REGULATING THE BIOSYNTHESIS AND SIGNALING OF THROMBOXANE A_2 IN HEMOSTASIS AND THROMBOSIS

by
Yan Li

A dissertation submitted to the department of Pharmacological and Pharmaceutical Sciences,
College of Pharmacy
in partial fulfillment of the requirements for the degree of

DOCTOR OF PHILOSOPHY

in Pharmacology

Chair of Committee: Ke-He Ruan, M.D., Ph.D

Committee Member: Richard A. Bond, Ph.D

Committee Member: Ken Fujise, M.D.

Committee Member: Yong-Jian Geng, M.D., Ph.D

Committee Member: Bradley K. McConnell, Ph.D

University of Houston
MAY 2020

ACKNOWLEDGEMENTS

I would like to express my deepest gratitude to my mentor, Dr. Ke-He Ruan. It cannot be possible to finish this dissertation without his constant support, valuable suggestions, guidance and encouragement throughout the entire research. His passion and knowledge towards research inspired me and broadened my vision in pharmacological research. I really appreciate this chance he provided to me to work on this interesting project. From Dr. Ruan, I learned not only the knowledge and the techniques, but also the ability of critical thinking and how to be a research scientist. I really enjoy my five-year Ph.D studies because of Dr. Ruan.

I would also like to thank all my committee members, Dr. Richard Bond, Dr. Ken Fujise, Dr. Yong-Jian Geng and Dr. Bradley McConnell for their helpful suggestions, precious time and constant encouragement to me and my research. Especially, I want to express my gratitude to Dr. McConnell. I spent my first one and half year in Dr. McConnell's lab, and I learned so many research skills and techniques during that time, which provides a solid foundation for my later research.

I would like to thank our department, the Department of Pharmaceutical and Pharmacological Sciences, for providing such a friendly, creative, open-minded and collaborative environment. I would like to thank Dr. Joydip Das for sharing their cell culture facilities with me. And Dr. Yang Zhang kindly provides their EOMA cell line for my research, and allowing me to use their imaging instruments and fluorescent

microscope and so do Dr. McConnell, Dr. Samina Salim and Dr. Das, Dr. Tahir Hussain, and Dr. Bin Guo. I couldn't finish my research without their supports.

I really want to thank all the graduate students and postdocs for the help and support. I will never forget the happy time we spent together. I couldn't thank more to my lab mates Dr. Qinglan Ling, Dr. Qunying Li, and Dr. Chang Chen. I learned so much from them.

Words fail me to express my appreciation towards my wonderful parents. They raise me with love and patience. They teach me how to be a good person. They try their best to give their two children the best education. They give me the freedom to let me choose to study in the United States. When I meet difficulties, they always stand by my side and never hesitate to show their supports. They are the best parents I could imagine in the world.

Five years ago, I came to United States alone, and I didn't expect I could meet my Mr. Right here. But life is unexpectable, the destiny let us find each other. I couldn't thank more to him, my wonderful husband, Mr. Haoran Zhao, and I am so grateful to have him in my life. His dedication, love, care and persistent confidence in me, has taken the load off my shoulder. He shares my happiness and sadness. He is not just a partner in my daily life, but also my best friend, and now, my family. He gives me a home, belonging us two, and a lovely dog and cat. I know no matter what happens in the future, as long as he holds my hands, I won't fear anything. Thank you, my love, my hero, my today and tomorrow, and I love you 3000!

Finally, I would like to thank all of my families, I couldn't come to today without your supports. My special appreciation to my dear brother, Jiasong and my dear sister-in law, Shan Xu. They took care of everything of me when I just came to United States, and not only the help, I got so much love from them. And I want to thank my dear angels, my niece Allison and my nephew Lucas. They provide so much happiness to my life. I feel so grateful to have the chance to watch them grow up healthily. I want to say thank you to my dearest friend, Shan Guo. She is the sunshine in my life and I am so lucky to grow up together with her. I would also like to express my appreciation of my dear friends, Liye Wang, Wei Zhao, Samanthreddy Kedika and Youngki You. I feel so thankful to have you all in my life.

ABSTRACT

Statement of the problem: TXA_2 is a main contributor in hemostasis. TXA_2 is mainly produced by the activated platelets, which can activate more platelets, induce platelet aggregation and facilitate the formation of platelet plug. The precursor of TXA_2 is AA, which can be metabolized by COX-1 into the unstable intermediate PGH_2. PGH_2 could be further isomerized by TXA_2 synthase (TXAS) to generate TXA_2. However, other prostanoid synthase can compete with TXAS for the same substrate PGH_2, to produce other prostanoids, such as PGI_2 and PGE_2, which are bleeding contributors. For the purpose of effective hemostasis, the production of TXA_2 should be increased and the productions of other prostanoids should be constrained. But one obstacle is that all of the prostanoid synthases have the similar affinity to PGH_2. Herein, we created a Single-Chain Hybrid Enzyme Complex (SCHEC), COX-1-10aa-TXAS, by linking the C-terminus of COX-1 to the N-terminus of TXAS through a 10 amino acid linker, to redirect the metabolism of AA toward the production of TXA_2. On the other hand, the signaling mediated by TXA_2 is highly involved in thrombosis. TXA_2 can activate its receptor TP, mediate the downstream pro-thrombotic Gαq-calcium signaling, which can mediate platelet aggregation and vasoconstriction. The effects of TXA_2 could be countered by PGI_2, through triggering the anti-thrombotic Gαs-cAMP signaling. However, the patients with thrombotic diseases, always have a higher level of TXA_2. The method to reverse the pro-thrombotic signaling activities of TXA_2 has not been

discovered yet. Therefore, this study was aimed to accomplish three aims. **Specific aim 1**: To Examine the biological functions of the novel hybrid enzyme, COX-1-10aa-TXAS. **Specific aim 2**: To investigate the application of COX-1-10aa-TXAS in hemostasis. **Specific aim 3**: To create a novel GPCR-G protein complex, which can reverse the pro-thrombotic signaling of TXA_2, and investigate the functions of the novel fusion protein complexes in platelet aggregation.

Procedure or methods: First, by expressing the hybrid enzyme in HEK 293 cells, the ability to redirect the metabolism of AA was studied. Considering the important role of TXA_2 in hemostasis, we investigated the functions of this novel hybrid enzyme *in vitro* platelet aggregation assays and *in vivo* mouse bleeding models. Secondly, we created two Single-Chain (SC) GPCR-G protein complexes, SC-TP-Gαq and SC-TP-Gαs. By stably expressing the fusion protein complexes in HEK cells, the signaling mediated by the protein complexes with TXA_2 stimulation was studied. In addition, through utilizing the platelet delivery system, the functions of SC-TP-Gαq and SC-TP-Gαs *in vitro* platelet aggregation were assessed.

Results: The HEK 293 cells stably expressing the hybrid enzyme, COX-1-10aa-TXAS, redirected the metabolism of AA to be in favor of TXA_2 production, and disfavor of other protanoids. Through being expressed in HEK cells, the hybrid enzyme indicated strong anti-bleeding functions both *in vitro* platelet aggregation assays and *in vivo* mouse tail-cut bleeding assays. The hybrid enzyme was also produced by using the *S. cerevisiae* yeast

protein expression system, and purified by ultracentrifugation and chromatography methods. The purified hybrid enzyme indicated strong ability to stop bleeding in mouse bleeding models. In HEK cells stably expressing SC-TP-Gαq and SC-TP-Gαs, triggered by TXA_2, the calcium signaling mediated by SC-TP-Gαq and the cAMP signaling mediated by SC-TP-Gαs were confirmed. Moreover, the platelets expressing SC-TP-Gαq could further promote platelet aggregation. While the platelets expressing SC-TP-Gαs could dramatically inhibit the aggregative activities of platelets.

Conclusions: These findings suggested that the hybrid enzyme, COX-1-10aa-TXAS, has great potential to be developed into a novel biological reagent in dealing with various hemorrhagic emergencies. And the fusion protein complex, SC-TP-Gαs, through the platelet delivery system, could be used to treat various thrombotic diseases, or be used to prevent the stent thrombosis or in-stent restenosis for the patients with the placement of stent. Additionally, this fusion protein method could also be applied to other GPCRs, in studying or manipulating the downstream signaling by linking to different G proteins.

Table of Contents

List of Figures

List of Abbreviations

COX, cyclooxygenase

PGG_2, Prostaglandin G_2

PGH_2, Prostaglandin H_2

TXA_2, Thromboxane A_2

TXAS, Thromboxane A_2 synthase

TP, TXA_2 receptor

PGI_2, Prostaglandin I_2

PGIS, prostaglandin I synthase

IP, PGI_2 receptor

PGE_2, Prostaglandin E_2

mPGES-1, microsomal prostaglandin E synthase-1

GPCR, G protein-coupled receptor

WT, wild type

TG, transgenic

NSAIDs, non-steroidal anti-inflammatory drugs

SCHEC, single chain hybrid enzyme complex

PLC, phospholipase C

PLA_2, Phospholipases A_2

IP_3, inositol triphosphate

AC, adenylate cyclase

cAMP, Cyclic adenosine monophosphate

PBS, phosphate buffered saline

DMSO, Dimethyl sulfoxide

BSA, Bovine serum albumin

PFA, Paraformaldehyde

RIPA, radioimmunoprecipitation assay

ANOVA, analysis of variance

PCR, polymerase chain reaction

LC-MS/MS, liquid chromatography-tandem mass spectrometry

PLP, platelet-like particle

PRP, platelet-rich plasma

PPP, platelet-poor plasma

ER, endoplasmic reticulum

ELISA, enzyme-linked immunosorbent assay

TPO, thrombopoietin

IV, intravenous

I. INTRODUCTION AND STATEMENT OF PROBLEM

Every year, around 1.5 million people from United States die from traumatic bleeding [1]. Generally, many bleeding emergencies, such as, can be very dangerous, and even life threatening. Arterial hemorrhage is always hard to control and is able to cause massive blood loss in a short time. TXA_2 is one of the most important factors to stop bleeding, due to its strong ability to activate platelets, induce aggregation of the activated platelets, and mediate vasoconstriction [2-6]. When bleeding occurs, a large number of arachidonic acid (AA) will be released from the cell membranes on the injured tissue, and quickly be metabolized into the unstable intermediate PGH_2 by COX-1, then PGH_2 will be further isomerized into TXA_2 by thromboxane synthase, TXAS, rapidly. However, TXAS need to compete with other pro-bleeding prostaglandin synthases, which means the production of TXA_2 is companied with other pro-bleeding prostanoids, and the efficiency of hemostasis is restricted. Thus, for the purpose of effective hemostasis, the metabolism of AA should be redirected toward the generation of TXA_2. But the redirection of AA metabolism is still unresolved, one key difficulty is that all of the prostanoid synthases have the similar affinity to the same substrate, PGH_2.

On the other hand, TXA_2 is closely related to the pathology of thrombosis [7]. Based on the statistics in 2010, thrombotic diseases were estimated to account for 1 in 4 deaths around the world, and are the leading causes of mortality [8].

Coronary artery is the artery to feed the heart muscles. When the coronary artery is narrowed down by the plaques, the blood flow will be reduced, resulting in chest pain. Even worse, the blood clotting could occur, which can block the blood flow completely, resulting in heart arrest [9]. Stent is a tiny wire mesh tube which can reopen the narrowed artery and recover the blood flow. But stent thrombosis may occur, which is a thrombotic occlusion of a coronary stent [10-15]. TXA_2 is a main player in inducing stent thrombosis [16]. In addition, another hazard may be caused by stenting, which is called in-stent restenosis. Restenosis means the blockage of the reopened coronary artery, which is mainly caused by the excessive tissue proliferation on the luminal surface of the stent [17-20]. Recent studies have suggested that by deletion of the TXA_2 receptor, TP, the restenosis could be prevented, which indicated the facilitation effects of signaling mediated by TXA_2 in restenosis. In contrast, deletion of the PGI_2 receptor, IP, can exacerbate restenosis, suggesting the inhibition of restenosis by PGI_2-mediated signaling. TXA_2 is mainly produced by activated platelets, and it can activate more platelets and cause further platelet aggregation. These pro-thrombotic effects are achieved by stimulation of its receptor TP, and activation of Gαq-mediated calcium signaling. Interestingly, these effects can be countered by PGI_2, which can induce Gαs-mediated anti-thrombotic cAMP signaling. What's more, more and more TXA_2 can be produced and accumulated on the thrombus area, causing the growth of thrombus. Therefore, the alteration of the downstream pro-thrombotic signaling of

TXA_2 may be very helpful for patients with thrombotic diseases, and prevent the stent complications, such as stent thrombosis and in-stent restenosis.

The long-term goal of this research is to investigate novel methods of control the biosynthesis and signaling of TXA_2 to treat life-threatening bleeding emergencies, and thrombotic diseases, especially stent thrombosis and in-stent restenosis. Based on our previous research, we engineered a novel single-chain hybrid enzyme complex (SCHEC), COX-1-10aa-TXAS, which was able to redirect the metabolism of AA toward the production of TXA_2. We hypothesize this hybrid enzyme can mediate effective hemostasis due to its capacity of producing a large number of TXA_2 rapidly; meanwhile, constraining the production of other pro-bleeding prostanoids. The rational of this research is that once the anti-bleeding properties of this hybrid enzyme is confirmed, it can be developed into a powerful anti-bleeding biological reagent to deal with a variety of severe bleeding situations. On the other hand, our previous studies indicated the powerful anti-thrombotic functions of PGI_2 through triggering Gαs-cAMP signaling. Thus, to mimic the anti-thrombotic effects of PGI_2, we constructed a novel GPCR-G protein complex, SC-TP-Gαs, which was able to change the downstream signaling of TXA_2 by linking the TP receptor to Gαs protein. We hypothesize this alteration of the TXA_2 downstream signaling activities should be able to convert its pro-thrombotic functions to anti-thrombotic effects. As long as the anti-thrombotic functions of SC-

TP-Gαs complex is verified, it can be used to treat various thrombotic diseases, such as stent thrombosis and in-stent restenosis.

To achieve the objectives of this research, we propose the following four aims. **Specific aim 1**: To Examine the biological functions of the novel hybrid enzyme, COX-1-10aa-TXAS. We will develop a cell line (HEK 293) stably express the cDNA of the hybrid enzyme. The biological functions of the hybrid enzyme will be determined by *in vitro* platelet aggregation assay and *in vivo* mouse bleeding models. In addition, aspirin-treated cell models and transgenic mouse models with bleeding tendency will also be utilized to test the functions of the hybrid enzyme. **Specific aim 2**: To investigate the application of COX-1-10aa-TXAS in hemostasis. We will utilize the *S. cerevisiae* yeast protein expression system to produce our hybrid enzyme. Then the produced hybrid enzyme will be purified and assessed for the functions in mouse bleeding models. **Specific aim 3**: To create a novel GPCR-G protein complex, which can reverse the pro-thrombotic signaling of TXA_2. To reverse the pro-thrombotic effects of TXA_2, the downstream Gαq protein will be replaced by the Gαs protein, creating a novel fusion protein complex, SC-TP-Gαs. The signaling mediated by SC-TP-Gαs triggered by TXA_2 will be assessed. **Specific aim 4**: To investigate the functions of the novel SC-TP-Gαs complex in platelet aggregation. In order to test our hypothesis, the megakaryocyte cell line, Meg-01 will be utilized. Firstly, the stable expression of SC-TP-Gαs will be induced in Meg-01 cells through electroporation method and G418 selection.

Then the maturation of the Meg-01 cells will be induced, releasing the platelet-like particles (PLPs) with the expression of SC-TP-Gαs, which are expected to become a novel type of platelets to absorb the excessive TXA_2 in blood circulatory system. The purpose of these platelets is not for transfusion, and is to serve as a carrier to express and deliver SC-TP-Gαs. We will test the anti-thrombotic effects of SC-TP-Gαs *in vitro* platelet aggregation assays.

II. LITERATURE SURVEY

II.1 Differences between COX-1 and COX-2

Cyclooxygenases (COXs) belongs to glycoproteins, and they are expressed abundantly on the ER membrane [21]. There are two catalytic sites were contained in these enzymes: the cyclooxygenase (COX) site and the peroxidase (POX) site. The COX site contains a tyrosine residue, which can metabolize AA into PGG_2. The POX site possesses a heme, by which PGG_2 is reduced into PGH_2. In addition, other products, such as PGH_1 and PGH_3, could also be produced by COXs from dihomo-γ-linolenic acid and 5,8,11,14,17-eicosapentaenoic acid, respectively [22].

About 63% of amino acid sequences are shared by COX-1 and COX-2. The molecular weights for both are 72 kDa. COX-1 is a 'housekeeping' enzyme, which is expressing constitutively and ubiquitously. The reason is that COX-1 doesn't have CAAT or TATA boxes, which are the promoter sequence to regulate

transcription [23] COX-2 is an inducible enzyme, and its expression is regulated by the promoter TATA box, NF-IL6 or CRE motif, AP-2, Sp1 and NF-κB sites [24]. The expression of COX-2 is only in response to diverse stimuli, including cytokines bacterial lipopolysaccharide, growth factors, etc.

Compared to COX-1, the N-terminus of COX-2 doesn't have the sequence of 17 amino acids [25]. It is still unknown about the differences of functions between COX-1 and COX-2 due to the different sequences on N-termini. Even though COX-2 has a shorter N-terminus compared to COX-1, COX-2 has an additional sequence of 18 amino acids at the C terminal domain [25]. COX-1 and COX-2 possess the same four residues, STEL, at the end of the C-termini. These four residues account for the attachment of both C-termini on the ER membrane. Differently, COX-2 is expressed on both of the ER membrane and the nuclear membrane, but COX-1 is only found on the ER membrane. Thus, the difference in C-termini between COX-1 and COX-2 might lead to the different subcellular localizations.

Based on the X-ray crystal structural studies, human COX-1 and CO-2 have almost the same 3D structures [26-27] except two residues, and all other residues on the substrate binding pocket and active sites, and other adjacent residues are completely identical. The two different residues are Isoleucine 434 and 523 in COX-1, while are Valine in COX-2. Due to the difference of the two residues, COX-

2 was found a larger active site than COX-1. This makes it possible to develop specific COX-2 inhibitors without affecting COX-1. However, if Ile 523 of COX-1 is mutated into Val, the selective COX-2 is able to bind to the COX-1 mutant, and thus the production of PGH_2 could be interrupted. The residue 434 is involved in the opening of the side pocket, which can contribute to the substrate selectivity on COX-2. After acetylation of COX-2, the residue Ser530 will become closer to the position 434, thus compared to Ile, the smaller bulk of Val allows larger entry space for substrates. Therefore, even after the acetylation by NSAIDs, AA still can enter to the COX-2 catalytic site [25]. For example, the COX site of COX-1 can be irreversibly acetylated by aspirin, and due to the large bulk of Ile 434, AA cannot enter into the active site of COX-1, which inhibit the oxidization of AA. But for COX-2, even acetylated by aspirin, AA can still be catalyzed into 15-HETE [25].

There is another important residue, Arg 120, which is an essential residue allowing AA, selective COX-1 inhibitor or nonselective NSAIDs to bind to COX-1 [28-31]. It is because a carboxylic acid in the structures of AA, selective COX-1 inhibitor and nonselective NSAIDs, which allow them to form an ionic bond with Arg 120 on COX-1. In contrast, selective COX-2 inhibitors do not be bound to the residue Arg 120, thus do not bind to COX-1.

II.2 Prostanoids and their roles in hemostasis

AA is a polyunsaturated fatty acid, which is abundantly expressed in the phospholipid of cell membranes. And AA is especially abundant in muscles, brain and liver. The enzyme PLA_2, could cleave off the AA from the phospholipid molecule and AA could be released from the cells. It's already known that three enzymes, COX, lipoxygenase and cytochrome P450 could metabolize AA [32]. In the lipoxygenase and cytochrome P450 pathways, AA can be metabolized into leukotrienes and epoxyeicosatrienoic acids (EETs), which can mediate asthma and vascular protection, respectively [33-34].

The COX pathway is the dominant pathway in AA metabolism. This is due to the higher affinity of COXs with AA. The COX pathway initiates with the hydrolysis of phospholipids in cell membrane, with the help of cLA_2, to free AA. The released AA can be metabolized by COXs into a transit intermediate, PGG_2, and PGG_2 will be quickly catalyzed by COXs again into the common intermediate, PGH_2. In the COX-1 pathway, PGH_2 is a common substrate for downstream prostanoid synthases, such as TXAS, PGIS and PGES, to synthesize individual prostanoid (TXA_2, PGI_2, and PGE_2) (Figure.1).

Thromboxane A_2 (TXA_2) is one type of thromboxane, which is mainly produced by activated platelets. TXA_2 is capable of activating platelets, induce aggregative

activities of the activated platelets, and promote the formation of platelet plug.

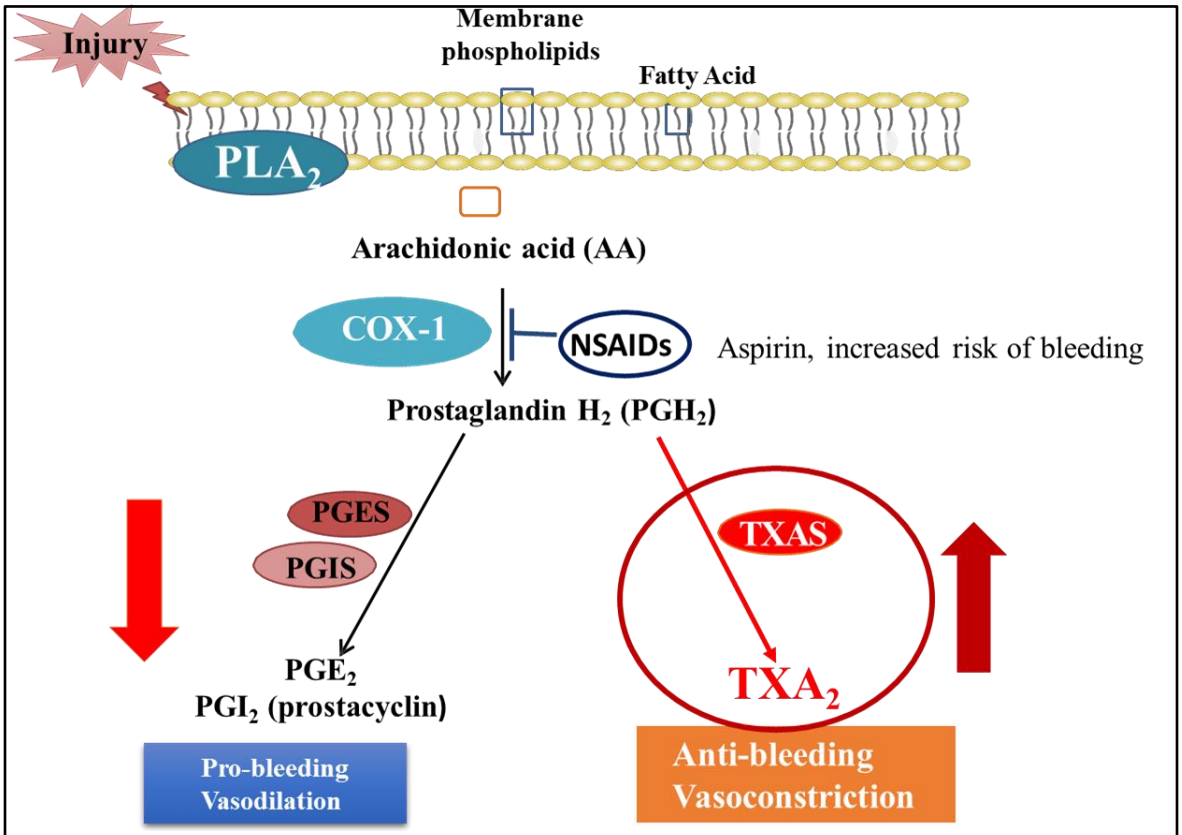

Figure 1. Illustration of the involvement of prostanoids in hemostasis.

AA is polyunsaturated fatty acid abundantly presenting in the phospholipids of cell membrane. When there are injury stimuli, PLA_2 can free AA from the phospholipid molecule. The released AA will be converted into the unstable intermediate PGH2 by COX-1, and further isomerized by different prostanoid synthases, including TXAS, PGES and PGIS, into individual prostanoid. Among these prostanoid, only TXA_2 suggests anti-bleeding and vasoconstriction effects, and all others exhibit the opposite functions. For the purpose of effective hemostasis, the production of

TXA_2 should be increased; meanwhile the production of other prostanoids should be constrained. In addition, the administration of NSAIDs could increase the risk of bleeding due to inactivation of COX-1, leading to prevent the generation of TXA_2 in platelets.

Besides, TXA_2 is a key factor in tissue injuries, because it demonstrates high impacts on mediating vasoconstriction. Generally, TXA_2 is produced through the chain triple catalytic reactions: in the bleeding site, massive AA released from the cells of the injured tissue is quickly metabolized by COX-1 into the transient intermediate prostaglandin G_2 (PGG_2), and rapidly catalyzed by COX-1 again into the unstable intermediate prostaglandin H_2 (PGH_2); rapidly, the intermediate PGH_2 is further isomerized by TXAS into the anti-bleeding prostanoid, TXA_2, in platelets. Besides the functions in hemostasis, TXA_2 is also suggested to have some impacts on the progression of cancer, tumor metastasis, as well as neurodegeneration. In addition, the administration of NSAIDs, such as aspirin, could increase the risk of bleeding. It is because that aspirin is a non-selective COXs inhibitor, and it can inactivate the functions of COX-1 irreversibly. Due to the no nuclei in platelets, the affected platelets cannot make new COX-1 enzyme. Thus the low-dose aspirin could permanently inactivate the functions of COX-1 in platelets, leading to the inhibition of the TXA_2 production, increasing the risk of bleeding.

PGE_2 is one key molecule in inducing inflammation. When inflammation occurs,

the level of PGE_2 is significantly elevated, and it has been identified to play very important roles in many inflammatory diseases, such as neurodegenerative diseases, atherosclerosis and cancer [35-37]. Many recent studies indicated that the PGE_2 synthase, mPGES-1 is involved in the Aβ plaques formation within the hippocampus in AD mouse models, as well as AD patients. The deletion of mPGES-1 through gene-knockout technique could reduce the formation of plaques [38]. PGI_2 is synthesized by PGIS from the COX-1-derived common intermediate, PGH_2. The majority of PGI_2 was synthesized in endothelial cells. It is well characterized as a cardiovascular protector [39-40] through mediating blood vessel dilation and inhibiting platelet aggregation [41]. Recent studies suggest that PGI_2 could promote progenitor cell regeneration in hindlimb ischemia [42], and prevent neurodegeneration of hippocampus in AD mouse models. In addition to the functions of PGE_2 and PGI_2 addressed above, PGE_2 and PGI_2 are also actively involved in hemostasis. Both of them exhibit pro-bleeding effects. When bleeding occurs, the released AA is rapidly metabolized into the common intermediate, PGH_2. The PGE_2 and PGI_2 synthases could instantly compete with the TXA_2 synthase. All of these prostanoid synthases demonstrate the similar affinity to PGH_2. Thus, the production of TXA_2 is limited through the competition, and the efficiency of hemostasis is constrained in this way.

II.3 The roles of TXA_2 and its receptor in thrombosis

II.3.1 The signaling mediated by TXA_2 and PGI_2

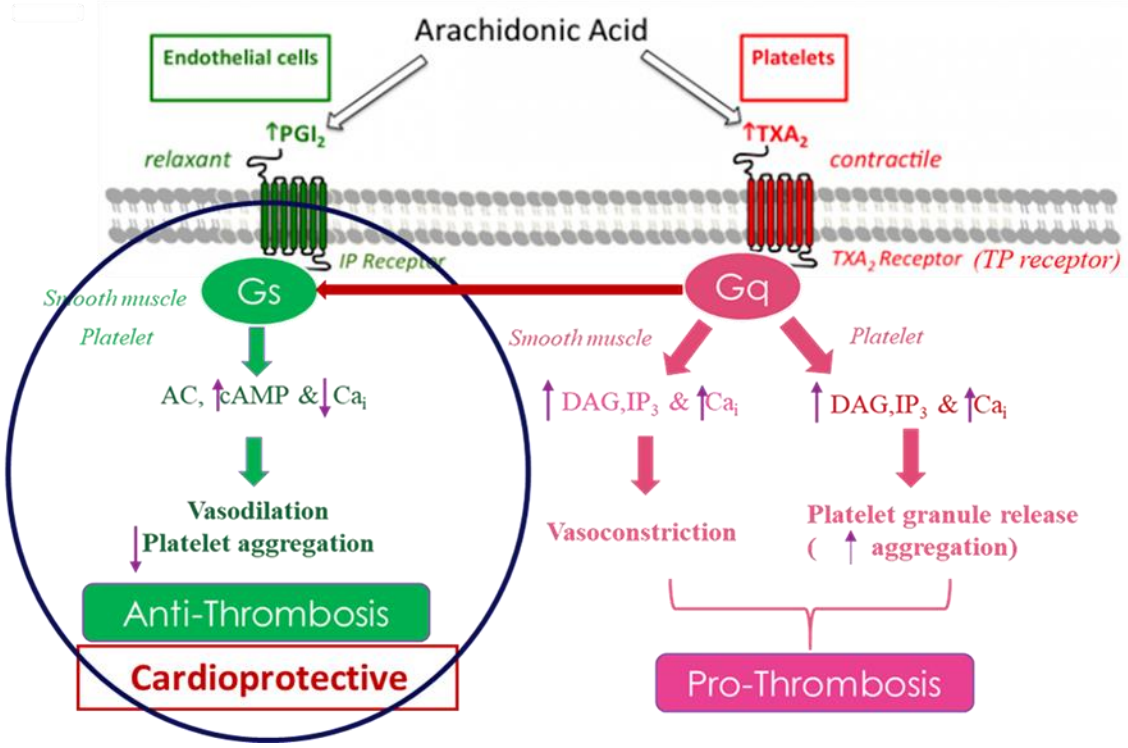

Figure 2. The different signaling cascades mediated by TXA_2 or PGI_2.

TXA_2 can activate TP, triggering Gαq-calcium signaling, which is able to mediate vasoconstriction and platelet aggregation. Thus the signaling mediated by TXA_2 exhibits pro-thrombotic effects. In contrast, PGI_2 can active IP, mediating the anti-thrombotic Gαs-cAMP signaling, which can mediate vasodilation and prevent the aggregation of platelets. Therefore, the signaling transductions mediated by PGI_2 is considered as cadioprotective.

The receptor of TXA_2 is TP. After TP is activated by TXA_2, the downstream Gαq signaling could be stimulated, which will promote Gαq to be association with PLC, triggering the release of the second messenger IP_3, and leading to the release of intracellular calcium. This calcium signaling cascades could mediate vasoconstriction, and promote platelet aggregation (Figure. 2). Thus the pro-thrombotic signaling mediated by TXA_2 is directly involved in some thrombotic diseases. On the other hand, PGI_2 can activate its receptor IP, and activate the downstream Gαs to be associated with AC, which catalyzes the cyclization of ATP, and leads to the production of cAMP. Different to TXA_2, the cAMP signaling transductions mediated by PGI_2 demonstrate anti-thrombotic effects. Thus PGI_2 is considered as vascular protector.

II.3.2 The isoforms of TP

There are two isoforms of human TP receptor. The two isoforms were derived from alternative splicing from the same gene. The one cloned from placenta is known as TPα, and the one cloned from endothelium is known as TPβ [43-45]. TPα and TPβ has 343, 407 amino acids in length, respectively, and they share the first 328 amino acids. The only difference between these two isoforms is the C-terminal. TPβ exhibits an extended C-terminal [46]. The transcription of two isoforms are activated by different upstream promoters, which also indicated the at least some independent functions [47-48]. In most tissues, both isoforms of TP receptor are

expressed, but the expression is not equal. Specially, only TPα is expressed in platelets [49]. The basic signaling of these two isoforms is through activating the G proteins of Gαq family [50], but in certain cell types, activation of TPα and TPβ may mediate different downstream cell signaling. In previous research, both isoforms were found to activate the high molecular weight G protein, Gh. However, the downstream signaling mediated by the Gh for the two isoforms are different. The activation of TPα can mediate Gh-induced, phospholipase C-mediated inositol phosphate production. But the activation of TPβ may mediate Gh-induced, Gαq-mediated inositol phosphate signaling [51]. Some studies also indicated that TPβ, not TPα may inhibit the adenylyl cyclase [52]. The intracellular trafficking mechanisms of the two isoforms is different also, and the TPβ depends on the direct interaction with Rab11 [53].

Both isoforms of TP receptors are regulated by phosphorylation-dependent desensitization [54]. However, the targets of agonists are different. Some studies demonstrated that only TPα, not TPβ is the desensitization target for nitric oxide and PGI_2 [55]. Compared to TPα, TPβ is more easily to undergo internalization, under both basal and activation status [56-57]. Thus, the expression level of TPβ is partially depended on the proteosomal degradation activities [58]. Another study indicated a C-terminal motif, only presenting on TPβ, was involved in tonic internalization and recycling of TPβ.

Some studies also indicated the distinct functions of the two TP isoforms in angiogenesis. Because in most mouse models, the lack of TPβ resulted in contrasting results at the beginning. Then people found the activation of TPα is able to promote angiogenesis [59]. In contrast, TPβ plays an important role in suppressing the blood vessel growth [60].

II.4 Hybrid enzymes

II.4.1 The hybrid enzymes, COXs linked to PGIS

From the topological and structural studies of PGIS and TXAS, it was suggested that the catalytic domains of PGIS and TXAS are located on the cytoplasmic side of the ER. And the N-terminal domains of PGIS and TXAS are anchored in the ER membrane [61-65]. In addition, based on the crystallographic studies of COX-1 and COX-2, it was suggested that the catalytic domains of the COX-1 and COX-2 are located on the luminal side of the ER. The C-terminal domains of COXs are anchored on the luminal side of the ER membrane [66-67]. The biosynthesis of prostanoids was accelerated by these enzyme configurations, which anchor COXs and different prostanoid synthases on the two sides of ER membrane, with the shortest distance. According to this information, the C-terminus of COX-2 was linked to the N-terminus of PGIS through 10 amino acids (10aa) or 22 amino acids (22aa) linkers. The residues of the linkers were derived from the helical transmembrane domain of bovine rhodopsin, whose crystal structure is already

available. The sequence of the 10aa linker is His-Ala-Ile-Met-Gly-Val-Ala-Phe-Thr-Trp, and the 22aa is His-Ala-Ile-Met-Gly-Val-Ala-Phe-Thr-Trp-Val-Met-Ala-Leu-Ala-Cys-Ala-Ala-Pro-Pro-Leu-Val. Then the cDNAs of the two hybrid enzymes, COX-2-10aa-PGIS, and COX-2-22aa-PGIS were cloned into pcDNA3.1(+) vectors, and reported by our lab in 2006 [68]. In addition, the cDNA of the reversed order, PGIS-10aa-COX-2, was also created and cloned into the vector to be used as a control. Both results of immunofluorescent staining and western blot confirmed the expression of the hybrid enzymes in HEK293 and COS-7 cell lines. Both of the hybrid enzymes, COX-2-10aa-PGIS and COX-2-22aa-PGIS suggested the ER pattern localization in cells, which was also observed in co-expression COX-2 and PGIS in the cells. These results suggested that these hybrid enzymes have the correct protein folding, and anchor across the ER membrane. In contrast, the expression of PGIS-10aa-COX-2 could not be identified in the western blot results and a very low level of expression was detected by immunostaining. Then the enzymatic activities of these hybrid enzymes were determined by ELISA and HPLC-Scintillation analysis through using [^{14}C]-AA as substrate. The results of the kinetic studies suggested a faster reaction of COX-2-10aa-PGIS in the first 0.5 – 1 minute compared to COX-2-22aa-PGIS, or co-expression of COX-2 and PGIS.

Later, in 2008, another hybrid enzyme, COX-1-10aa-PGIS was reported by our group [69]. Compared to previous COX-2-10aa-PGIS, the COX-1-10aa-PGIS hybrid enzyme indicated advantages in stable expression due to the replacement

of the inducible COX-2 by the constitutive COX-1 (Figure. 3a). The expression of COX-1-10aa-PGIS was identified by western blot and immunofluorescent staining. The ER pattern localization of COX-1-10aa-PGIS was also observed, which was the same with the co-expression of COX-1 and PGIS. In addition, the enzyme kinetics studies of co-expression of COX-1and PGIS, and COX-1-10aa-PGIS were almost identical (about Km = 5 μM, Vmax = 400 μM). The stable expression and catalytic activities of COX-1-10aa-PGIS were confirmed in HEK293 cells. But the expression and enzymatic activities of COX-2-10aa-PGIS decreased significantly after a few days expressed in HEK 293 cells. A recent study, which applied the hybrid enzyme COX-1-10aa-PGIS in a mouse hind-limb ischemic model, indicated impressively improved endogenous regeneration.

II.4.2 The hybrid enzyme, COX-2-10aa-mPGES-1

The hybrid enzyme, COX-2-10aa-mPGES-1, by linking COX-2 to mPGES-1, was first reported by our group in 2009 [70]. Four transmembrane domains of mPGES-1 spanning on the ER membrane. Same with previous hybrid enzymes, the C-terminal domain of COX-2 was linked to the N-terminal domain of mPGES-1 through a 10aa linker (Figure. 3b). The results of fluorescent immunostaining indicated the ER pattern localization of this hybrid enzyme, which was also identified in co-expression of COX-2 and mPGES-1. This indicated that this hybrid enzyme, COX-2-10aa-mPGES-1, was also anchored in the ER membrane. By

using [^{14}C]-AA as substrates, more effective triple-catalytic activities were observed in this hybrid enzyme by HPLC analysis (Figure. 3b), which can constrain the productions of other molecules, inducing more production of [^{14}C]-PGE_2. In addition, in the first 30 seconds, slightly faster kinetics were identified. The Km value was 0.5 μM.

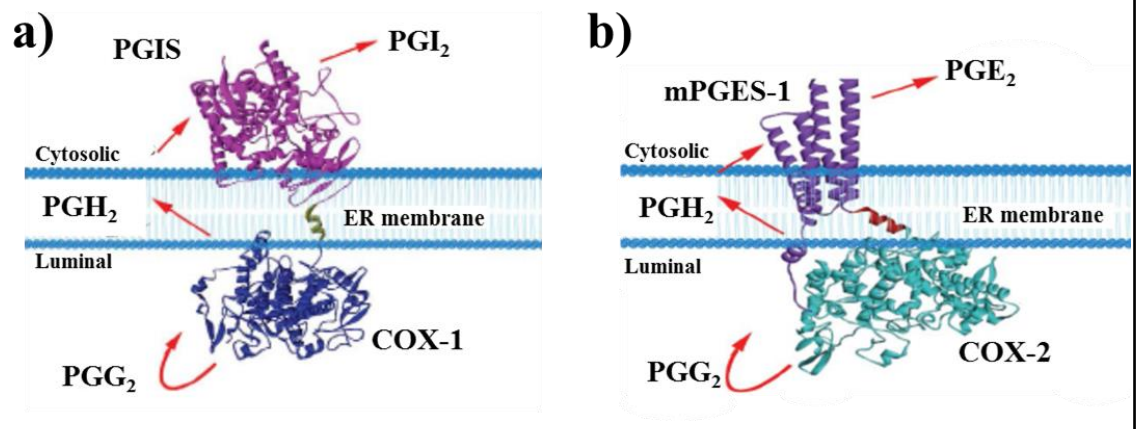

Figure 3. The structural modeling for the two hybrid enzymes.

a) The computational modeling for COX-1-10aa-PGIS. The C-terminus of COX-1 is linked to the N-terminus of PGIS through a 10aa linker. The triple-catalytic activities could be performed by the hybrid enzyme. b) The computational modeling for the hybrid enzyme, COX-2-10aa-mPGES-1. The C-terminal domain of COX-2 is also linked to the N-terminal domain of mPGES-1. This hybrid enzyme can also perform the chain triple-catalytic activities.

II.5 Currently widely-used topical hemostatic agents

II.5.1Collagen-based hemostatics.

In the collagen-based agents, the collagen molecules, which are non-covalently bound to some amino acid groups, consist of the microfibrillar structure [71]. The large surface provided by the helical structure can attach to the bleeding surface, attract platelets, and induce platelet aggregation, since the platelets can adhere to the collagen fibrils and degranulation. This can promote the formation of platelet plug on the injury site. To enhance the effects, this agent is always combined to a procoagulant substance, always thrombin. The commercial agents belong to this category including Avitene®, D-Stat®, InstatRM, CoStasis®, and Helistat®. The adverse effects for this type of agent include formation of granulomatous masses, adhesion formation, allergic reactions, and interference with the healing of skin edges [72].

II.5.2 Gelatin-based hemostatics.

It is believed that there is no involvement of blood clotting in gelatin-based haemostats. Surface effects play the main role [73]. For example, FloSeal ® Matrix, a typical hemostatic agent in this category, works through mechanical and pharmacological mechanisms. The granules can swell up to 20% when in touch with blood or body fluids, and the bleeding is stopped by a tamponade effect. The

safety of these gelatin-based agents has not been fully investigated, but some animal models indicated the potential dangerous side effects due to thrombotic obstruction through the swelling of granules [74].

II.5.3 Cellulose-based hemostatics.

These hemostatic agents, such as Surgicel®, have been used for decades. Their actions include blood absorption, interactions with surface proteins, attraction of platelets, and most important, local activation of the coagulation cascade. They don't contain any coagulation substances, and they work through stimulation of blood clotting and providing a favorable structure for clot organization [75]. However, the limitations of these agents have been demonstrated by many studies. Because these agents primarily activate the local coagulation cascade, the intact functional coagulation system is necessary. For example, when a traumatic bleeding occurs on a patient with platelet-deficient bleeding disorder, the cellulose-based agents will fail to induce platelet aggregation. In addition, these agents were demonstrated not effective in wet environment, due to their poor adhesion to tissue [76]. Also, many research indicated these agents can provide nidus for bacteria, and thus promote infection and abscess.

II.5.4 Synthetic albumin-derived adhesives.

The most widely-used agent in this category is BioGlue®, which consists of purified bovine serum albumin (45%) and glutaraldehyde (10%) [77]. The mechanism of action is based on the covalent bond between albumin and tissue surface proteins, and glutaraldehyde can form covalent bonds with both albumin and surface proteins and cross-link the two, which forms a mechanical seal at the bleeding site. Importantly, this hemostatic process is completely independent of the patient coagulation system, so maybe useful to be used on the patients with coagulation-deficient bleeding disorders. However, it is inconvenient to use these agents since albumin and glutaraldehyde must be kept separately until application, which may waste time when facing life-threatening bleeding emergencies. In addition, some studies indicated the potential tissue toxicity of glutaraldehyde [78].

II.5.5 Polysaccharide-based hemostatics.

Chitosan, commercial known as CELOXTM and HemCon®, is produced by deacetylation of Chitin (poly-N- acetyl glucosamine). This is a novel local hemostatic agent, which involves in activation of platelets, and form electrophysiologic interactions between red blood cells and tissue surfaces [79-81]. The full mechanism and adverse effects have not been fully elucidated.

II.5.6 Inorganic hemostatics.

The commercial product of this category in known as QuickClot®. The component, zeolite, can absorb water from the injury site, and thus can concentrate the platelets and clotting factors and facilitate the coagulation system. And the water absorption is achieved by an exothermic reaction [82]. This agent was designed to treat severe arterial hemorrhage. However, the exothermic reaction, which is responsible for the efficacy, was indicated to produce injuries, such as potentially partial or full-thickness burns, and the peak temperature may even reach up to 140.4oC [83-84].

II.5.7 Fibrin adhesives.

The fibrin adhesives are composed of thrombin and purified fibrinogen (bovine or human). They mimic the last step of the blood coagulation system, to stabilize the blood clot in the injury site through fibrin. They were demonstrated to reduce adhesion formation and promote wound healing [85]. Due to the limitations of only involvement in the final step, these agents, such as TisseelTM, FlosealTM, are always combined with thrombin, factor XIII, and/or other antifibrinolytic agent, to amplify the effects.

II.5.8 Comparison of our hybrid enzyme to these commercial hemostatic agents

Our hybrid enzyme COX-1-10aa-TXAS, indicates many significant advantages compared to the above commercial hemostatic agents. The only substrate to

initiate the effects of the hybrid enzyme is the endogenous AA. AA is a polyunsaturated fatty acid, which is abundant in cell membrane. When bleeding occurs, a lot of AA will be released from the cell membrane on the injury site. The application of the hybrid enzyme can rapidly utilize the massive arachidonic acid (AA) released on the injury site as substrates, to produce the strong anti-bleeding prostanoid, thromboxane A_2 (TXA_2), through the chain catalytic reaction. The biosynthesis of TXA_2 is very fast, which indicates higher efficiency in hemostasis. Compared to other hemostatic agents, our hybrid enzyme doesn't need any exogenous substrates, and the blood coagulation system will be initialized by TXA_2, since TXA_2 can activate platelets, induce platelet aggregation and promote the formation of platelet plug [86]. Since this hybrid enzyme can mimic the natural biosynthesis of TXA_2, it won't cause significant immune response compared with other synthetic chemical hemostatic agents. In addition, distinct from all above hemostatic agents, the hybrid enzyme can also mediate vasoconstriction [87], which may be very helpful in dealing with arterial hemorrhage. In conclusion, compared to the existing hemostatic agents, our COX-1-10aa-TXAS, can overcome many of their shortages, and exhibit significant improvements.

II.6 Stent thrombosis, restenosis and current medical treatments

II.6.1 Stent thrombosis and restenosis

When the arteries are blocked, angioplasty is a safe and effective method to unblock the blood vessel and recover the blood flow [88]. During the angioplasty, a catheter with a deflated balloon will be utilized and pass through the atherosclerotic plaque in an artery, then the balloon will be inflated. The blockage of the artery will be opened and the plaque will be compressed. To keep the widened artery from collapsing down, the stent, a small metallic spring-like device, is then placed on the blockage site [89]. This inserted stent works as a scaffold to keep the artery open. However, both of the procedures in angioplasty and stent placement are not gentle, actually cause the trauma to the blood vessel wall.

Restenosis refers to the unblocked blood vessels become narrowed or blocked again. Without the support of stent, the treated arteries are more easily to block again, which is known as restenosis [90-91]. The main reason is as we addressed above, the procedures of angioplasty are not gentle, which can cause trauma on the vessel wall. And plaques start to build up where the arteries are damaged. Thus, more plaques will be formed following angioplasty and restenosis always occurs within the six months of the procedures. The chance of restenosis has been decreased by placing the stent after angioplasty. However, restenosis can still occur, which is known as in-stent restenosis [91]. In addition to in-stent restenosis, another hazard of stent is known as stent thrombosis. One of the most common reasons for stent thrombosis is the trauma formed during the stenting, and platelets will start to aggregate on the injury site accompanied by an immune response, and

induce thrombosis. Another reasons to cause stent thrombosis include impaired re-endothelization, hypersensitivity reactions, neoatherosclerosis, stent malapposition, and stent dismantling. In-stent restenosis is the result of cell proliferation in the media, the smooth muscle layer of the artery wall [92]. After a stent is inserted in a blood vessel, new tissue will start to grow inside the stent. Actually this is how the stent woks, that the struts of the stent are covered by the new tissue, forming the new endothelium lining of the arterial wall, and the new lining allows the blood to flow smoothly without clotting. However, later on, the scar tissue may begin to form underneath the healthy lining (mainly consist of vascular smooth muscle cells), which is indeed a 'healing process' resulting from the trauma caused by stenting. The excessive cell growth can cause the scar tissue become thicker and thicker and eventually obstruct the blood flow and result in a severe blockage.

II.6.2 Current medical treatments for prevention of in-stent restenosis and stent thrombosis

To prevent the stent thrombosis, the administration of anti-platelet drugs, the IIb/IIIa inhibitors, the blood thinner drugs immediately after the stenting might prevent the occurrence. However, the long-term administration of these drugs can cause many adverse effects, such as bleeding complications, hemorrhagic stroke or GI bleeding. To prevent in-stent restenosis, the drug-eluting stent (DES) are

utilized [92]. The drugs, such as rapamycin, and paclitaxel are coated on the stent, released slowly and mediate local activities. They work through inhibiting the cell proliferation, which will inhibit the formation of neointimal, and thus reduce restenosis. However, the limitations of these are also very significant, because they can also inhibit the proliferation of endothelium, which means inhibition of the formation of the new endothelium lining inside stent. And this may lead to dangerous late stent thrombosis. Brachytherapy is also used to prevent restenosis through delivering β and γ radiation to inhibit cell proliferation [92]. However, some severe side effects might also be caused, such as promotion of media remodeling, edge restenosis at the end or outside of stent (low radiation doses), delayed healing process of medical dissections, and delayed re-endothelialization.

II.6.3 Comparison of the above medical treatments with our SC-TP-Gαs

Compared to the above treatments to prevent stent thrombosis and restenosis, the application of our GPCR-G protein complex, SC-TP-Gαs, may indicate significant improvements. Due to the trauma caused by stent placement, a lot of TXA_2 will be produced, then the TXA_2 will stimulate its receptor TP, and activate Gαq, mediating the intracellular calcium signaling [93]. This signaling cascades can lead to vasoconstriction, and platelet aggregation, which contributes to the first stage of restenosis. On the other hand, PGI_2 has been reported to be helpful to prevent stent thrombosis, because it can stimulate the IP receptor, and activate the Gαs,

mediating cAMP signaling [94]. The cAMP signaling can suppress the calcium signaling, mediate vasodilation, and inhibit platelet aggregation, which can prevent the occurrence of thrombosis. Our SC-TP-Gαs can mimic the natural signaling of PGI_2: when stimulated by TXA_2, the Gαs-cAMP signaling will be activated instead. Thus, the application of SC-TP-Gαs, can prevent the stent thrombosis, with the minimal side effects compared with any drug administration. The vascular smooth muscle cell proliferation is the main cause of the in-stent restenosis. A lot of studies has addressed the protective effects of PGI_2 by suppressing the proliferation of vascular smooth muscle cells, and promoting the formation of endothelium lining [94]. Thus, via expression the SC-TP-Gαs in arteries, the in-stent restenosis can be prevented by mimicking the signaling of PGI_2. Another improvement is that we will utilize platelet delivery system to use platelets as carriers, delivering SC-TP-Gαs into the blood circulatory system, without any later drug administration. The platelets expressing SC-TP-Gαs can be applied through IV transfusion and last for around two weeks.

III. MATERIALS AND METHODS

III.1 Materials

The HEK 293 cell line and Meg-01 cell line were purchased from ATCC (Manassas, VA). Cell culture medium, supplements and antibiotics were purchased from Life Technologies (Grand Island, NY). TPO was from R&D systems (Minneapolis, MN). Yeast culture medium and supplements were purchased from Invitrogen (Carlsbad, CA).The COX-1, Gαq and Gαs antibodies were purchased from Cayman (Ann Arbor, MI), and the CD41a and CD42b antibodies were from Invitrogen (Carlsbad, CA).

III.2 Cell culture

HEK293 cells and cells from HEK293 cell lines were cultured in high-glucose Dulbecco's modified Eagle's medium (DMEM),

Meg-01 cells were cultured in RPMI 1640 medium, supplemented with 10% fetal bovine serum (FBS), and 1% Antibiotic- Antimycotic at 37 °C, in a humidified 5% CO_2 incubator. Since this is a suspension cell line, the subculture was performed

through centrifugation at a speed of 200g for 5 minutes. Then the cell pellet was resuspended in fresh culture medium.

III.3 Subcloning of the hybrid enzyme

The cDNA of COX-1-10aa-TXAS was produced by PCR. The subcloning procedures have been described previously [95-98]. The cDNA of the hybrid enzyme was successfully subcloned into the pcDNA 3.1(+) vector between the two BamHl sites, through the PCR method. The correct inserted size of cDNA was assessed by restriction enzyme digestion and DNA sequencing was performed to test the sequence of the hybrid enzyme.

III.4 Expression of the hybrid enzyme in HEK cells

The method to establish stable cell lines expressing the hybrid enzyme and other control enzymes has been addressed in previous studies [99-100]. Briefly, the cells were transfected with the cDNA vectors by using the Lipofectamine 2000 approach, following the manual provided by the manufacturer (Invitrogen). After 48h of transfection, G418 (400ug/ml) was added to the medium for screening and selection of HEK cells expressing the recombinant proteins. The selection always lasts for 8 weeks.

III.5 Immunostaining

The procedures for immunostaining have been described in detail previously [101]. Briefly, the cells cultured on cover slides were fixed, and then stained with the primary antibody in the presence of 0.25% saponin. Then PBS will be used to wash away the unbound primary antibodies after 1h incubation at room temperature, followed by stained with the fluorescent secondary antibodies. Then the slides were examined under the Zeiss Axioplan 2 epifluorescence microscope.

III.6 HPLC-scintillation analysis

First, the transfected cells were washed by PBS for three times then resuspended in PBS. Then [^{14}C]-AA was added to the cells with 3 μM of the final concentration. PBS was used to balance the final volume to 100 μL. 5 minutes later, the addition of buffer A (50 μL of 0.1% acetic acid containing 35% acetonitrile) terminated the reaction. Then the sample was centrifuged at 12,000 rpm for 5 min. The mixture was separated by the C18 column (4.5 × 250 mm) and buffer A with a gradient of 35-100% of acetonitrile for 45min at a 1.0mL/min flow rate. The metabolism of [^{14}C]-AA was monitored by the liquid scintillation analyzer (Packard 150TR) connected to the HPLC.

III.7 Platelet aggregation assay

500μL of human PRP, from Gulf Coat Blood Bank (Houston, TX) was incubated with 30 μL cells for 2 minutes. Platelet aggregation was induced by the addition of 10uL of AA with a final 3μM concentration to the PRP mixture. Aggregometer (CHRONO-LOG, PA) monitored the aggregative activities of platelets at a real time mode. The readings obtained indicated the percentage of platelet aggregation. In the dilution assay, the PRP was diluted by PPP for 5 times. PPP was the obtained supernatant after 20 minutes of centrifugation of PRP at 2400 G for 20 minutes.

III.8 Mouse tail-cut bleeding assay

A 0.5cm-length of mouse tail was cut by a sharp blade to cause arterial bleeding. The bleeding tail was immediately treated by the hybrid enzyme for 30 seconds. Then the bleeding tail was blotted on a filter paper with a 10 seconds interval or placed in the PBS solution. The end point is the blood dot unable to be detected or the disappearance of the blood in the solution. The total bleeding time for the blotting method was calculated as the following formula:

$$\text{Bleeding time (s)} = \text{number of dots} \times 10$$

III.9 Expression of the hybrid enzyme in *S. cerevisiae* protein expression system.

The pYES2 vector containing the sequence of the hybrid enzyme was transformed into the competent INVSc1 yeast cells. Then the cells were selected on the SC-U selective platelets for 4 days. One single colony was picked up and scaled up in 15mL SC-U medium containing 2% raffinose at 30^{o}C with shaking overnight. Next morning, the cells were pelleted at 1500G for 5 minutes at 4^{o}C. The cell pellet was resuspended in 1mL induction medium, which was the SC-U medium containing 2% galactose. Then the mixture was inoculated into 50mL induction medium, grown with shaking at 30^{o}C for 8 hours. The cells were harvested by centrifugation at 1500 G for 5 minutes, at 4^{o}C. The cell pellet was washed by 500µL sterile water and pelleted again in a microcentrifuge at the top speed for 30 seconds.

III.10 Western blot

The steps of western blot were performed were followed by the protocol provided on Abcam (Cambridge, MA) website. First the cells were washed with cold PBS, then scratched and harvested into a 1.5mL Eppendorf tube. The cells were centrifuged at 2000rcf for 3min and the supernatant was discarded. 200µL lysis buffer (1 x RIPA buffer, 1mM PMSF, 1 x Protease inhibitor) was added mixed well with the cell pellet. Then the cell lysates were incubated on ice for 30min with vortexing on and off. The cell lysates were then centrifuged at 16, 000rcf for

20min at 4ºC. The supernatant was obtained and transferred into a new tube. 10µl of lysate was used to perform a protein assay (Pierce 660nm Protein Assay, Thermo Scientific). 30µg protein was subjected to electrophoresis with lab-made gradient SDS-PAGE gel (4% stacking gel and 10% separation gel). Then the samples on the gel were transferred onto PVDF membrane (Bio Rad). COX-1, Gαs or Gαq antibody was diluted at 1:300 in 1% bio-grade milk. β-actin and secondary antibodies were from ThermoFisher Scientific, and the dilution ratio is 1:2500 in 1% bio-grade milk.

III.11 Subcloning the cDNAs of the protein complexes into pcDNA3.1(+) vector

The sequence of Gα subunit covalently linked to the GPCR, TP, was generated by PCR. And the procedures of subcloning were provided by the vector company (Invitrogen), and described previously [102-105]. Then the resulting cDNA was successfully subcloned into the pcDNA 3.1 vectors through PCR, at EcoRI and XhoI sites containing a cytomegalovirus (CMV) early promoter. The correct size of the cDNA sequences was confirmed by both DNA sequencing and restriction enzyme digestion analyses.

III.12 Ligand binding assay

The procedures were described previously [106]. Briefly, 800ug cell pellet was incubated with 3 nM [3H]SQ29,548 (30,000 cpm, 30 Ci/mol, PerkinElmer Life

Sciences) in 25 mM Tris-HCl buffer, pH 7.4, containing 5 mM CaCl2. This 0.1 ml reaction volume was kept at room temperature for one hour with vigorous shaking, and then this reaction was terminated by adding 1ml ice-cold washing buffer, which was 25 mM Tris-HCl, pH 7.4. Whatman GF/C glass filter (Whatman, Clifton, NJ, ice-cold washing buffer presoaked) was used to filter the unbound ligand under vacuum. The radioactivity of the TP-bound [3H]SQ29,548 was counted in 4 ml of scintillation mixture using a Beckman counter (Fullerton, CA).

III.13 Live cell calcium signaling assay

This method has been described in our previous studies [107]. Briefly, Fluo-8 AM dye (excitation 490nm, emission 525nm) was used as an indicator in this live cell calcium signaling assay. The cells were cultured in 12-well glass bottom plates, and incubated with loading buffer (Fluo-8 dissolved in Modified Hank's buffered salt solution (HBSS, without calcium and magnesium) containing 10mM HEPES, pH 7.6, and 0.1% bovine serum albumin (HBSSHB buffer))for 20 min. Then the cells were washed three times with the washing buffer (2.5mM Probenecid acid and 0.1% Pluronic F-68 in HBSSHB buffer) for perturbation, and incubated for another 10 min. Afterwards, calcium signaling mediated by TP was conducted through adding IBOP (TP agonist). The signaling was monitored by Nikon Ti-S eclipse microscope system (40x objective). Three trails were performed for each assay.

III.14 Determination of SC-TP-Gαs signaling using cAMP assay

Based on the manufacture instructions, cAMP assay was conducted to analyze the signaling transduction capacity of Gs-coupling TP receptor. The stable cell lines were seeded in 96-well plates with DMEM and 10% FBS and kept at 37 ^{o}C, 5% CO_2 and humidified atmosphere overnight. Next day, the cells were incubated with 0.01, 0.1, 1, 10, 100, 1000, 3000 nM IBOP (TP agonist) at 37^{o}C in culture medium for 10 min, then the culture medium was removed and the cells were lysed. Afterwards, the amount of intracellular cAMP produced by IBOP stimulation was quantified in the 96-well microplates by enzyme immunoassay (EIA) through a cAMP Biotrak system. A set of three trials were conducted. The cAMP in Gαs-knockout HEK cells expressing wild type TP or SC-TP-Gαq as controls were compared with that of the SC-TP-Gαs stimulated by IBOP.

III.15 Flow cytometry analysis

The PRP or PLP was incubated with the FITC-conjugated CD41a antibody or APC-conjugated CD42b antibody for 10 minutes at a dilution ration 1:10. Then the stained sampled were mixed gently and AA was added to induce aggregation at a final concentration of 3μM. 10 minutes later, the sample was injected into the flow cytometry machine for analysis.

IV. RESULTS

IV.1 Molecular modeling of human TXAS and the modeling of coordination between the upstream COX-1 and the downstream prostanoid synthases, including TXAS, mPGES-1 and PGIS on the bleeding site.

To perform a molecular modeling for the purpose of a structure-based hybrid enzyme complex, one key step is to analyze the 3D crystal structure of the enzymes. Until now, the 3D structures of COX-1, mPGES-1 and PGIS have been discovered. However, the crystal structure of TXAS has not been resolved yet. In this research, we utilized the homology modeling approach to create a 3D structure model for human TXAS by using the 3D crystal structure of human PGIS as a template (Figure 4). The structure of PGIS has the highest identity and similarity with human TXAS. It shall also be indicated that a curved line was used to represent the N terminus of TXAS in the structural modeling, due to the lack of the crystal structure for the N-terminal domain of human PGIS. Based on the previous crystallographic studies of detergent-solubilized COXs, it has been indicated that the catalytic domain of the enzyme lies on the luminal side of ER. Besides, the catalytic domain is anchored toward the ER membrane by the hydrophobic side chains of the amphipathic helices A-D, and the entrance channel for the substrate, AA, is also formed by these hydrophobic domains [108-110] (Figure 4). On the other hand, based on the results of our topological and structural studies that

performed by the homology modeling and immunostaining, it has been suggested that TXAS is anchored to the cytoplasmic side of the ER membrane toward COXs [111-114] (Figure 4). Thus, COX-1 and TXAS locate at the different sides of ER, and it is also known that the C-terminus of COX-1 is toward the N-terminus of TXAS on the ER. When bleeding occurs, the released AA will be metabolized into PGH_2 by COX-1 and further isomerized into the anti-bleeding prostanoid TXA_2 by TXAS, on ER cytosolic side in vascular cells and platelets (Figure 3, red circle). But the intermediate PGH_2 could also be isomerized into other prostanoids in these vascular cells, such as the bleeding contributors PGE_2 and PGI_2, by PGES and PGIS in the ER environment, respectively (Figure 3, blue rectangle). Therefore, elevating the production of TXA_2, while reducing the production of the other prostanoids, PGI_2 and PGE_2, could be able to increase the anti-bleeding effects. This hypothesis has led to the consideration of engineering a novel enzyme complex, which can control the onsite AA metabolism to be in favor of TXA_2, while disfavor of PGE_2 and PGI_2.

IV.2 Design of a novel hybrid enzyme, COX-1-10aa-TXAS, performing triple-catalytic chain reactions continually to control AA metabolism toward TXA_2 specifically.

First of all, considering that the substrate channels of COX-1 and TXAS open at different sides of the ER membrane, it should be safe to hypothesize that the

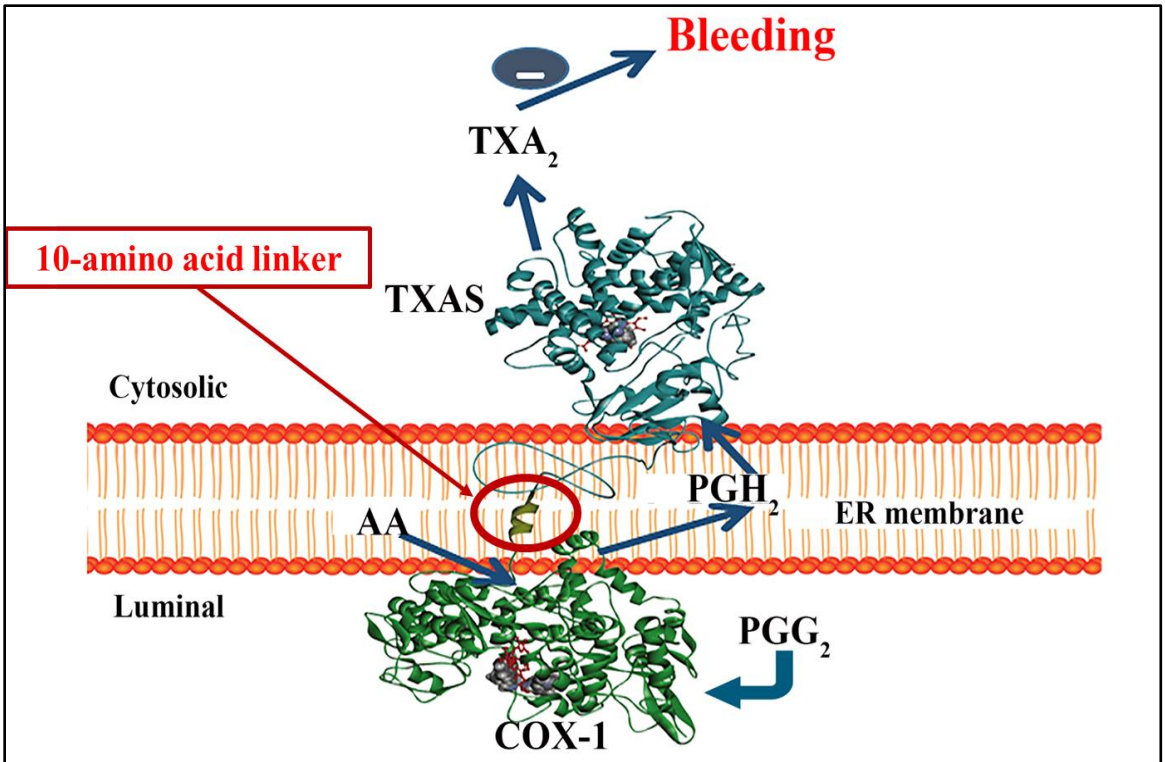

Figure 4. The design of the novel hybrid enzyme, COX-1-10aa-TXAS.

This novel hybrid enzyme was created by linking the C-terminal domain of COX-1 to the N-terminal domain of TXAS, through a 10-residue amino acid linker (-10aa). The structural model of this hybrid enzyme has the triple-catalytic chain reactions as described below: The AA can be metabolized by COX-1 into the transient intermediate PGG_2 and quickly, metabolized by COX-1 again into the PGH_2; then PGH_2 will be passed to TXAS through the 10aa linker and be isomerized into the anti-bleeding prostanoid, TXA_2.

Distance between the two channels could not be long. Then considering the spatial structures and the distribution of the substrate channels of COX-1 and TXAS, COX-1-10aa-TXAS, a novel single chain hybrid enzyme complex, was created (Figure 4). This novel hybrid enzyme holds an extension of the C-terminus of COX-1, through a 10-residue amino acid linker (His-Ala-Ile-Met-Gly-Val-Ala-Phe-Thr-Trp), which is a transmembrane helical sequence, then anchoring to the N-terminal domain of TXAS. The purpose of this design is to shorten the traveling distance for PGH_2, from COX-1 to TXAS, compared to that from COX-1 to other prostanoid synthases, such as PGES and PGIS.

IV.3 Creating the cDNA of the novel hybrid enzyme, COX-1-10aa-TXAS, by utilizing PCR approach and subcloning the cDNA clone into an expression vector

The cDNA encoding the hybrid enzyme, COX-1-10aa-TXAS, was created through the PCR and subcloning approaches. Firstly, the full cDNA of human TXAS was cut from the previously created vector, pcDNA3.1(+)-TXAS, and amplified by the PCR (Figure 5a). On the other hand, the existing cDNA vector, pcDNA3.1(+)-COX-1-10aa-PGIS was used as a template. The sequence of PGIS was cut off by restriction enzyme digestion method, and the cDNA of COX-1-10aa was kept intact. Next, the cDNA of TXAS was ligated with the cDNA of COX-1-10aa to create the new vector, pcDNA3.1(+)-COX-1-10aa-TXAS. The new vector is suitable to express the hybrid enzyme, COX-1-10aa-TXAS in the mammalian cells. The

detailed steps, including the vectors, the cutting sites, PCR, ligation were demonstrated in Figure 5. After the expression vector of COX-1-10aa-TXAS was created, the restriction enzyme digestion was performed to verify the insert of the cDNA within the cloned pcDNA3.1-COX-1-10aa-TXAS vector. In this experiment, the cDNA fragment containing the entire encoded TXAS and the linker, 10aa, was cut off. The correct insert size (1.6kb) and the correct remaining size (7.3kb) were confirmed in Figure 5b.

IV.4 Establishment of a stable mammalian cell line expressing the recombinant hybrid enzyme, COX-1-10aa-TXAS

Since cell lines are easy to obtain and culture, firstly we will express the hybrid enzyme in the immortalized human embryonic kidney cell line, HEK 293 cell line. HEK 293 cells were generated by transfecting the normal human embryonic kidney cells with the sheared adenovirus 5 DNA. HEK 293 cells indicate reliable growth and easy to transfect. Besides this, the reason we chose HEK 293 cell line is that naturally HEK cells don't express TXAS, which means naturally HEK cells don't have the biosynthesis of TXA_2. So HEK cells can provide us a null background to test the functions of the hybrid enzyme. Basically the HEK 293 cells were transfected with the cloned pcDNA3.1(+)-COX-1-10aa-TXAS vector. Forty-eight hours later, were further selected and maintained by adding G418 antibiotic into

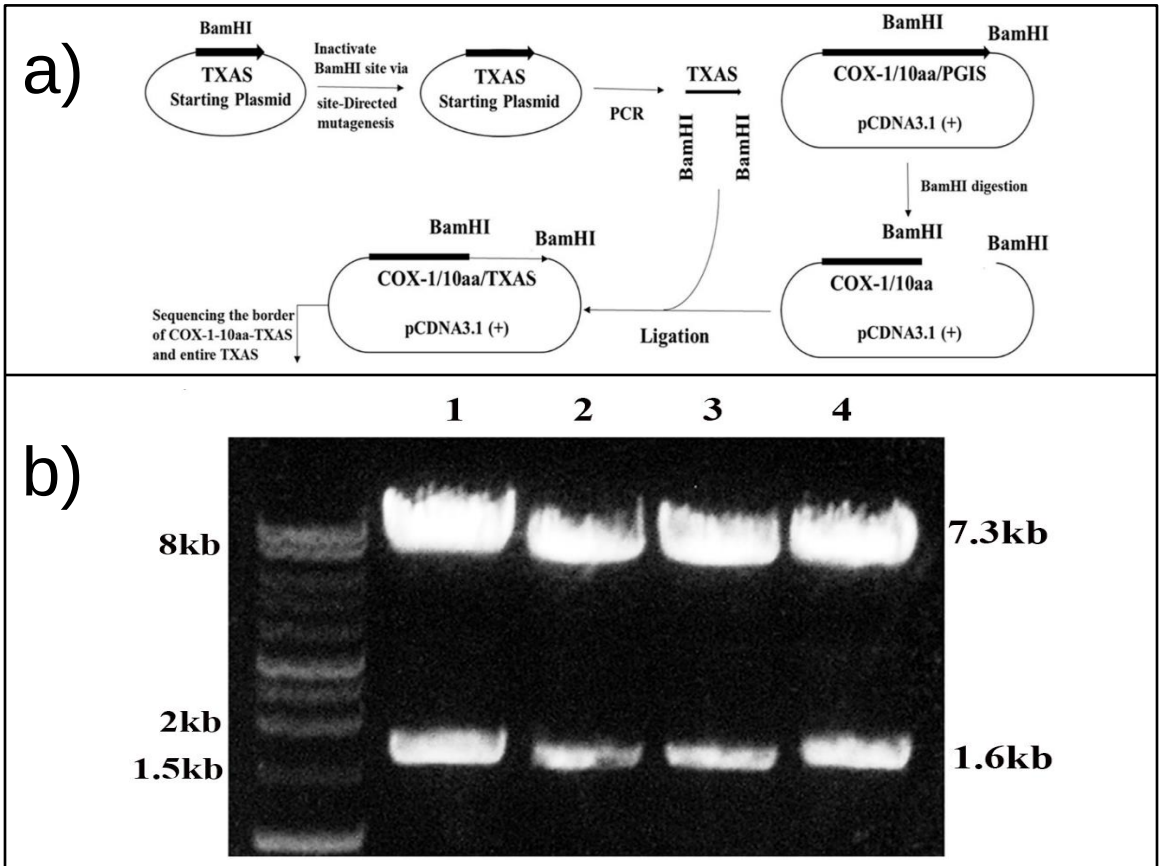

Figure 5. Subcloning of the cDNA of the hybrid enzyme into a mammalian expression vector, pcDNA3.1(+).

a) The starting plasmids of pcDNA3.1(+)-TXAS and pcDNA3.1(+)- COX-1-10aa-PGIS were prepared previously (JCMM 13). After inactivating the BamHI site of the TXAS vector through site-directed mutagenesis, the full cDNA of TXAS was obtained. On the other hand, the cDNA fragment of PGIS was cut off from the pcDNA3.1(+)- COX-1-10aa-PGIS vector. Then the cDNA fragment of TXAS was ligated and the new expression plasmid, pcDNA3.1(+)- COX-1-10aa-TXAS, was

formed. b) The restriction enzyme digestion was performed to confirm the correct insert size of the pcDNA3.1(+)-subcloned COX-1-10aa-TXAS vector. It was cut twice at BamHI recognition sites and two DNA fragments was obtained: one fragment was the pcDNA3.1(+) vector with COX-1-10aa, and the size of the vector plus COX-1-10aa should be equal to 7.3 kb (5.4kb of vector +1.9kb of COX-1-10aa); the other fragment was TXAS, and the size of TXAS cDNA should be equal to 1.6kb. Later, DNA sequencing of the inserted region of 10aa-TXAS was done to further verify the cDNA sequencing of COX-1-10aa-TXAS in the plasmid (Data not shown).

the culture medium, to obtain the cells which can stably express the hybrid enzyme. The rationale of the selection is that the cells expressing the cloned pcDNA3.1(+)-COX-1-10aa-TXAS vector can develop resistance to G418. After two months of selection, the cells were lysed and the expression of the hybrid enzyme was firstly confirmed by western blot using anti-COX-1 monoclonal antibody (Figure 6a, lane 2). The HEK293 cells transfected with the empty pcDNA3.1(+) vector were used as control (Fig.6b, lane 1).

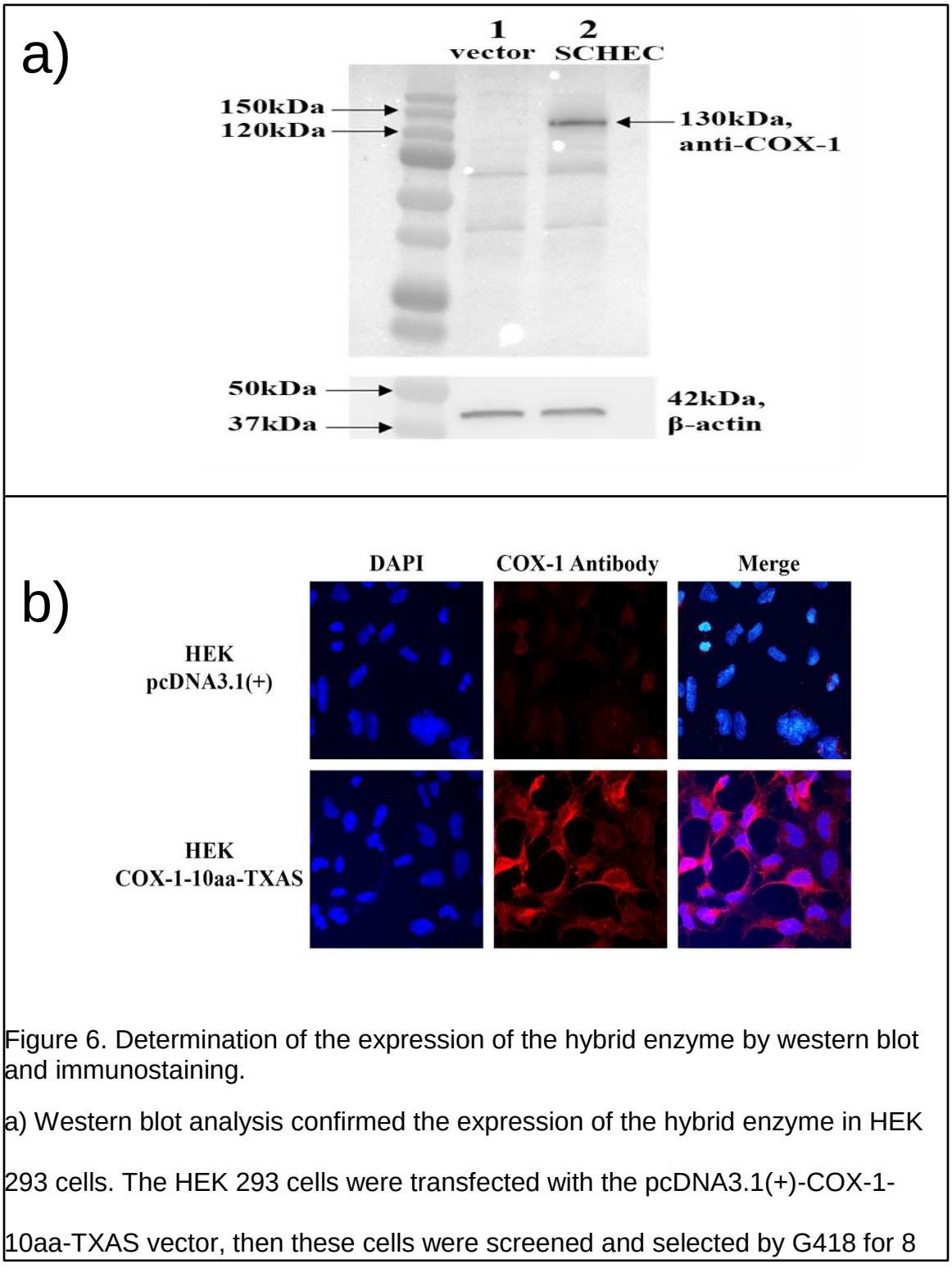

Figure 6. Determination of the expression of the hybrid enzyme by western blot and immunostaining.

a) Western blot analysis confirmed the expression of the hybrid enzyme in HEK 293 cells. The HEK 293 cells were transfected with the pcDNA3.1(+)-COX-1-10aa-TXAS vector, then these cells were screened and selected by G418 for 8

weeks. After the cells were lysed, about 20ug proteins were subjected to Western blot analysis by using 10% SDS-PAGE and COX-1 monoclonal antibody. Lane 1 was the negative control, which was the cells transfected with the empty vector. The correct size of the hybrid enzyme (~130kDa) was indicated in lane 2. b) The results of the immunostaining further confirmed the expression of the hybrid enzyme in these cells. The cells either stably expressing the hybrid enzyme (bottom) or transfected with the empty vector (negative control, top) were cultured on the cover-slides. Then the cells were permeabilized by 4% PFA, incubated with the mouse monoclonal COX-1 antibody and stained by rhodamine-labeled goat anti-mouse IgG. The slides were imaged under a confocal fluorescent microscope.

IV.5 Further identifications of the expression and subcellular localization of the hybrid enzyme in HEK 293 cells by immunostaining analysis

To further investigate the expression of the hybrid enzyme, COX-1-10aa-TXAS in HEK293 cells, the established stable cell line was analyzed by fluorescent immunocytochemistry. Furthermore, the high resolution immunostaining results (by confocal fluorescent microscope) should be able to reveal the subcellular localization of the expressed hybrid enzyme. The specific domain of COX-1-10aa-TXAS was identified by the monoclonal COX-1 antibody (Fig. 6b, bottom panel, central, red fluorescence), which confirmed the expression of the hybrid

enzyme in these cells. In contrast, no red fluorescence can be detected in the cells only transfected with the pcDNA3.1(+) vector, which indicated no endogenous COX-1 staining (Fig. 6b, top panel, central). When the staining of the cell nuclei (DAPI, blue) and COX-1 (red) was merged together, a clear ER pattern localization of the hybrid enzyme can be recognized (Fig. 6b, bottom panel, central). This data further confirmed the stable expression of the hybrid enzyme in the established stable cell line, and identified the subcellular localization of the hybrid enzyme is on the ER membrane. This ER pattern localization is accordant with our expectation, because the native COX-1 and TXAS are localized on the different sides of ER membrane. These results indicated the similar protein folding, posttranslational modification, and ER topological arrangement of the hybrid enzyme with the wild type COX-1 and TXAS in the mammalian cells. Meanwhile, the data also indicated that the engineered hybrid enzyme, COX-1-10aa-TXAS, could also be as stable as the wild types of the individual enzymes in biological activities.

IV.6 Identification of the triple-catalytic properties of the hybrid enzyme by using the reliable HPLC-scintillation analysis method

As we mentioned before, based on our expectation, this novel hybrid enzyme should be able to directly convert the substrate AA into the anti-bleeding

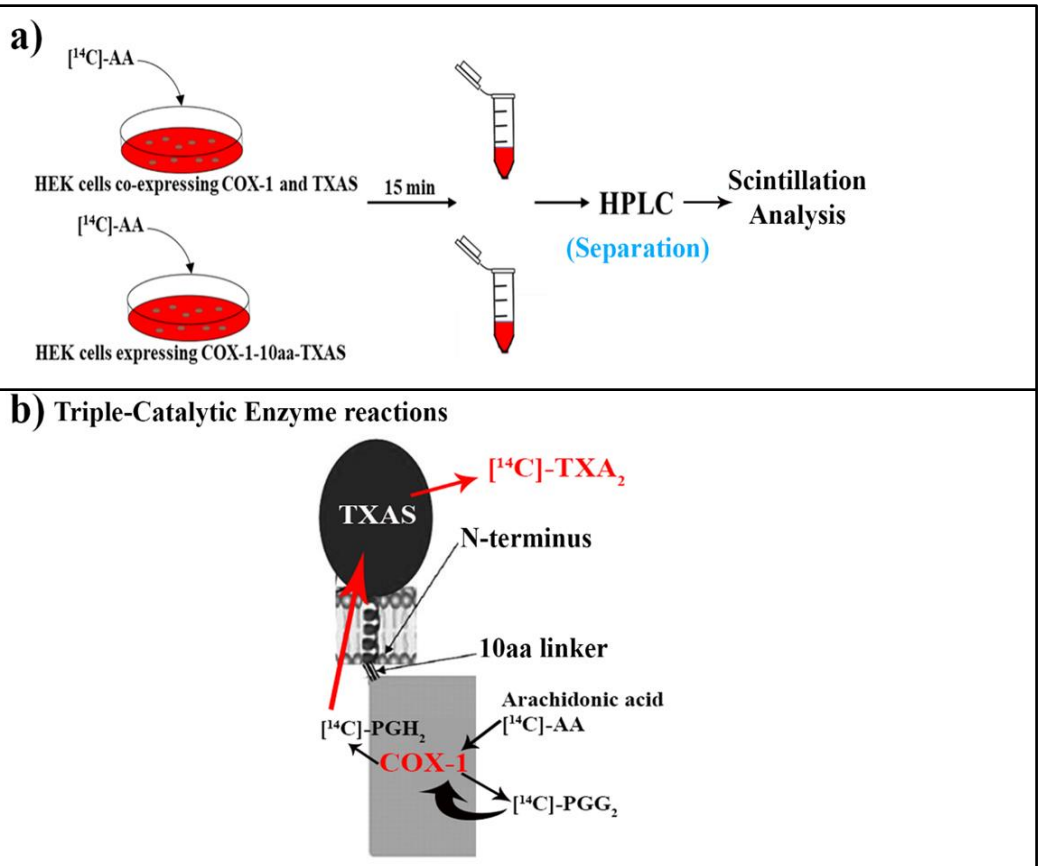

Figure 7. Schematic presentation for demonstration of the triple-catalytic chain reactions of the expressed hybrid enzyme, COX-1-10aa-TXAS, by using the highly sensitive and reliable HPLC-scintillation analysis method.

a) In this assay, the specific isotope-labeled exogenous AA, [^{14}C]-AA was used as the substrate. 3 µM of [^{14}C]-AA was added to the cells and incubated for 15 minutes. Then the metabolites of [^{14}C]-AA were extracted out by buffer A (35% acetonitrile in 0.1% acetic acid). Next the metabolized compounds were subjected to HPLC analyzer through C-18 column (4.5 × 250 mm), starting with

buffer A and following by a linear gradient of buffer B (100% acetonitrile) for 45 minutes. Then the eluents were directly analyzed by a Scintillation analyzer, which picked up the [^{14}C]-labeled compounds catalyzed by the hybrid enzyme. b) In this assay, [^{14}C]-AA was quickly metabolized by the hybrid enzyme into the transient intermediate, [^{14}C]-PGG_2. Then the [^{14}C]-PGG_2 was further metabolized by the hybrid enzyme into [^{14}C]-PGH_2. The [^{14}C]-PGH_2 could be metabolized by the hybrid enzyme again into the [^{14}C]-TXA_2. This is the triple-catalytic activities conducted by the hybrid enzyme.

prostanoid, TXA_2, while reduce the production of other metabolites of AA, such as the bleeding contributors, PGE_2 and PGI_2 (Figure X). To test our hypothesis, a very sensitive and reliable assay, the HPLC-scintillation analysis method was utilized to test the functions of the hybrid enzyme in the HEK 293 cells stably expressing COX-1-10aa-TXAS (Figure 7a). In this assay, through accurately monitoring the metabolism of [^{14}C]-AA by the HPLC-scintillation analyzer, it was able to profile [^{14}C]-AA to be metabolized into [^{14}C]-TXA_2, through triple catalytic activities of the hybrid enzyme (Fig. 7b). The detailed experimental steps and conditions were demonstrated in methods.

Two different stable cell lines were used in this assay. One was transfected with the cDNA of the hybrid enzyme, COX-1-10aa-TXAS; the other one was co-transfected with the cDNA vectors of individual COX-1 and TXAS (for positive

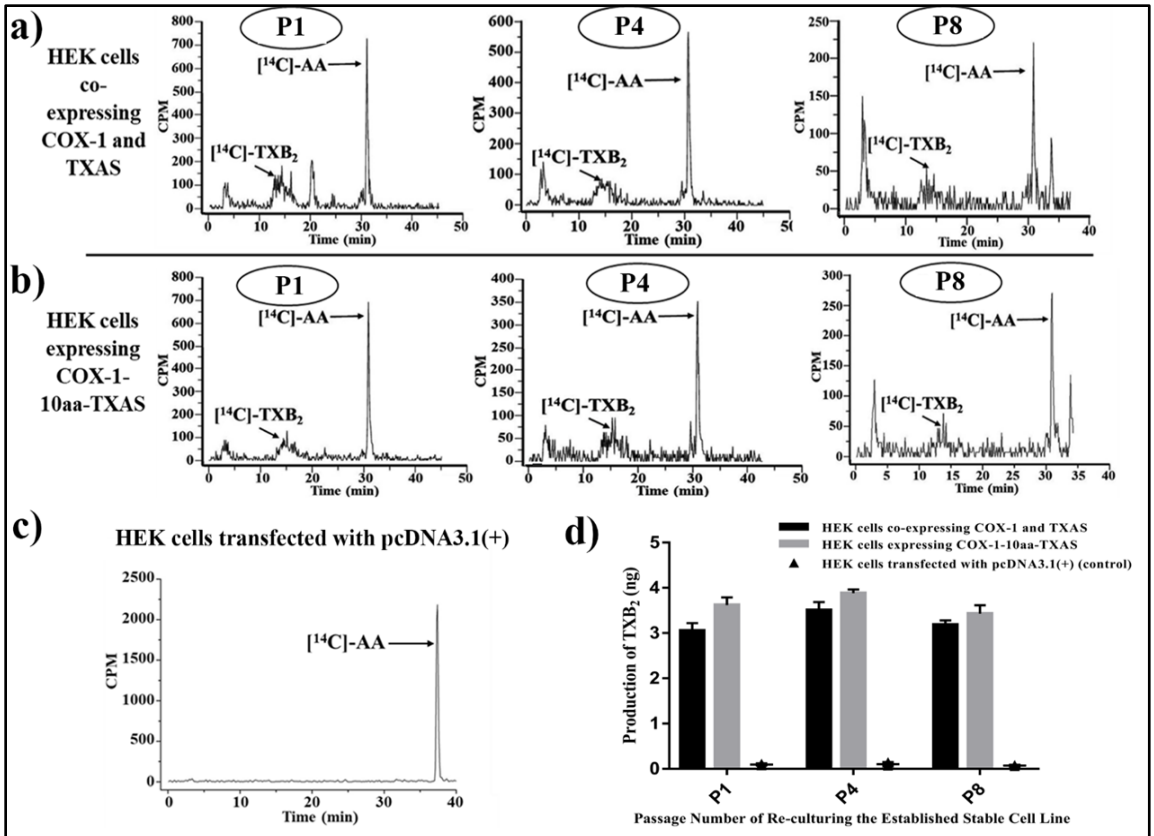

Figure 8. Determination the catalytic activities in the cells expressing the hybrid enzyme, COX-1-10aa-TXAS, and compared to that of the cells co-expressed individual COX-1 and TXAS.

HEK 293 cells were transfected with either the cDNA of the hybrid enzyme (b) or the cDNA vectors of individual enzyme, COX-1 and TXAS (a). After screened and selected by G418 for 8 weeks, the two stable cell lines were freeze in liquid nitrogen. After re-cultured the cells, the catalytic activities were tested in P1, P4 and P8 cells. Since re-culture, the cells firstly reaching 100% confluence were

marked as P1 cells; one week later, the cells with 100% confluence with three passages were marked as P4 cells; and another week with four passages were the P8 cells. The method demonstrated in Figure 7 was used to indicate the production of the [^{14}C]-compounds, enzymatically metabolized from the added [^{14}C]-AA, by the functions of the expressed hybrid enzyme (b) or the co-expressed individual COX-1 and TXAS (a). The peaks of [^{14}C]-TXB_2 and its derivatives, with the retention time of 10-20 minutes, representing the production of TXA_2, were pointed by the arrows labeled with [^{14}C]-TXB_2. The remaining [^{14}C]-AA (retention time: 30-40min) was also indicated in each assay. The cells transfected with the empty vector only were used as a negative control (c). The quantitative results of the production of [^{14}C]-TXB_2 isomerized from [^{14}C]-AA was shown in d).

control). After transfection, the cells were screened and selected by G418 for 8 weeks. The established stable cell lines were freeze in the liquid nitrogen. After re-cultured the cells, the cells firstly reaching 100% confluence were marked as P1 cells. One week later, after three passages, the cells reaching 100% confluence were marked as P4 cells, and another week with four passages were the P8 cells. A serial of tests for the enzymatic activities were accomplished for P1, P4 and P8 cells (Fig. 8). By using the assay mentioned above, the chain triple-catalytic reactions in the HEK cells expressing COX-1-10aa-TXAS were compared to that in the cells co-expressing individual COX-1 and TXAS. It has to

be addressed that [^{14}C]-TXA_2 is very unstable and could be further isomerized into multiple stable metabolites, including [^{14}C]-TXB_2 and its derivatives. So in Figure 8 a and b, there were a group of broad peaks with retention time between 10 and 20 minutes, representing [^{14}C]-TXB_2 and its derivatives. But definitely, the HPLC-Scintillation analysis is the most reliable approach to profile the metabolism of AA. Because in this assay, [^{14}C]-AA was utilized, which can be distinguished from the endogenous AA. The data of Figure 8b has suggested that the expressed hybrid enzyme, COX-1-10aa-TXAS, in HEK 293 cells was able to directly convert the [^{14}C]-AA to the final product [^{14}C]-TXB_2 and its derivatives, through the triple- catalytic chain reactions. Moreover, the catalytic functions of the hybrid enzyme were identical to that of the wild-type enzymes, COX-1 and TXAS (Figure 8c and d). In contrast, there was no [^{14}C]-TXB_2 could be detected in the HEK293 cells transfected with pcDNA3.1(+) vector only, which can exclude the interferences from the endogenous COX-1 and TXAS in the HEK293 cells. Herein, these results suggested that the hybrid enzyme, COX-1-10aa-TXAS, was able to perform the three-step reactions to metabolize AA toward the production of TXA_2.

IV.7 Investigation of the biological functions of the hybrid enzyme in platelet aggregation assay

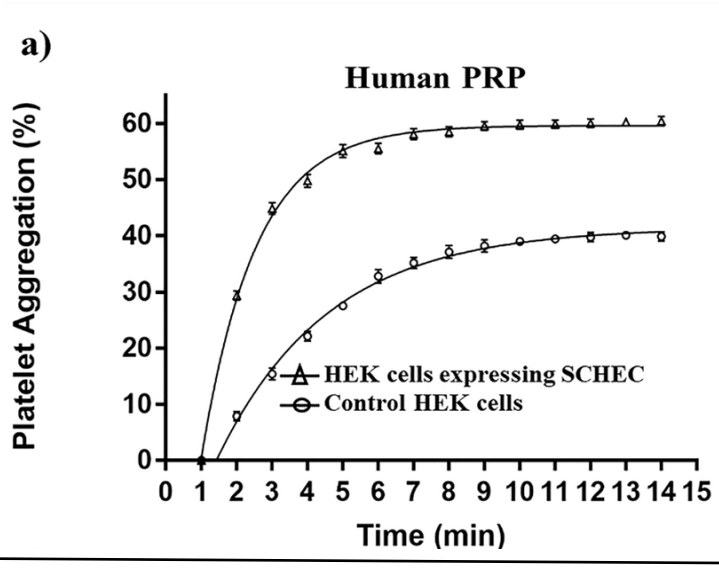

b)

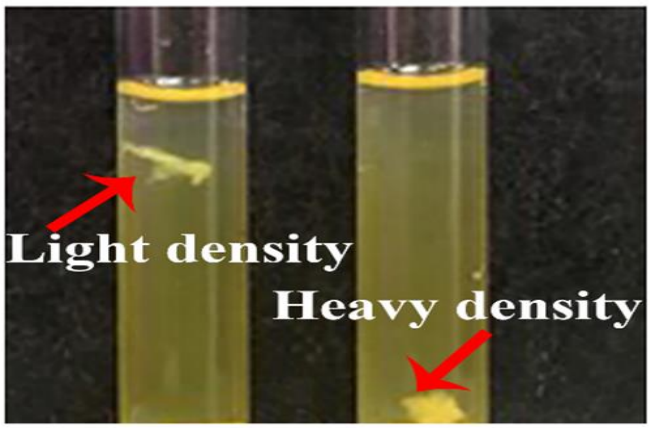

Figure 9. Determination of the biological functions of the hybrid enzyme by using normal platelet aggregation assay.

a) PRP was incubated with HEK 293 cells expressing the hybrid enzyme (open triangles) or the cells transfected with the empty vector (HEK control, open circles) for two minutes, and followed by the addition of 10 µL AA (3uM of final

concentration). The aggregative activity was monitored by the platelet aggregometer. b) The fibers were formed by the aggregated platelets. The fibers formed in the presence (right) or absence of the hybrid enzyme (left) were shown in this figure.

In Figure 9a, it was observed that the hybrid enzyme, COX-1-10aa-TXAS, could dramatically promote platelet aggregation. Compared to the control group, the percentage of maximal aggregation was increased from 38% to 60%. In addition, the ½ time for the maximal aggregation was decreased from 3.2 to 1.8 minutes by the expressed hybrid enzyme. This result was also supported by the data in Figure 9b. The fibers in Figure 9b were formed by the aggregated platelets. The fiber with the presence of the hybrid enzyme exhibited a much heavier and solid form (Figure 9b, right) than that of the control (Figure 9b, left).

IV.8 Determination of the biological activities of the hybrid enzyme to rescue the aggregative functions of NSAIDs-treated platelets

One major side effect of administration of aspirin, or other NSAIDs, is to cause bleeding. To investigate if the novel hybrid enzyme can rescue the NSAIDs-resulted platelet dysfunction, the human PRP was pretreated with aspirin for 20 minutes, then centrifuged to remove the excessive aspirin. The pelleted platelets were dispensed by PPP. The restoration of the platelet aggregation activities was compared between two groups: one was incubated with the cells expressing the

hybrid enzyme and the other one with control cells. It was observed that through the aspirin treatment, the aggregative activities of platelets were almost completely inhibited (Fig. 10, triangles). But with the help of the hybrid enzyme, the platelets recovered almost full aggregative functions (Fig. 10, circles).

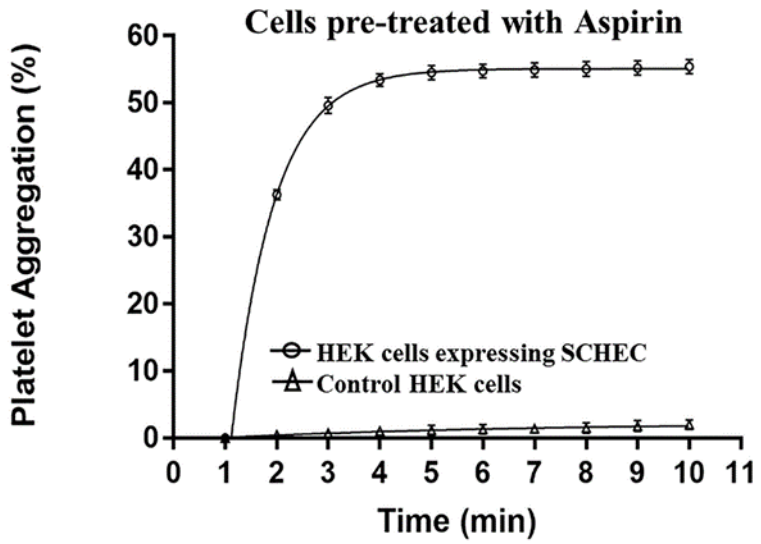

Figure 10. Determination of the biological activities of the hybrid enzyme in platelet aggregation by pretreatment of aspirin.

First, the human PRP was pre-treated with 10mM aspirin for 20min, then the excessive aspirin was removed by centrifugation. Next the human PRP was dispensed by PPP, and incubated with either the cells expressing the hybrid enzyme (open circles) or control cells (open triangles) for 2 minutes. Then 10 µL AA (3uM of final concentration) was added and the aggregative activity was monitored by the platelet aggregometer.

IV.9 Further characterization of the biological functions of the hybrid enzyme using platelet aggregation assay in the mimicked platelet-deficient situations.

Many diseases or even clinical treatments, such as chemotherapies, may cause the deficiency of platelets in patients. Life-threatening bleeding may possibly occur in these patients due to their damaged hemostatic functions. To mimic the platelet-deficient situations, the normal human PRP was diluted by PPP to generate a concentration of the platelets being only 20% of the normal level. The diluted PRP was incubated with the cells expressing the hybrid enzyme or the control cells for two minutes, followed by the addition of 3uM (final concentration) AA. The results suggested that the hybrid enzyme could effectively promote the platelet aggregation under platelet-deficient situations (Fig. 11a). Thus, this hybrid enzyme, COX-1-10aa-TXAS, has great potential to be developed into a novel type of bio-enzymatic treatment for the platelet-deficient resulted bleeding disorders.

IV.10 Investigating the functions of the hybrid enzyme to restore the aggregative activities of the expired PRP

Generally, the functions of PRP can only last for less than two weeks under 4^{o}C storage. To determine the potential application of the hybrid enzyme in extending the storage period of PRP, the PRP were stored for 45 days before performing the tests, which means these PRP has passed the expiration date for more than

one month. Based on the results of the aggregation assay, it was observed that the responses of the expired platelets upon AA stimulation were very weak (Figure.11b, triangles). But the expressed hybrid enzyme can dramatically restored the aggregative activities (Figure. 11b, circles). This result indicated that

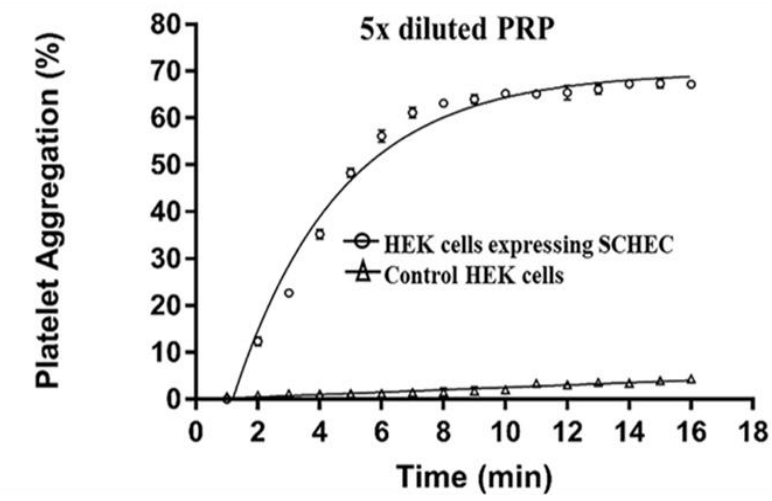

Figure 11. Determination of the biological activities of the hybrid enzyme in platelet aggregation by using diluted or expired PRP.

a) To mimic the pathological situations in some platelet-deficient diseases, the human PRP was diluted by PPP (ration 1:4, 5 X). The aggregation activities were monitored in the presence (open circles) or absence (open triangles) of the hybrid enzyme after the addition of AA (3uM of final concentration). b) PRP was stored at 4^{o} C for 45 days, which exceeded the expiration date. The long-term storage resulted in the loss of the majority of platelet aggregation activities. Then the expired PRP was incubated with the cells with (open circles) or without (open triangles) expressing the hybrid enzyme, and followed by the addition of AA to the 3uM of final concentration. The restoration of the aggregative activities was monitored as described above.

the hybrid enzyme might be developed to be used to extend the reasonable storage period for functional PRP.

IV. 11 Determination of the anti-bleeding effect of the hybrid enzyme *in vivo* mouse bleeding model.

The tail-cut bleeding mouse model was used to test the anti-bleeding functions of the hybrid enzyme *in vivo*. The mice were divided into two groups: the first group was treated with the HEK cells expressing the hybrid enzyme, and the second group was treated with the control cells. Basically, 0.5 cm of tail was cut off by a sharp blade, which can cause the arterial bleeding, then the bleeding tail was treated differently as described above. The average arterial bleeding time for the

control group was approximately 13.2 minutes (Figure.12c, left). But with the treatment of the hybrid enzyme, the average arterial bleeding time was decreased significantly to approximately 3.1 minutes (Figure. 12c, right). This

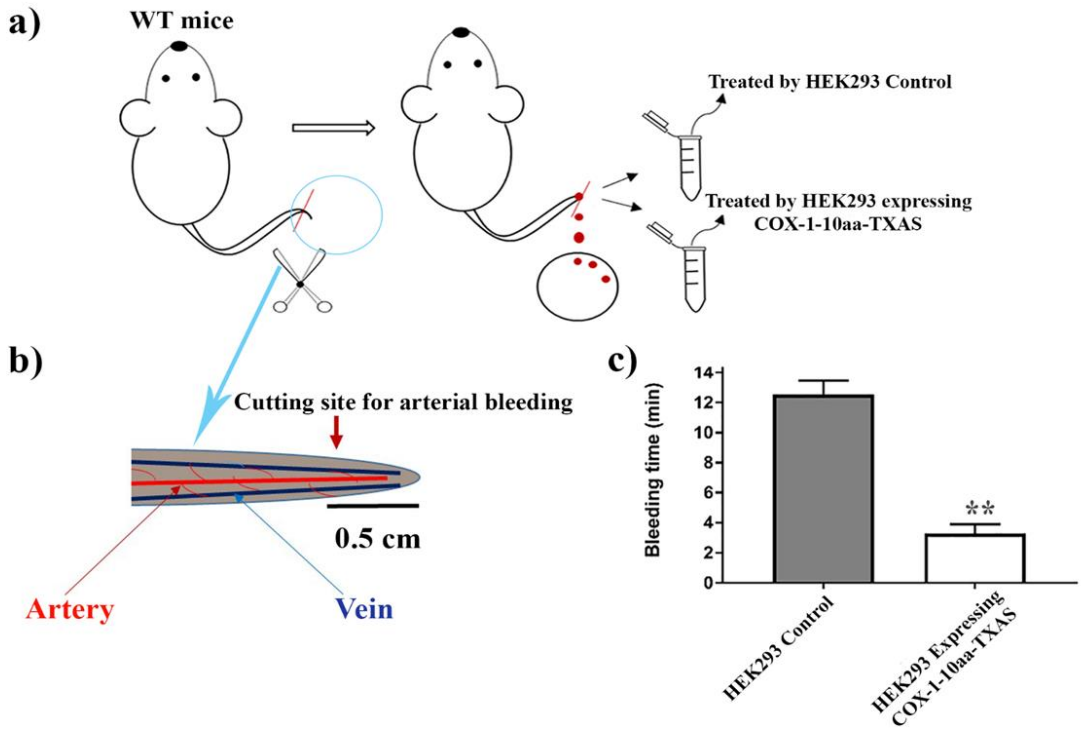

Figure 12. Examination of the anti-bleeding functions of the hybrid enzyme by using mouse tail-cut bleeding model.

a) 0.5-cm of tail was cut by the blade to cause arterial bleeding. Then the bleeding tail was dipped into the tubes containing either the cells expressing the hybrid enzyme or the control cells. Next the blood was blotted on the paper every ten seconds until no blood dots can be recognized. b) The distribution of artery

and vein in mouse tail was displayed here. c) The bleeding time for the control group is around 13.2 minutes. By the treatment of the hybrid enzyme, the bleeding time was decreased to around 3.1 minutes.

result provided strong proof that this novel hybrid enzyme could efficiently stop arterial bleeding *in vivo*.

IV. 12 Further determination of the anti-arterial bleeding functions of the hybrid enzyme by using a transgenic mouse model with a bleeding tendency.

Recently, our lab successfully created a transgenic mouse model by overexpressing another hybrid enzyme we mentioned above, COX-1-10aa-PGIS *in vivo* [115]. On these transgenic mice, the overexpressed COX-1-10aa-PGIS could redirect the metabolism of AA toward the production of the bleeding contributor, PGI_2, which can prevent platelet aggregation and induce vasodilation. The purpose of creating this transgenic mouse model is to prove that the hybrid enzyme, COX-1-10aa-PGIS, is able to be against thrombotic stroke and ischemia *in vivo*. The detailed steps for creating and characterization of this transgenic mouse model has been addressed previously [115]. Briefly, a single chain cDNA of the hybrid enzyme, COX-1-10aa-PGIS, was prepared, and injected into the mouse embryo to create the transgenic mice (Fig. 13a). Considering the functions of the hybrid enzyme, COX-1-10aa-PGIS, to redirect the metabolism of AA toward the production of PGI_2, and furthermore, to

dramatically decrease the production of TXA_2, we hypothesized these transgenic mice should indicate bleeding tendency with extended bleeding time. The similar

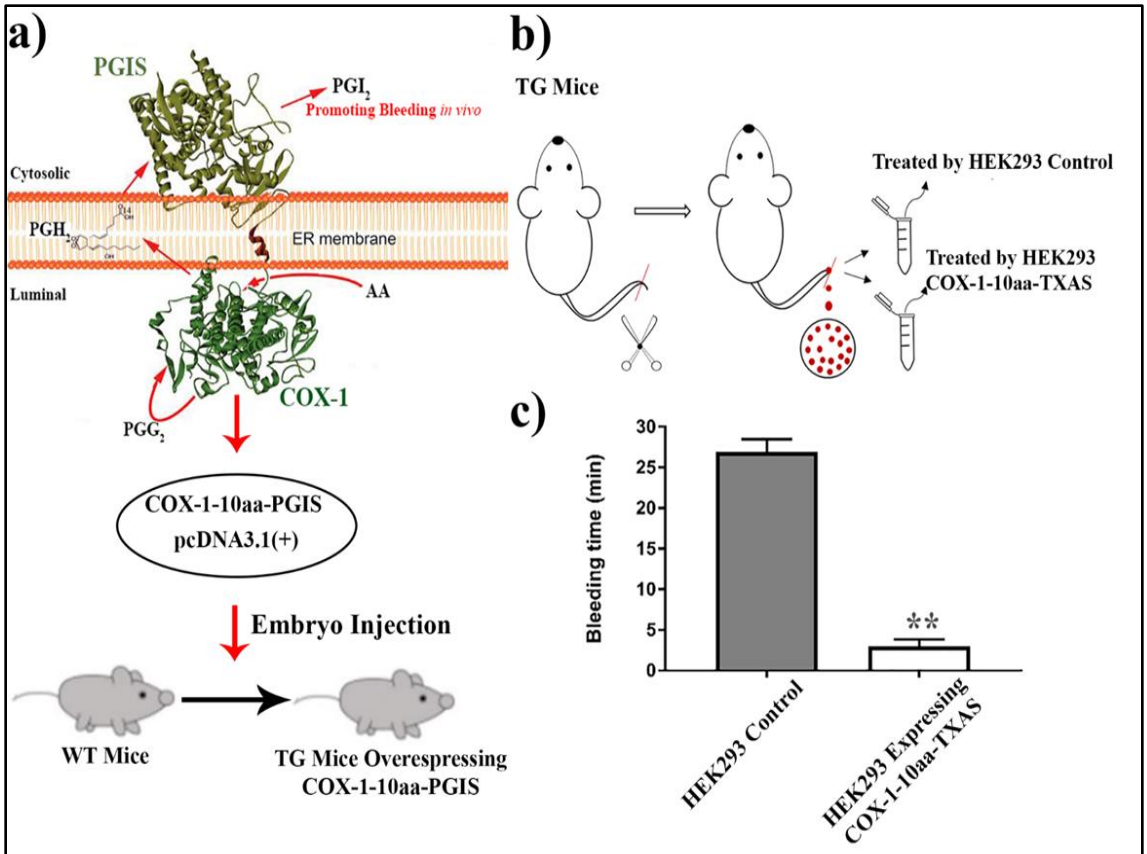

Figure 13. Further identification the anti-bleeding functions of the hybrid enzyme in mouse tail-cut bleeding assay by using a transgenic mouse model with bleeding tendency.

a) The transgenic mouse model was created by injecting the linear cDNA of COX-1-10aa-PGIS into the embryos of the mice (JCMM 13). Then COX-1-10aa-PGIS was overexpressed in the established transgenic mouse model. b) The

same tail-cut bleeding assay was performed on these transgenic mice. These mice were also divided into two groups: one group was treated with the hybrid enzyme and the other one was treated with the control cells. c) In the control group, the bleeding time of the transgenic mice was about 26.5 minutes, which was almost doubled compare to that of the wild type mice. By treating with the hybrid enzyme, the bleeding time was reduced dramatically to around 2.8 minutes. The difference is very significant.

tail-cut bleeding assay was performed on these transgenic mice, and found the arterial bleeding time was extended about two-fold in the transgenic mice (an average of 26.5 minutes, Figure. 13c, left), compared to that of the wild type mice (an average of 13.1 minutes, Fig. 12c, left). By treating with the hybrid enzyme, COX-1-10aa-TXAS, the bleeding time was decreased to around 2.8 minutes (Fig. 12c, right), which was highly significant. Therefore, the results suggested that the hybrid enzyme, COX-1-10aa-TXAS, has the ability to overcome the TXA_2-deficiencient bleeding tendency. Moreover, this hybrid enzyme is able to rebalance the ratio of PGI_2 and TXA_2 to stop bleeding *in vivo*.

IV.13 Investigation of the application of the hybrid enzyme in hemostasis by utilizing *S. cerevisiae* yeast protein expression system

The *S. cerevisiae* yeast cells were known as a ‘cell factory’, and the *S. cerevisiae* yeast protein expression system is widely used for the production of industrial

enzymes and pharmaceutical proteins. Thus, we wanted to utilize the *S. cerevisiae* yeast protein expression system to produce the hybrid enzyme for the purpose of application. The cDNA sequence of the hybrid enzyme, COX-1-10aa-TXAS, was successfully subcloned into the pYES2 vector, which is a vector for inducible expression of recombinant proteins in *S. cerevisiae* yeast cells. Then the pYES2-COX-1-10aa-TXAS vector was transformed into the competent INVSc1 yeast cells, and the transformants were grown on the selective plates. Four days later, the single colonies were observed on the selective platelets (Figure.14a). Next step we did a screening for six colonies to pick up one colony with higher expression level of the hybrid enzyme. The expression of the hybrid enzyme in these colonies was induced through the addition of galactose. After 5 hours of induction, the yeast cells were lysed and performed western blot. The result suggested that the colony #3 has a relative higher expression level than the other five colonies (Figure.14b). To optimize the conditions of induction to maximize the production of the hybrid enzyme, one time-course experiment was done to select the best induction duration. It was suggested after 8 hours' induction, the expression of the hybrid enzyme reached the highest level (Figure.14c).

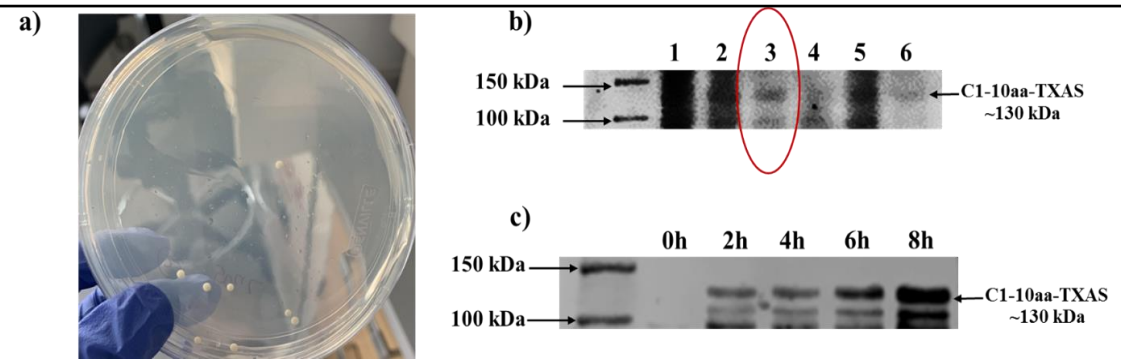

Figure 14. Optimization of the conditions of induction to maximize the production of the hybrid enzyme.

a) The cDNA sequence of the hybrid enzyme was subcloned into the pYES2 vector by following the manual from the vector company (Invitrogen). Then the pYES2-COX-1-10aa-TXAS was transformed into the competent INVSc1 yeast cells, and the transformants were grown on the SC-U selective plates for four days. The single colonies were shown on the selective plates. b) A screening test was performed for 6 colonies. By growing in the induction medium for 5 hours, the yeast cells were lysed and analyzed by western blot. Compared to other colonies, the colony #3 showed a relative higher expression of the hybrid enzyme. c) A time-course experiment was done to test the expression of the hybrid enzyme at different time point. It was suggested that 8h induction could maximize the production of the hybrid enzyme.

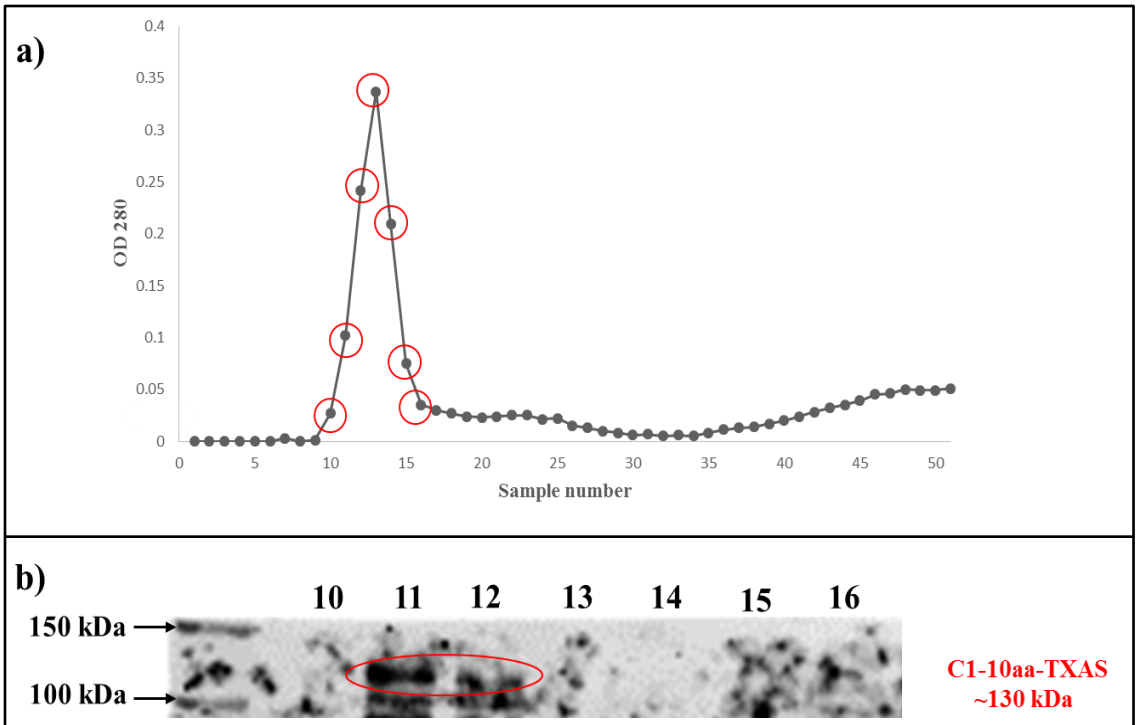

Figure 15. The purification of the hybrid enzyme sample.

a) The lysed protein sample was first purified and concentrated by ultracentrifugation. Then Sephadex G75 protein fractionation was performed to further purify the concentrated protein sample. By testing the OD 280, the presence of protein was suggested in sample #10 to #16. b) Western blot was done for the sample #10 to #16, and the expression of the hybrid enzyme was found in sample #11 and #12.

After the conditions of induction was confirmed, a large scale expression of the hybrid enzyme was induced. Then the yeast cells were pelleted and lysed by the glass beads and beads beater. The protein sample was first purified and

concentrated by ultracentrifugation. Then the concentrated protein sample was further purified by Sephadex G75 protein fractionation. In protein fractionation, each collection tube collected 1ml of protein samples. 50 samples were collected in total. Then OD 280 was tested for these samples. The samples #10 to #15 indicated a peak in OD 280 (Figure. 15a), which indicated the presence of protein in these samples. Next the western blot analysis was performed for the samples #10 to #15, and the expression of the hybrid enzyme was found in sample #11 and #12 (Figure. 15b).

IV.14 Determination of the anti-bleeding functions of the purified hybrid enzyme in mouse tail-cut bleeding model

After the expression of the hybrid enzyme was detected in sample #11 and #12, the two samples were mixed together, concentrated and purified again by ultracentrifugation. Then the anti-bleeding functions of the purified hybrid enzyme was tested in mouse tail cut bleeding model. This time, after cutting the tail to cause the arterial bleeding, on drop of the hybrid enzyme sample was applied on the bleeding tail and left for 1 minute. Then the bleeding tail was placed in the PBS solution, and the end point of the bleeding could be easily identified by the disappearance of blood (Figure. 16a). The treatment of the hybrid enzyme can reduce the bleeding time from 12 minutes to 2.3 minutes (Figure. 16b). The anti-bleeding functions of the hybrid enzyme was very significant.

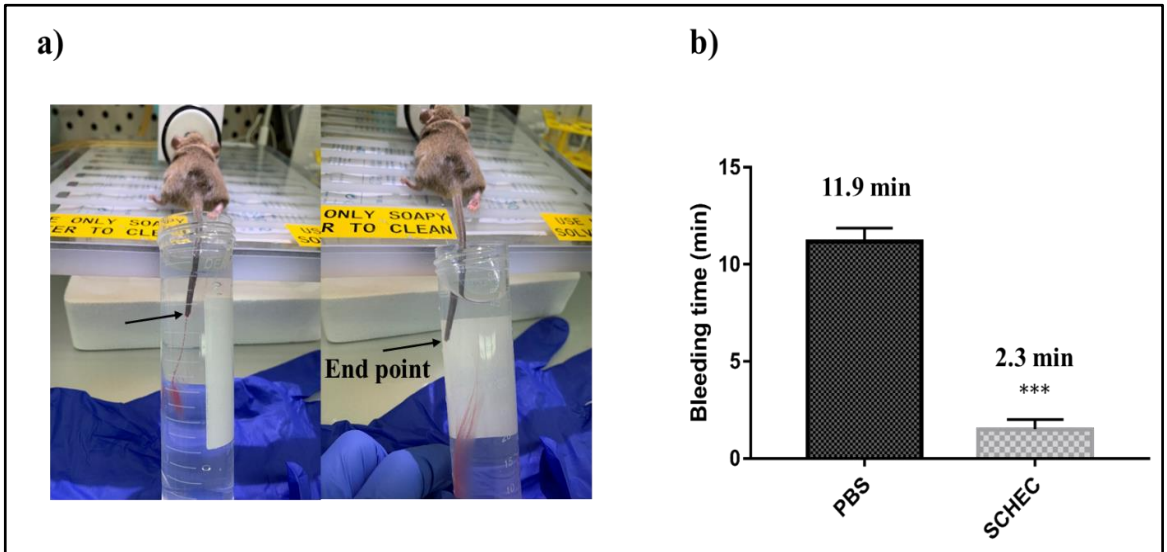

Figure 16. The determination of anti-bleeding functions of the hybrid enzyme in mouse tail-cut bleeding assay.

a) A 0.5-cm length of tail was cut to cause arterial bleeding on these mice. Then the mice were divided into two groups. One group was treated with one drop of PBS, and another was treated with one drop of the hybrid enzyme. The treatment was last for 1 minute. Then the bleeding tail was placed in the PBS solution, and the end point could be clearly observed. b) By treatment of the hybrid enzyme, the bleeding time was decrease dramatically, from 12 minutes to 2.3 minutes.

IV.15 Design and cloning of a functional single-chain GPCR-G protein complex, SC-TP-Gαq complex, to mimic endogenous calcium signaling activity conducted by native TP selectively coupling to Gαq

The SC-TP-Gαq complex was designed based on our previous studies, which characterized the structural and functional interactions of TP and Gαq [116-119]. In designing of an active fusion protein to mimic the three-dimensional configuration of TP and Gαq, firstly we started to look into the details of the structural and functional information for the prostanoid receptors, TP and IP, which are the receptors of TXA_2 and PGI_2, individually. Based on the structural conformations of TP in solution with Gαq subunit and prostacyclin receptor (IP) with Gαs subunit, which were described previously [116-117], it was predicted that the flexible C-terminus of TP could be constrained and liked to the flexible N-terminus of the Gαq or Gαs to form a single chain GPCR-Gα complex, which should not alter the GPCR and Gα folding and membrane anchoring. By utilizing the natural coupling of TP to Gαq as a model, firstly, a recombinant cDNA (Figure. 17a) encoding the single-chain human TP linked to Gαq (SC-TP-Gαq, Figure.17b) was created and then subcloned into pcDNA3.1 (+) vector (Figure. 18). The Ecor1 and Xho1 sites used to link the cDNAs of human TP and Gαq together to form a single-chain cDNA of SC-TP-Gαq were indicated in the Figure. 14a, and Figure. 15. Because the crystal structure of TP has not been resolved yet, a structural modeling for TP, which was established by our previous research

Figure 17. The design of the single-chain GPCR-Gαq complex, SC-TP-Gαq. (a) The full-length cDNA sequence of SC-TP-Gαq. The underlined sequence were the recognition sites for the restriction enzymes. (b) Schematic presentation of the novel single-chain GPCR-Gα complex, SC-TP-Gαq. In this novel protein-protein complex, the C-terminus of TP is covalently linked to the N-terminus of Gαq, to mimic the natural coupling between TP and Gαq when TP is stimulated by a receptor agonist and starts the signaling transduction.

[120-123], was used in this study. Thus, the model of the 3D conformation of the single-chain TP-Gαq protein complex was visualized by the protein modeling approach, in which the human TP model and the crystal structure of Gαq [124] were utilized(Figure 15).

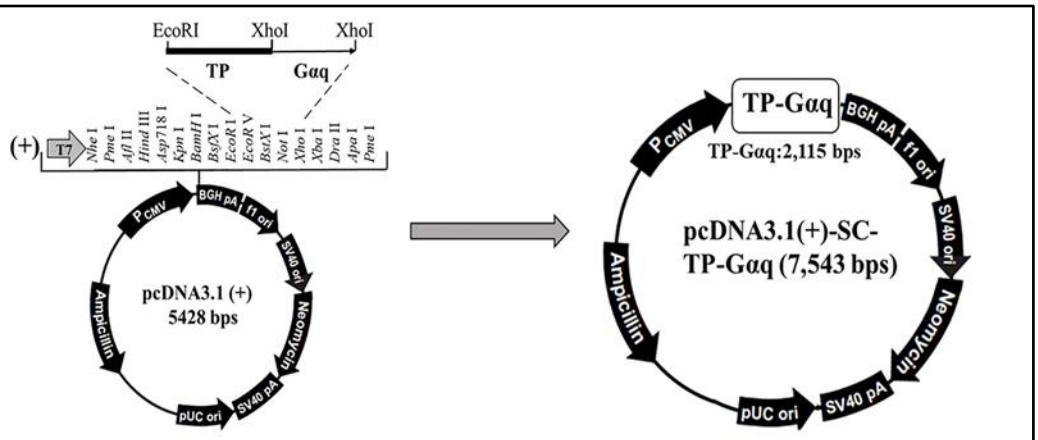

Figure 18. Construction and subcloning of the cDNA of the novel single-chain GPCR-Gα complex, SC-TP-Gαq, into the pcDNA3.1(+) vector.

The full length DNA sequence of TP linked to Gαq was generated by PCR. Following the subcloning procedures provided by the vector company (Invitrogen), the resulting cDNA clones were successfully subcloned into the pcDNA3.1(+) vector at EcoRI and XhoI sites.

IV.16 Establishment of a stable human cell line to express the recombinant SC-TP-Gαq protein complex

The expected molecular weight for SC-TP-Gαq should be approximately 90 kDa, which consists of full sizes of amino acid compositions of TP and Gαq, and additional glycosylation of TP. Firstly, we chose a human cell line, the HEK 293 cell line in this study. The reason we chose HEK cells is that naturally these cells don’s express TP receptor, which means these cells can provide null background

to test the functions of the protein complex, SC-TP-Gαq. Furthermore, CRISPR-edited Gαq-knockout HEK293 cells (HEK-ΔGαq cells) were used in this study to be transfected with the cDNA of SC-TP-Gαq. These cells can further exclude the interferences from the endogenous Gαq-mediated downstream signaling. 48 hours after transfection, the cells were screened and selected by G418 for two months to establish a stable cell line expressing SC-TP-Gαq protein complex. Western blot was performed to confirm the expression of the SC-TP-Gαq by using the Gαq antibody, and the correct size (~90kDa, Figure. 16a, lane 4) was indicated. Wild type HEK 293 cells (HEK-WT) and HEK-ΔGαq cells were used as negative controls (Figure. 19a, lanes 2 and 3). The expression and subcellular localization of SC-TP-Gαq were further examined by immunofluorescent staining analyses (Figure. 19b). In this immunostaining assay, the green fluorescence indicated the presence of Gαq, by using the Gαq antibody. Compared with HEK-WT (Figure. 19b, left penal), the green fluorescence of Gαq could not be detected in HEK-ΔGαq cells (Figure. 19b, middle penal). But in the stable cell line, HEK-ΔGαq expressing SC-TP-Gαq, the green fluorescence of Gαq was identified (Figure. 19b, right penal); moreover, the membrane-bound localization of SC-TP-Gαq was also observed (Figure. 19b, right penal). It shall be indicated that the CRISPR-Cas9 -edited HEK-ΔGαq cell line has been established, and well-characterized previously, and kindly provided by our co-author, Dr. Inoue, Asuka [125-126].

IV.17 Examination of the ligand binding activities of SC- TP-Gαq protein complex

Firstly, the ligand binding activities of the SC-TP-Gαq complex was tested in HEK-WT cells. The HEK-WT cells were divided into three groups and transfected with individual cDNA vector: 1) pcDNA3.1(+) vector only; 2) pcDNA3.1(+) TP-WT vector; 3) pcDNA3.1(+)SC- TP-Gαq vector. After transfection, G418 screening and selection were performed as we described above to develop three different stable cell lines. After the successful establishments of the stable cell lines, the assay for determination of the ligand binding activities were performed.

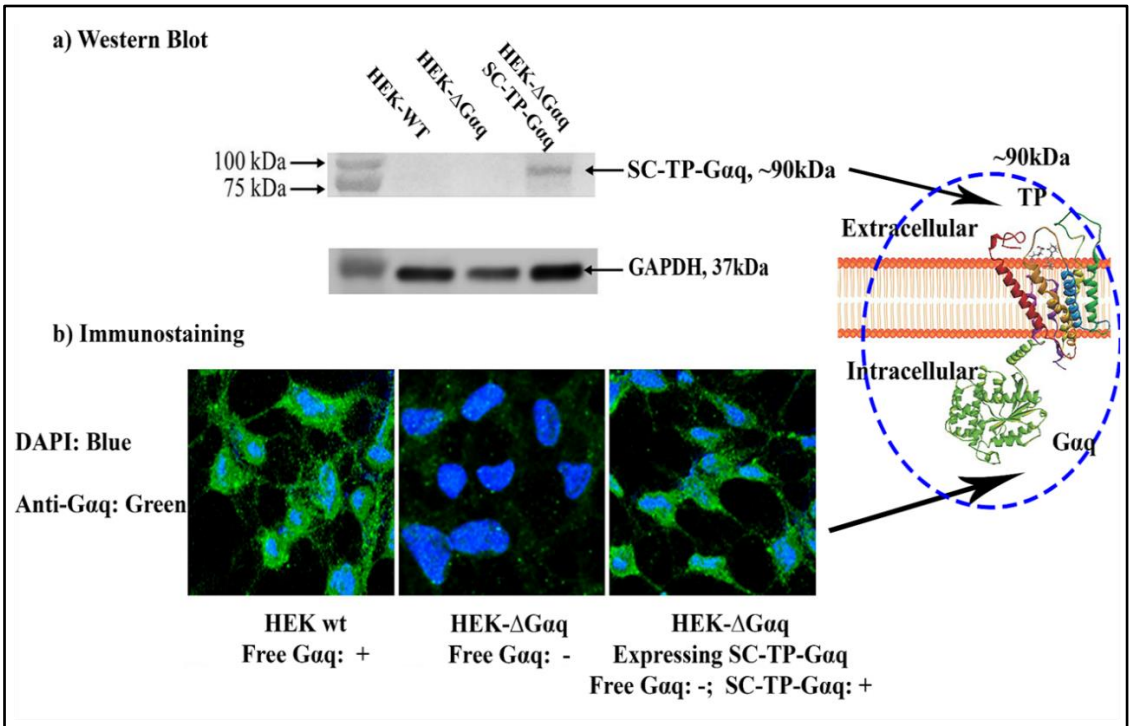

Figure 19. Expression of the recombinant SC-TP-Gαq protein complex in CRISPR/Cas9 modified Gαq-knockout HEK293 cell line.

(a) Western blot was performed to detect the expression of SC-TP-Gαq in HEK-ΔGαq cells. The arrow indicated the correct size (~90kDa) of SC-TP-Gαq protein complex. Lanes: 1) HEK-WT cells, negative control; 2) HEK-ΔGαq cells, negative control; and 3) HEK-ΔGαq cells expressing SC-TP-Gαq protein complex. (b) Furthermore, immunofluorescent imaging was performed to examine the expression and subcellular localization of SC-TP-Gαq complex in the established stable cell line, HEK-ΔGαq expressing SC-TP-Gαq. The cells were cultured in the cover slides and three types of cells were used: HEK-WT cells (left); HEK-ΔGαq cells (central); and HEK-ΔGαq cells expressing SC-TP-Gαq protein complex (right). The cells were permeabilized by Triton-100 and then incubated with mouse anti-Gαq antibody. The bounded primary antibodies were stained by Alexa Fluor 488 goat-anti-mouse IgG (green, Gαq). The cover slides were mounted by the mounting medium with DAPI (blue, nucleus). The slides were imaged under confocal fluorescent microscope. The green fluorescence representing the presence of Gαq was detected in HEK-WT cells (left), while not in HEK-ΔGαq cells (central). But in HEK-ΔGαq cells expressing SC-TP-Gαq protein complex (right), the green fluorescence indicating the expression of Gαq, was identified. In addition, the membrane-bound localization of SC-TP-Gαq was also observed (right).

SQ 29,548 is a common ligand of TP. Due to the lack of TP in HEK-WT cells, by utilizing [^{3}H]-labeled SQ 29,548 in the assay, the signal of the isotope in the

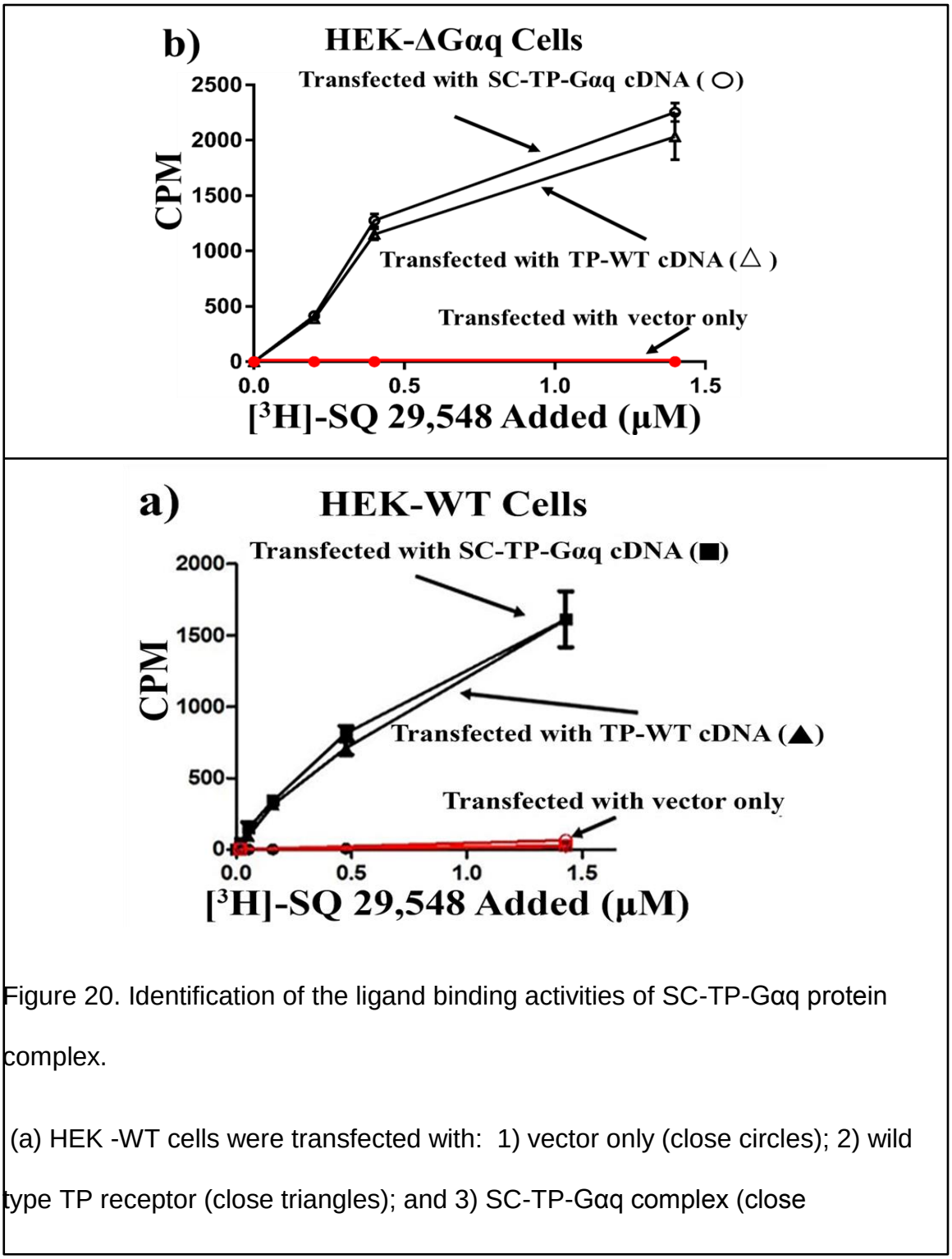

Figure 20. Identification of the ligand binding activities of SC-TP-Gαq protein complex.

(a) HEK -WT cells were transfected with: 1) vector only (close circles); 2) wild type TP receptor (close triangles); and 3) SC-TP-Gαq complex (close

rectangles). After 48 hours of transfections, the cells were screened and selected by G418 for two months to generate stable cell lines. After the stable cell lines were established, the cells were harvested and around 800ug cell pellet from each cell line was incubated with 3 nM [^{3}H]SQ29,548, the highly selective TP ligand, at room temperature for one hour with vigorous shaking. Then this reaction was terminated by the addition of 1ml ice-cold 25 mM Tris-HCl, pH 7.4. The unbound ligand was filtered under vacuum. Afterwards, the radioactivity of the TP-bound [^{3}H]-SQ29,548 was counted. (b) To further check the ligand binding activities of SC-TP-Gαq, HEK-ΔGαq cells were used. These cells were transfected with: 1) vector only (close circles); 2) wild type TP receptor (close triangles); and 3) SC-TP-Gαq complex (close rectangles). Then the stable cell lines were developed as described previously. The same ligand binding assay was performed in each stable cell line and the radioactivity of the TP-bound [^{3}H]-SQ29,548 was counted.

samples can indicate the ligand binding activities. In Figure 20a, SC-TP-Gαq protein complex indicated very similar ligand binding activities compared to that of the expressed TP-WT. To further determine the ligand binding on SC-TP-Gαq protein complex, another group of cells were utilized, the HEK-ΔGαq cells. Except the established stable cell line as we described above, the HEK-ΔGαq cells expressing SC-TP-Gαq, other two stable cell lines were also created by using the same method: the HEK-ΔGαq cells expressing the pcDNA3.1(+) vector

only; and the HEK-ΔGαq cells expressing TP-WT. By performing the same ligand binding assay, it was double-confirmed that SC-TP-Gαq indicated the same ligand binding activities with the wild-type TP (Figure. 20b).

IV.18 Identification of the signaling mediated by SC-TP-Gαq protein complex

Next step, the signaling of the SC-TP-Gαq complex was studied. We expected the same signaling transductions in SC-TP-Gαq complex with the normal signaling mediated by TP activation. Based on our design, upon agonist stimulation, TP can activate the linked Gαq and promote Gαq to be associated

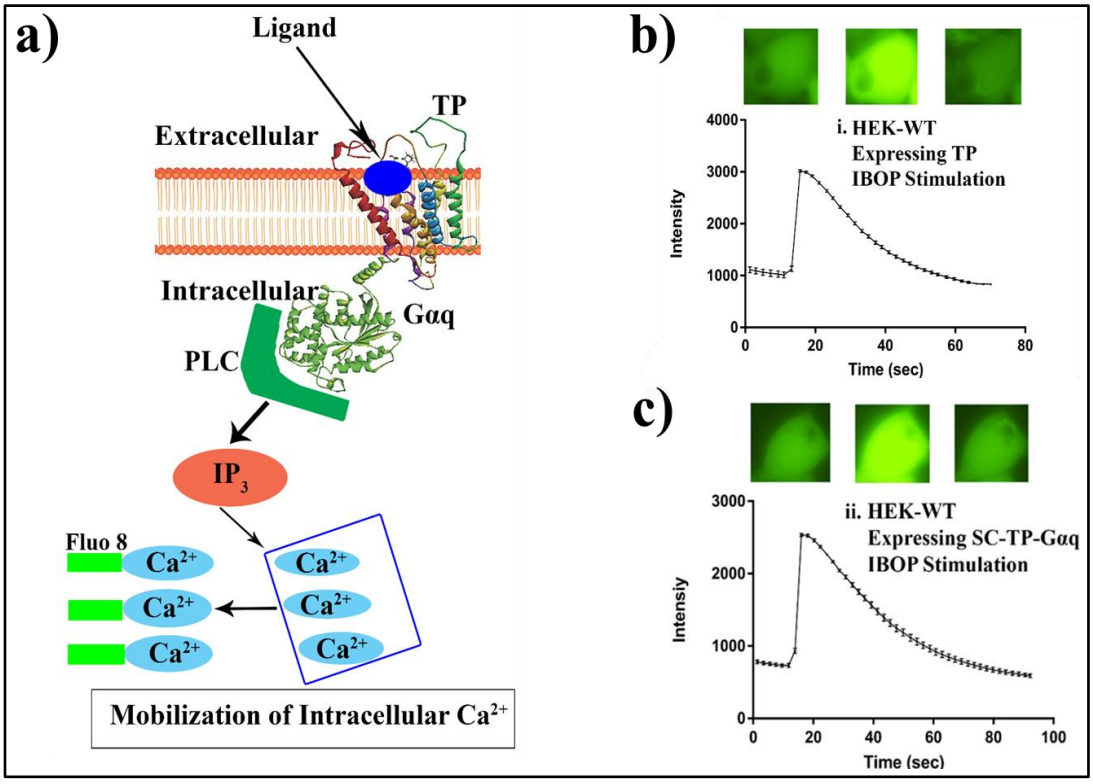

Figure 21. The determination of the calcium signaling mediated by SC-TP-Gαq. (a) Schematic presentation of the signaling transduction mediated by SC-TP-Gαq. After TP was stimulated by agonist, Gαq signaling pathway could be directly activated and promote Gαq to be associated with phospholipase C (PLC), which triggers the release of the second messenger inositol trisphosphate (IP_3), leading to the release of intracellular calcium. Fluo-8 is an intracellular fluorescent calcium binding dye. So if the calcium signaling is mediated, a flash of the green fluorescence should be observed. (b) An established stable cell line, HEK-WT expressing TP-WT was used to perform the real-time calcium signaling assay. IBOP, an agonist of TP, was used to trigger the signaling transduction. Basically, the cells were cultured in 12-well glass-bottom plates, and incubated with Fluo-8 AM dye. After 20 minutes incubation, the cells were washed three times by PBS. Calcium signaling mediated by WT TP was induced by applying IBOP on the live cells. The signaling was monitored by Nikon Ti-S eclipse microscope system (40x objective). Three trails were performed. (c) Another established stable cell line, HEK-WT expressing SC-TP-Gαq was used to perform the real-time calcium signaling. The procedures were described above.

with phospholipase C (PLC), which can induce the release of the second messenger inositol trisphosphate (IP_3), leading to the release of intracellular

calcium (Figure. 21a). To test the functions of SC-TP-Gαq, the real-time calcium signaling system was utilized, which utilized the pre-loaded flour-8 as a calcium binding indicator to monitor the intracellular calcium signaling under a fluorescent microscopy (Figure. 21) [127]. Firstly, two established cell lines were used: HEK-WT expressing TP and HEK-WT expressing SC-TP-Gαq. In both types of cells, a flash of the green fluorescence was clearly observed after activating TP by its agonist, IBOP, which indicated the release of the intracellular calcium (Figure. 21b, c).

However, the results above cannot exclude the interferences from the endogenous Gαq-mediated calcium signaling. Therefore, the CRISPR-Cas9 modified HEK-ΔGαq cells were utilized to eliminate the background Gαq-calcium signaling. We already established two stable cell line based on the HEK-ΔGαq cells as we described above, HEK-ΔGαq expressing TP-WT and HEK-ΔGαq expressing SC-TP-Gαq. The same real-time calcium assays were performed on these cells. Because no Gαq can mediate the downstream calcium signaling, after IBOP stimulation, the HEK-ΔGαq expressing TP-WT cells cannot indicate the calcium signaling (Figure. 22a). In contrast, a clear flash of green fluorescence was detected in HEK-ΔGαq expressing SC-TP-Gαq cells, which indicates TP agonist activation can trigger the release of intracellular calcium in these cells (Figure. 22b). Therefore, this SC-TP-Gαq protein complex was able to

mimic the natural signaling cascades of TP coupling to Gαq, which is TP- Gαq-calcium signaling.

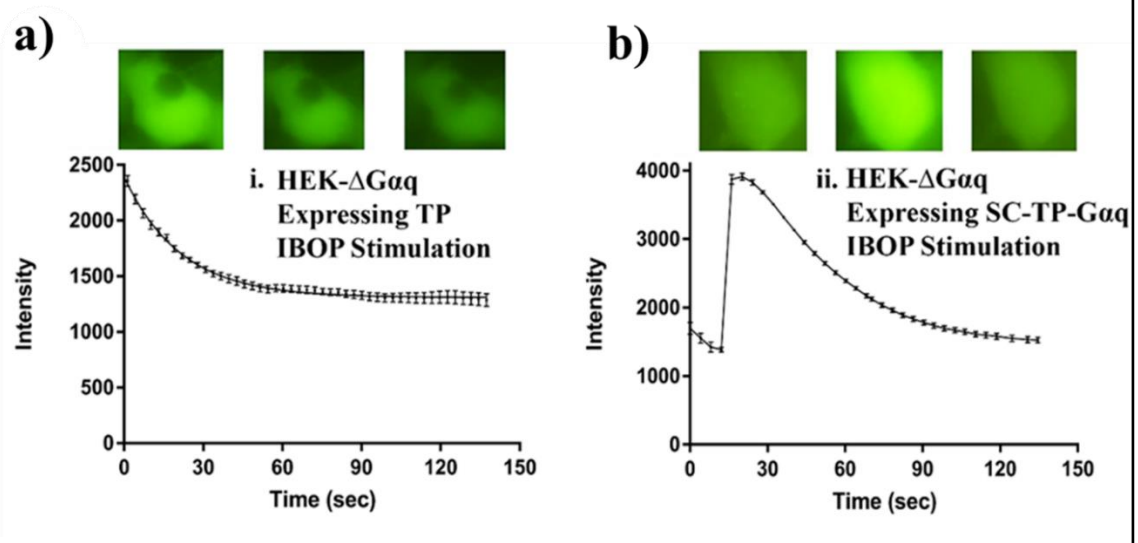

Figure 22. Further identification of the calcium signaling mediated by the SC-TP-Gαq protein complex.

To eliminate the native Gαq signaling, CRISPR/Cas9 modified HEK-ΔGαq cells were utilized. The real-time calcium signaling assay were conducted in two former established stable cell lines which were based on the HEK-ΔGαq cells, HEK-ΔGαq expressing TP-WT and HEK-ΔGαq expressing SC-TP-Gαq cell lines. a) The calcium assay was performed as described above in HEK-ΔGαq expressing TP-WT cells. There was no calcium signaling was detected. b) The same real-time calcium assay was performed in HEK-ΔGαq expressing SC-TP-

Gαq cells. An obvious flash of green fluorescence was detected, which indicated the calcium signaling was triggered in these cells.

IV.19 Application of the design of SC-TP-Gαq on another GPCR-G protein complex, SC-TP-Gαs protein complex, to alter the downstream signaling of TP

The success of the design for SC-TP-Gαq has indicated that the approach might be applied to create other active GPCR-G protein complex, which might achieve the control of selective coupling of GPCRs to the specific G-proteins, to modify the downstream second messenger signaling. The control of GPCR-G-protein coupling could become a fundamental breakthrough for various diseases related research because this approach may reverse the pathological GPCR signaling.

In cardiovascular research, TXA_2 is a well-known player to induce the pathogenic signaling for thrombotic diseases, by activating its receptor TP, and mediating the Gαq-calcium signaling cascades. The TP- Gαq-calcium signaling can promote platelet aggregation and induce vasoconstriction, which may cause the formation of thrombus. On the other hand, PGI_2, which is a known cardio-protective prostanoid, can activate the receptor IP and initiate the downstream Gαs-cAMP signaling, which could prevent platelet aggregation and lead to vasodilation. This anti-thrombotic effects of the IP- Gαs-cAMP signaling cascades can be very beneficial for the patients with thrombotic diseases. Based on our hypothesis, the

novel approach might control the GPCR coupling to a specific G protein, thus we

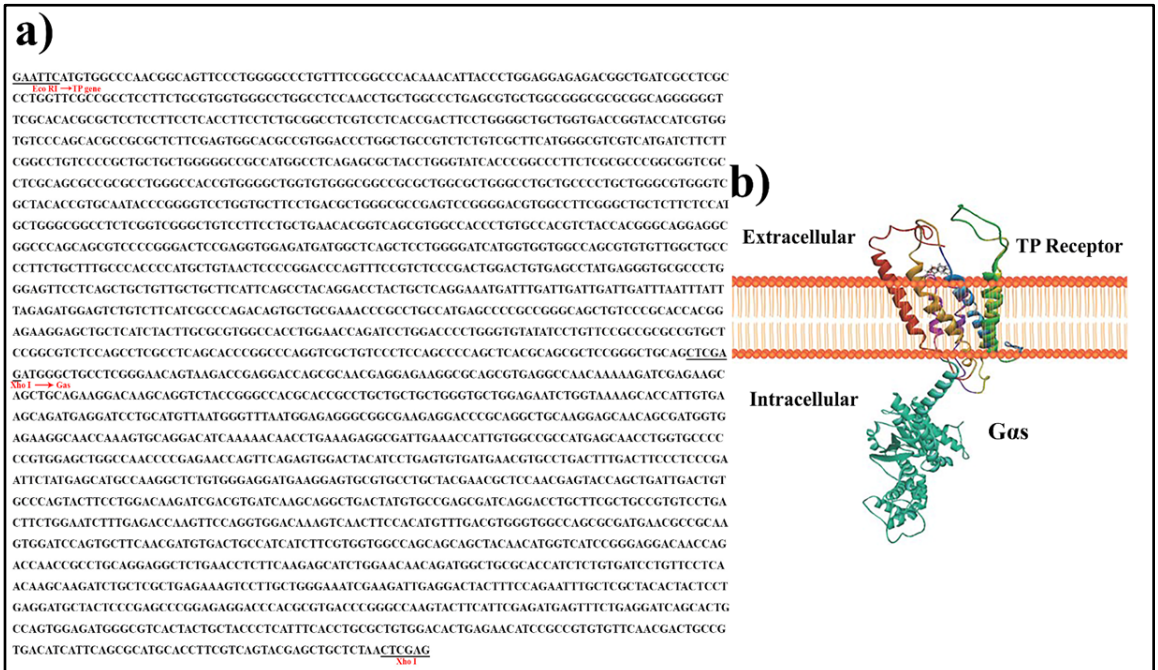

Figure 23. The design of the single-chain GPCR-Gα complex, SC-TP-Gαs.

(a) The full length cDNA sequence of SC-TP-Gαs. (b) Schematic presentation of the novel single-chain GPCR-Gα complex, SC-TP-Gαs, in which the C-terminus of TP was covalently linked to the N-terminus of Gαs, to convert the pro-thrombotic downstream signaling and physiological effects under TXA_2 activation of TP.

proposed to change the coupling of the TXA_2 to Gαs instead of Gαq, to reverse the pro-thrombotic Gαq-calcium signaling. This is the first time to propose a

method to reverse the activities of the endogenous ischemic-mediator TXA_2 within the local vascular system.

Herein, by using the same method to design SC-TP-Gαq, a recombinant cDNA (Figure. 23a) encoding the single-chain human TP linked to Gαs (SC-TP-Gαs) was created, in which the C-terminus of TP was linked to the N-terminus of Gαs subunit (Figure. 23b). The full-length of the DNA sequence for SC-TP-Gαs was generated by PCR. Then the recombinant cDNA was subcloned into pcDNA3.1 (+) vector by following the procedures of the vector company (Figure. 24). The Ecor1 and Xho1 sites used to link the cDNAs of human TP and Gαs together to form a single-chain cDNA of SC-TP-Gαs were indicated in the Figure. 23a.

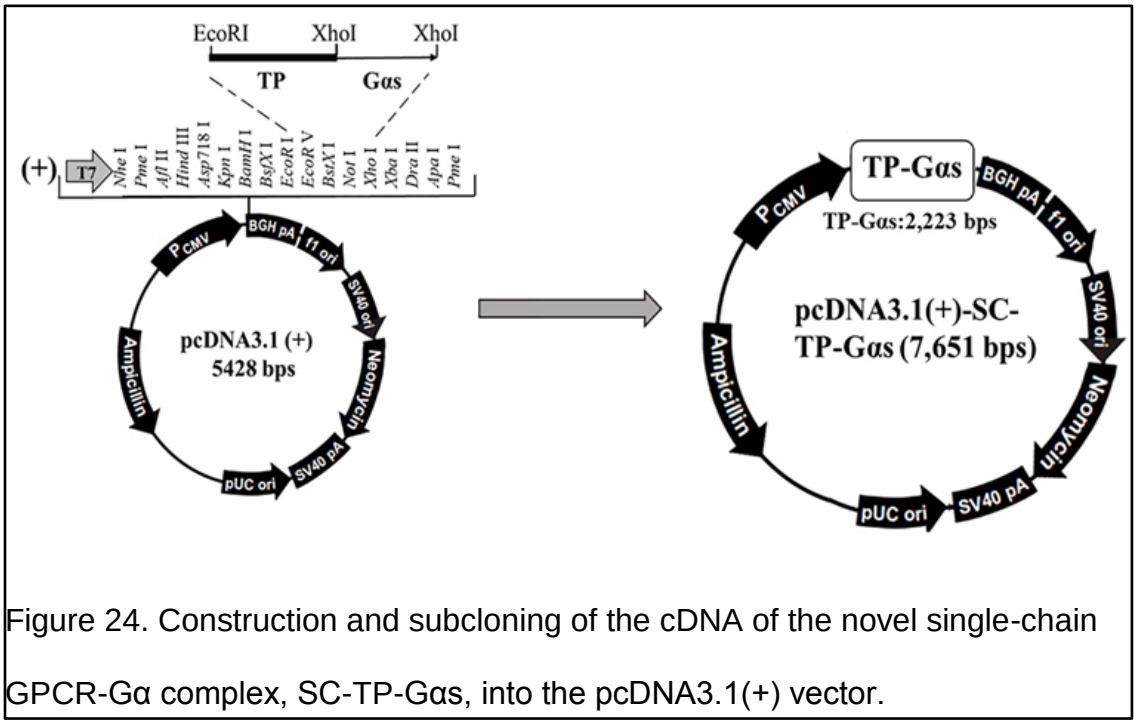

Figure 24. Construction and subcloning of the cDNA of the novel single-chain GPCR-Gα complex, SC-TP-Gαs, into the pcDNA3.1(+) vector.

The full length DNA sequence of TP linked to Gαs was generated by PCR. Following the subcloning procedures provided by the vector company (Invitrogen), the resulting cDNA clones were successfully subcloned into the pcDNA3.1(+) vector at EcoRI and XhoI sites.

IV.20 Establishment of human stable cell line to express the recombinant SC-TP-Gαs protein complex

As we mentioned before, HEK-WT cells don't express TP, which is ideal to test the signaling and functions for the recombinant protein complex. In addition, the CRISPR-edited Gαs-knockout HEK293 cells (HEK-ΔGαs cells), were also utilized in this research to exclude the interferences from the endogenous Gαs. It must be also indicated that the HEK-ΔGαs cells has been well characterized and generously provided by Dr. Inoue, Asuka's laboratory [125-126].

Firstly, the HEK-ΔGαs cells were transfected with the cDNA of SC-TP-Gαs, then were developed into a stable cell line to express SC-TP-Gαs protein complex. The procedures to generate the stable cell line has been addressed above. The expression of the SC-TP-Gαs in the stable cell line was confirmed by western blot with the correct size of 90kDa (Figure. 25a, lane 3). Following the strategies in studying the SC-TP-Gαq, the expression and subcellular localization of SC-TP-Gαs were further tested by immunofluorescent staining analyses (Figure. 25b). Just the same as we expected, the green fluorescence of Gαs was not detected

in HEK-ΔGαs cells (Fig. 25b, middle penal) which was different from HEK-WT cells. But in the stable cell line, HEK-ΔGαs expressing SC-TP-Gαs, the green fluorescence of Gαs was detected, which double-confirmed the expression of the SC-TP-Gαs in these cells. In addition, the membrane-bound subcellular localization of SC-TP-Gαs was also identified (Figure. 25b, right penal).

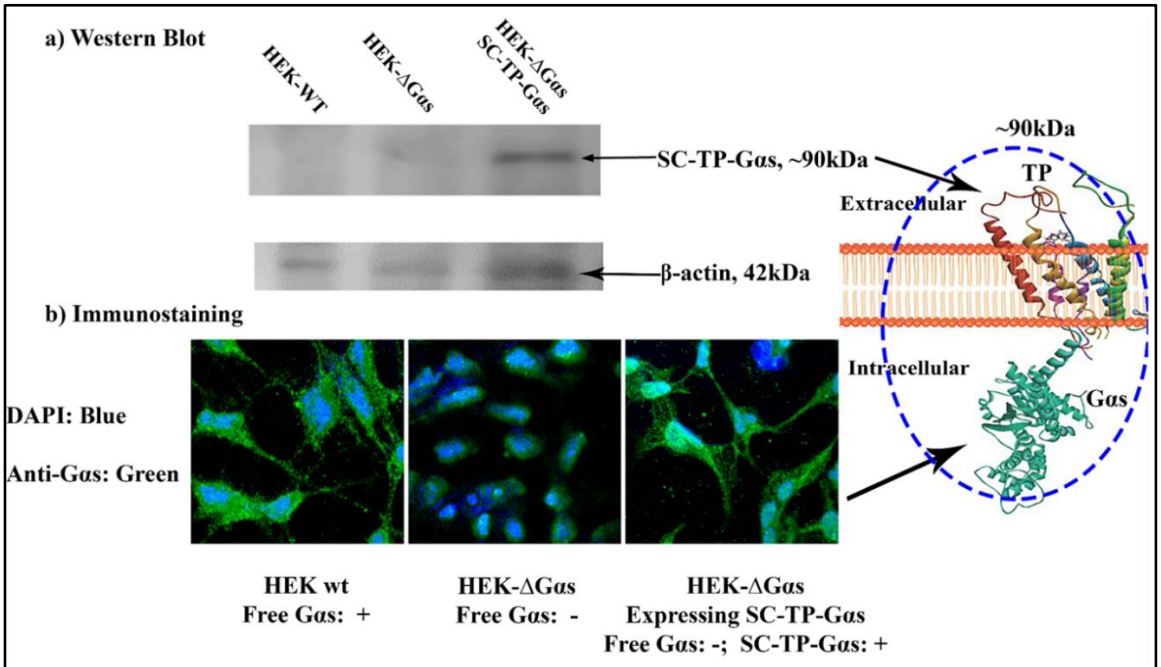

Figure 25. Expression of the recombinant SC-TP-Gαs protein complex in CRISPR/Cas9 modified HEK-ΔGαs cells.

(a) The stable cell line, HEK-ΔGαs expressing SC-TP-Gαs, was generated by following the procedures described previously. Western blot was performed to detect the expression of SC-TP-Gαs in the stable cell line. The arrow indicated

the expression of SC-TP-Gαs at 90kDa. Lanes: 1) HEK-WT cells, negative control; 2) HEK-ΔGαs cells, negative control; and 3) HEK-ΔGαs expressing SC-TP-Gαs. (b) Immunofluorescent imaging was performed to further examine the expression and subcellular localization of SC-TP-Gαs in the established stable cell line. Three types of cells were cultured on the cover slides: HEK-WT cells (left); HEK-ΔGαs cells (central); HEK-ΔGαs expressing SC-TP-Gαs (right). The cells were permeabilized by Triton-100 and then incubated with mouse anti-Gαs antibody. The bound primary antibodies were stained by Alexa Fluor 488 goat-anti-mouse IgG (green, Gαs). The cover slides were mounted by the mounting medium with DAPI (blue, nucleus). Finally, the slides were imaged under confocal fluorescent microscope. It was observed that there was no green fluorescence of Gαs in HEK-ΔGαs cells (central). But in the HEK-ΔGαs expressing SC-TP-Gαs cells, the green fluorescence of Gαs was detected (right). And the membrane-bound subcellular localization of Gαs was also identified in these cells.

IV.21 Comparison of the ligand binding activities between the novel SC-TP-Gαs protein complex and TP WT

The same isotope [^{3}H]-labeled SQ 29,548, a highly selective ligand of human TP, was utilized to perform the ligand binding assay. First of all, three stable cell lines were developed: HEK-WT expressing vector only, HEK-WT expressing TP-WT,

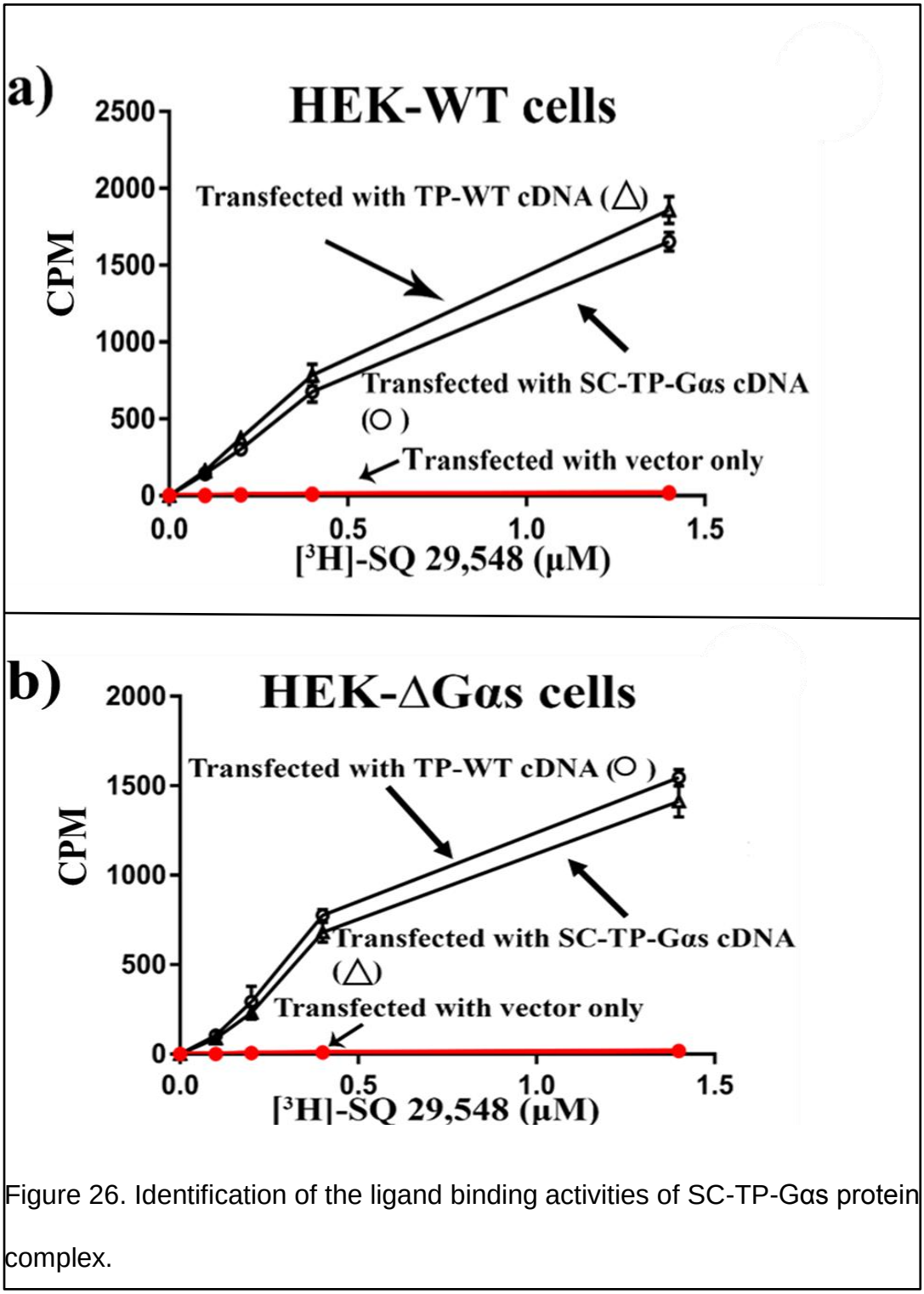

Figure 26. Identification of the ligand binding activities of SC-TP-Gαs protein complex.

a) Three stable cell lines were established here: HEK-WT expressing empty vector only (close circles); HEK-WT expressing TP-WT (close rectangles); and HEK-WT expressing SC-TP-Gαs close triangles. Generally, after harvesting the cells, 800ug of cell pellets from each stable cell line was incubated individually with 3 nM [^{3}H]SQ29,548, the highly selective TP ligand, at room temperature for one hour with vigorous shaking, then this reaction was terminated by adding 1ml ice-cold 25 mM Tris-HCl, pH 7.4. The unbound ligand was filtered under vacuum. Afterwards, the radioactivity of the TP-bound [^{3}H]SQ29,548 was counted. In HEK-WT expressing empty vector cells, no binding signal was observed. While in the cells from HEK-WT expressing TP-WT and HEK-WT expressing SC-TP-Gαs, the similar ligand binding signals were detected. b) Another three stable cell lines were used to perform the same ligand binding assay: HEK-ΔGαs expressing vector only (close circles), HEK-ΔGαs expressing TP-WT (close rectangles), and HEK-ΔGαs expressing SC-TP-Gαs (close triangles). The steps of the ligand binding assay were the same as above. The SC-TP-Gαs protein complex indicated the similar ligand binding signal compared to that of the TP-WT, and no binding signal in the cells from HEK-ΔGαs expressing vector only.

and HEK-WT expressing SC-TP-Gαs. The procedures to develop the stable cell lines have been described above. In the HEK-WT expressing vector cells, there was no signal of radioactivity. This was due to the lack of TP expression in HEK-WT cells. But in the cells from the other two stable cell lines, HEK-WT expressing

TP-WT, and HEK-WT expressing SC-TP-Gαs, the SC-TP-Gαs indicated the similar ligand binding activities with the TP-WT (Figure. 26a).

To double-check the ligand binding activities of SC-TP-Gαs, additional three stable cell lines were used in this test: HEK-ΔGαs expressing vector only, HEK-ΔGαs expressing TP-WT, and HEK-ΔGαs expressing SC-TP-Gαs. The HEK-ΔGαs expressing SC-TP-Gαs stable cell line has been established in the previous experiments, and the other two stable cell lines were generated by using the same method. Not surprisingly, the SC-TP-Gαs protein complex indicated the similar ligand binding activities compared to that of the TP-WT in these cells (Fig. 26b). These results indicated that this SC-TP-Gαs protein complex passed the first examination, in which the SC-TP-Gαs can bind to the ligand of TP successfully.

IV.22 Determination of the signaling mediated by the SC-TP-Gαs protein complex upon the TP agonist stimulation

It is known that the TP agonist, IBOP (an analogue of TXA_2), normally induces calcium signaling upon stimulation of TP, which was in accordance to the results we got above (Figure. 21 and 22). While the purpose of designing the SC-TP-Gαs protein complex is to convert the pro-thrombotic Gαq-calcium signaling into the anti-thrombotic Gαs-cAMP signaling. We hypothesize that in the SC-TP-Gαs protein complex, when TP is activated by an agonist, the coupled Gαs will be

triggered instead of Gαq. Then Gαs, rather than Gαq, will be in association with adenyl cyclase (AC), which catalyzes the cyclization of adenosine triphosphate (ATP) into the second messenger cyclic adenosine monophosphate (cAMP) (Figure. 27a).

To verify our hypothesis, the cAMP ELISA assay was performed to determine the signaling mediated by the SC-TP-Gαs protein complex. Three stable cell lines were used in this assay: HEK-ΔGαs expressing TP-WT, HEK-ΔGαs expressing SC-TP-Gαs and HEK-ΔGαs expressing SC-TP-Gαq. The former two stable cell lines have been established in previous experiments, and the third one was generated by using the same method. The HEK-ΔGαs can completely exclude the possible native Gαs-cAMP signaling. In the cells from HEK-ΔGαs expressing SC-TP-Gαq (Fig.27b, open squares) and HEK-ΔGαs expressing TP-WT (Figure. 24b, open triangles), IBOP stimulation was unable to induce the production of cAMP. In contrast, in the HEK-ΔGαs expressing SC-TP-Gαs cells, the production of cAMP was clearly observed upon the identical IBOP stimulation (Figure. 27b, open circles). To conclude, after the activation by TP agonist, the SC-TP-Gαs protein complex can activate the coupled Gαs, instead of the Gαq, thus trigger the downstream cAMP signaling. These results demonstrated that the recombinant GPCR-G protein complex, in which the GPCR was pre-coupled to a particular G-protein, can effectively regulate the downstream signaling and even the physiological effects.

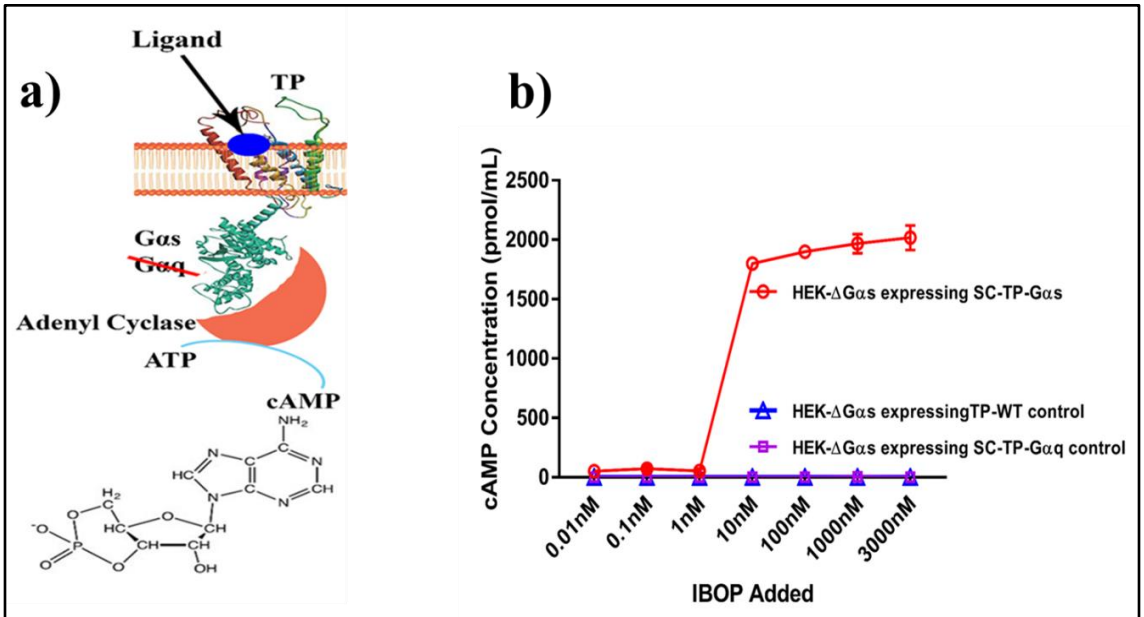

Figure 27. Identification of the signaling mediated by SC-TP-Gαs.

a) Schematic presentation of the predicted signaling transductions mediated by SC-TP-Gαs. When TP agonist stimulates the SC-TP-Gαs protein complex, the pre-coupled Gαs, instead of Gαq, will be activated, then induces the association of Gαs with AC, which catalyzes the cyclization of ATP, and leads to the production of the second messenger, cAMP. b) cAMP ELISA assay was performed to test the signaling transductions mediated by SC-TP-Gαs. Three stable cell lines were utilized in this assay: HEK-ΔGαs expressing TP-WT (open triangles), HEK-ΔGαs expressing SC-TP-Gαs (open circles) and HEK-ΔGαs expressing SC-TP-Gαq (open squares). The steps to generate the stable cell

lines were described previously. The cells from the three stable cell lines were seeded in 96-well plates and cultured overnight. Next day, the cells were incubated with different concentrations of IBOP at 37^{o}C in culture medium for 10 min, then the culture medium was removed and the cells were lysed. Afterwards, the amount of intracellular cAMP produced by IBOP stimulation was quantified in the 96-well microplates by enzyme immunoassay (EIA) through a cAMP Biotrak system. A set of three trials were conducted. It was observed that the production of cAMP was detected only in the HEK-ΔGαs expressing SC-TP-Gαs cells (open circles), upon IBOP stimulation.

IV.23 Establishments of stable megakaryocyte cell lines to stably express SC-TP-Gαq or SC-TP-Gαs

After confirming the protein complexes could mediate the signaling transductions as we expected, we started to consider using platelets as a carrier to deliver the protein complexes into the human body. We planned to utilize the human pluripotent stem cells, and program the stem cells into the immature megakaryocytes. Then these immature megakaryocytes will be transfected with the cDNAs of SC-TP-Gαq or SC-TP-Gαs, and be developed into two stable cell lines. Next the immature megakaryocytes from the two stable cell lines will be induce maturation by the addition of megakaryocyte growth and development factors (MGDFs), which can release the platelets expressing SC-TP-Gαq

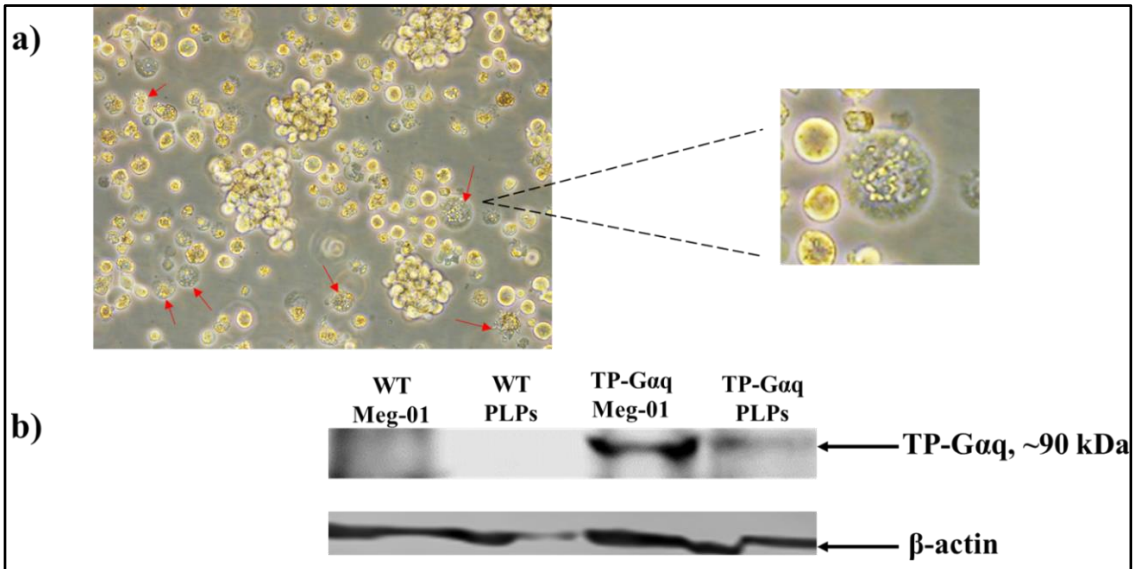

Figure 28. Induction of the maturation of the Meg-01 cells expressing SC-TP-Gαq.

a) The pro-platelet structure was identified. b) The expression of SC-TP-Gαq in PLPs was confirmed by western blot.

or SC-TP-Gαs. The procedures to produce the clinically applicable platelets from human pluripotent cells have been well developed [129]. To test this platelet delivery system, firstly, we chose a megakaryocyte cell line, Meg-01 cell line as a cell model. The Meg-01 cell line was derived from a patient with chronic myelogenous leukemia. But Meg-01 cells are very similar to the human megakaryocytes, and the platelets released from the Meg-01 cells are also very

similar to the human platelets. The Meg-01 cells were transfected with the

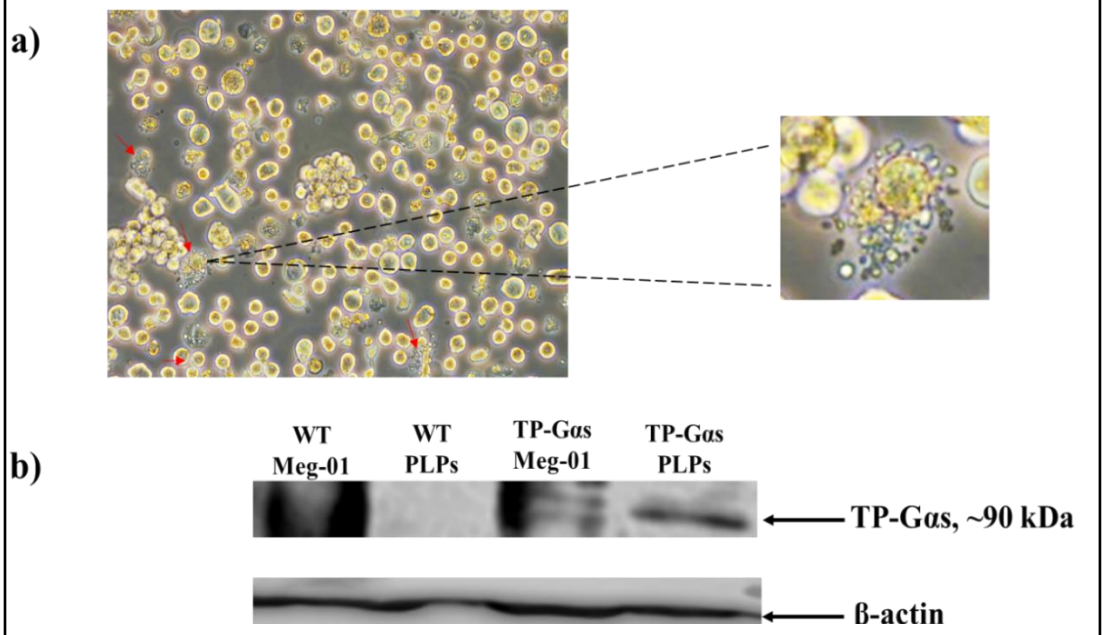

Figure 29. Induction of the maturation of the Meg-01 cells expressing SC-TP-Gαs.

a) The pro-platelet structure was also identified under microscope. b) The expression of SC-TP-Gαq in PLPs was also confirmed by western blot.

cDNAs of SC-TP-Gαq or SC-TP-Gαs, then were developed into two stable cell lines. The procedures to generate the stable cell lines were addressed before. Then the cells were induced maturation by adding the MGDF, TPO, for 72 hours. The pro-platelet structures were identified under microscope (40x Objective) (Figure. 28a and Figure 29a). The released platelet-like particles (PLPs) were isolated by centrifugation. The isolated PLPs and megakaryocytes were lysed

and the expression of the protein complexes in platelets were confirmed by western blot (Figure. 28b and Figure. 29b).

IV.24 Determination of the functions of PLPs by using flow cytometry

Based on the signaling cascades mediated by SC-TP-Gαq and SC-TP-Gαs, we hypothesized that the PLPs expressing SC-TP-Gαq might further promote platelet aggregation, while the PLPs expressing SC-TP-Gαs might prevent the aggregation activities. To test our hypothesis, the flow cytometry method was used to monitor the aggregation of platelets. In this assay, two common platelets markers were utilized, FITC-conjugated CD41a and APC-conjugated CD 42b. Basically, we stained half of the PRP sample with the CD41a antibody, and another half of sample with CD42b antibody. Then the samples were mixed and induced aggregation by the addition of AA (final concentration: 3μM). Then the sample was analyzed by the flow cytometry. The signals shown double-stained by both CD41a and CD 42b indicate the aggregation activities.

First, to determine the positive and negative result for each staining, we analyzed three groups of samples. The first group was just the platelets without any staining treatments (FITC-, APC-), which was the negative control of this assay. The area where the cells present was prescribed as Q3 Quadrant (Figure. 30a). The second group was the mixture of FITC-conjugated CD41a stained platelets and negative platelets. After analyzed by flow cytometry, two populations were

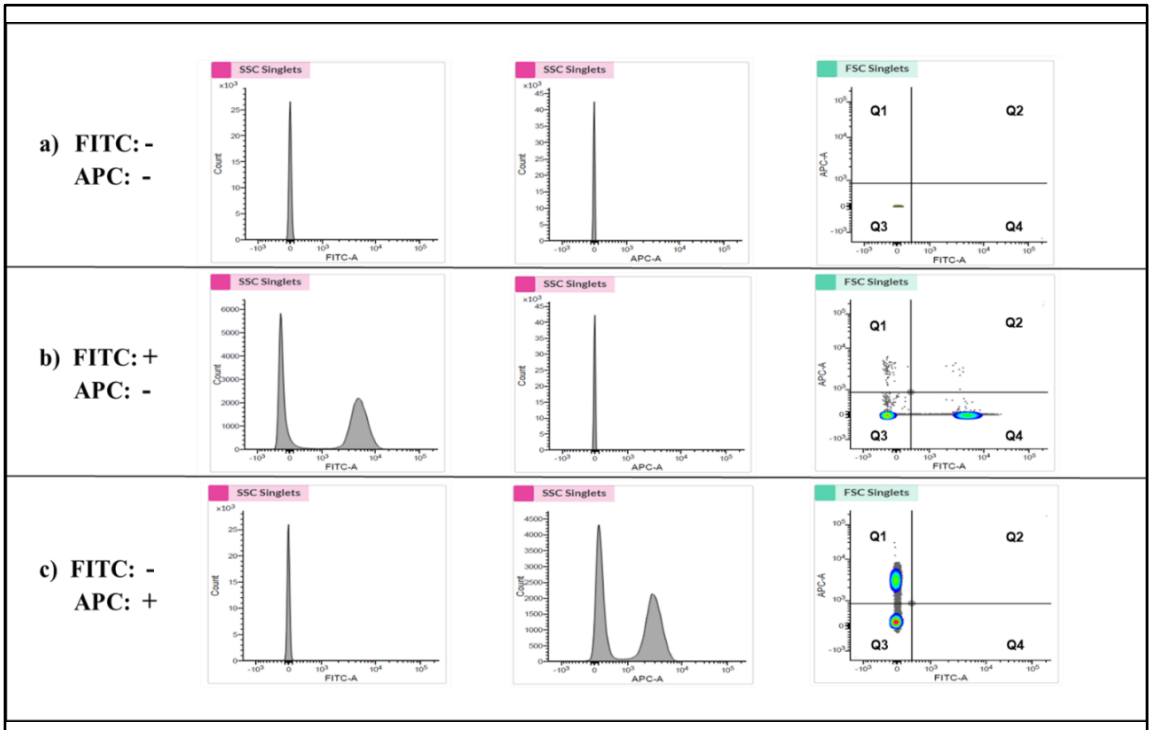

Figure 30. Determination of the specific quadrant to indicate the platelet aggregative activities.

a) The analysis of platelets without staining was shown. The Q3 Quadrant represents the negative platelets without fluorescence. b) The platelets stained with the FITC marker was mixed with the negative platelets. The shown left population represents the FITC negative platelets, and the right population (Q4 Quadrant) represents the FITC positive but APC negative platelets. c) The mixture of APC marker stained platelets and negative platelets was analyzed. The bottom population represents the ACP negative platelets, and the upper one (Q3) represents the APC positive while FITC negative platelets. The Q4

Quadrant, which represents the double staining by both FITC and APC, might indicate the platelet aggregative activities.

present (Figure. 30b. Left: FITC-; Right: FITC+). The area where the FITC positive cells present was defined as Q4 Quadrant (Figure. 30b). The third group was the APC-conjugated CD 42b stained platelets mixed with negative platelets. Through the analysis of flow cytometry, also two populations were present. The upper population was the APC-positive platelets, and that area was defined as Q1 Quadrant (Figure. 30c). Then the Q2 Quadrant was described as the double-staining population, which indicated the aggregation of platelets.

Three groups of platelet mixture were performed flow cytometry to determine the aggregation activities. And three trials were conducted in each group. The first group was the mixture of 200μL PRP and 200μL PLP released by WT Meg-01 cells. After inducing aggregation by AA, around 67% percentage of aggregation was recognized in Q2 double-staining Quadrant (Figure. 31a). The next group was 200μL PRP mixed with 200μL PLP expressing SC-TP-Gαq. The aggregative activity was induced by the addition of AA, and an increased aggregation percentage (~74%) was identified (Figure. 31b). This is because SC-TP-Gαq can mediate calcium signaling, which could further promote platelet aggregation. The last group was the mixture of PRP with the PLP expressing SC-TP-Gαs. The aggregative reaction was also triggered by adding AA, and it was found that the

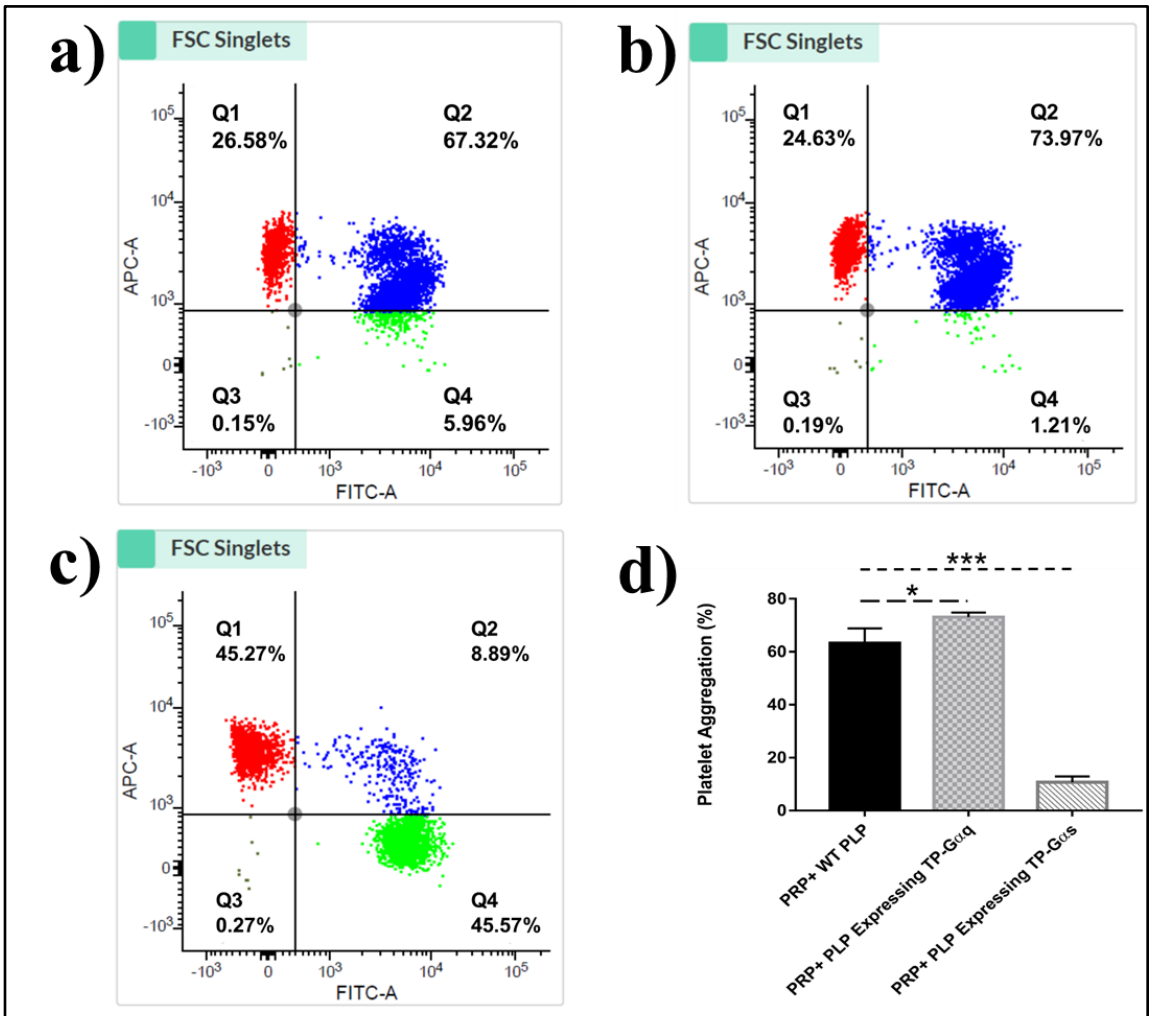

Figure 31. Identification of the PLPs expressing the protein complexes in platelet aggregation assays.

a) 200µL PRP was mixed well with 200µL WT PLPs. The mixed sample was divided equally into two groups: one was stained with the FITC-conjugated CD41a antibody and another was stained with the APC-conjugated CD 42b antibody. After the staining, the two groups were mixed again thoroughly and AA

was added to induce aggregation (3μM). Then the sample was analyzed by flow cytometry. About 67% of aggregation was recognized. b) 200μL PRP was mixed completely with 200μL PLPs expressing SC-TP-Gαq. Then the above procedures were repeated. The flow cytometry analysis indicated about 74% of aggregation. c) The mixture of 200μL PRP and 200μL PLPs expressing SC-TP-Gαs was used to repeat the above steps. Around 9% of aggregation was demonstrated in this group.

aggregation percentage was decreased to about 9% (Figure. 31c). This should result from the cAMP signaling mediated by SC-TP-Gαs, which could inhibit platelet aggregation. The statistical analysis of the results has indicated that the SC-TP-Gαq protein complex could significantly promote the platelet aggregative activities, while SC-TP-Gαs could dramatically prevent the aggregation of platelets, which might exhibit benefits in treating thrombotic diseases (Figure. 31d).

V. DISCUSSION

In this study, the novel hybrid enzyme, COX-1-10aa-TXAS, is able to mimic the triple-catalytic chain reactions mediated by the wild type COX-1 and TXAS in metabolizing the cellular AA into TXA_2. Therefore, this hybrid enzyme has provided very valuable information to understand the active ER configuration of the wild type COX-1 and TXAS in the biosynthesis of TXA_2. The further structural

studies of COX-1-10aa-TXAS might be very helpful to uncover the detailed structural and functional relationship between COX-1 and TXAS in the chain catalytic reactions during the biosynthesis of the key molecule, TXA_2, which is directly involved in hemostasis, as a blood coagulation mediator.

In addition, this research allows to predict that the distance between the COX-1 and TXAS on the ER membrane is very close to that in the hybrid enzyme, which has not been proposed yet. In the hybrid enzyme, COX-1 and TXAS was connected by a 10 amino acid linker, whose helical structure and separation distance (with a 14.4Å separation) has been studied in our previous research [128]. This hybrid enzyme approach could accurately define the distance between the two proteins during the chain reactions because the primary structures and part of the 3D structures for most proteins are known due to the protein structure studies in the past years, which can be used for the computational structural modeling. Based on this concept, we have successfully measured the 3D configuration and distance between the COXs and PGIS or mPGES-1 on the ER membrane during the chain catalytic reactions, through the active hybrid enzyme approach, using COX-1-1-10aa-PGIS and COX-2-10aa-mPGES-1 as tools previously.

This hybrid enzyme, COX-1-10aa-TXAS, might have several promising medical applications. First, it could be developed into a biological reagent to treat

bleeding emergencies. Compared to other hemostatic agents, one major advantage of this hybrid enzyme is that it is able to use endogenous AA as a substrate. Just as we introduced before, AA is polyunsaturated fatty acid presenting in the phospholipids of cell membrane. When there is a bleeding stimulus, a lot of AA will be released from the cells very quickly. And the large number of AA could become the substrates of the hybrid enzyme and initiate the production of TXA_2. Because the triple-catalytic activities of the hybrid enzyme could continually and instantly convert the released AA into TXA_2 in the bleeding site, it should be able to stop the bleeding quickly. In addition, different from other hemostatic agents, TXA_2 can not only mediate blood coagulation, but also mediate vasoconstriction. This can further improve the hemostatic efficiency. In this study, we utilized *S. cerevisiae* yeast expression system to produce the hybrid enzyme. After purification, the hybrid enzyme exhibited strong ability to stop bleeding. Thus, COX-1-10aa-TXAS has great potential to be developed into a biological reagent to treat various bleeding emergencies.

Second, the biological functions of TXA_2 in mediating platelet aggregation and vasoconstriction in hemostasis are well-characterized, but its roles on other diseases are poorly understood. It has been reported that TXA_2 could promote cancer cell proliferation in recent studies [127]. TXA_2 was also indicated to be involved in post- neuronal cell damages after stroke [123]. The success of the creation of this hybrid enzyme, COX-1-10aa-TXAS , which specifically redirects

the metabolism of AA, by passing the common intermediate PGH_2 to TXAS directly, was the first to make it possible to control cellular AA metabolism toward TXA_2, and disfavoring for other prostanoids. Through transfecting the cDNA of COX-1-10aa-TXAS to different cells, such as neuronal and tumor cells, could be used as cell models to uncover the roles of the TXA_2 on various diseases, such as neurodegeneration, cancer development and metastasis.

Moreover, the imbalance between the production of TXA_2 and other prostanoids, is one major cause for the formation of thrombi in thrombotic diseases, such as stroke, heart arrest, ischemia, pulmonary arterial hypertension, and deep vein thrombosis. Specific inhibition of the production of TXA_2 is a key step to rescue TXA_2-mediated ischemia. And aspirin is used as the first-line blood-thinner medication to prevent blood clotting by decreasing the production of TXA_2. However, aspirin is a non-selective COX inhibitor, which could also suppress the production of other important prostanoids, such as PGI_2, which exhibits important vascular protective effects that prevents damages from excess TXA_2. More and more studies indicated that aspirin might also promote cardiovascular diseases by preventing the production of the vascular protector, PGI_2. However, the drug specifically controlling TXA_2 production, with the property of maintaining the level of PGI_2, has not been discovered yet. Herein, we could use the established hybrid enzymes as targets for screening the new drugs, which only inhibit the functions of TXAS without affecting PGIS and COX-1, by combining our

previously developed COX-1-10aa-PGIS with this new hybrid enzyme, COX-1-10aa-TXAS. Therefore, the COX-1-10aa-TXAS could have a great impact to be used as a drug target for discovering the next generation of NSAIDs, which have fewer side effects on cardiovascular diseases. Even though this novel hybrid enzyme has multiple advantages, there might be some limitations concerning about its application. This hybrid enzyme is ideal in treating aspirin-resulted bleeding disorders, especially for the patients taking aspirin as a daily medication. The clearance of the restrictions to platelet functions from aspirin always takes more than 10 days until the affected platelets replaced completely by the newly-generated platelets. However, in some emergent situations, the medical treatments must be taken immediately on these patients without waiting for another 10 days. So this hybrid enzyme could be life-saving in the surgical procedures to treat the possible bleeding disorders. However, one major concern about this hybrid enzyme is that if this hybrid enzyme induces excessive platelet aggregation, it could also cause another serious hazard, the formation of the thrombus. So more studies will be done in the future in concerning about the safety of this hybrid enzyme during the clinical application.

In the second part of my research, we proposed a new technology to pre-couple the GPCR with a particular G protein, in order to manipulate the downstream signaling through controlling the activation of a specific G protein. In this study, based on the innovative and active fusion-protein approach, the previously

established modeling structure of TP was linked to the resolved crystal structures of Gαq or Gαs.

Except for the purpose of controlling the downstream signaling and reverse the physiological effects mediated by the GPCR, as we described in previous studies, this fusion protein approach could also be used as a tool to characterize the 3D configuration for the active protein-protein interaction and measure the protein-protein distance. This approach has advantages compared to other approaches, such as chemical linkage, and fluorescence resonance energy transfer (FRET) [128]. This approach allows to study the protein-protein interaction in the active forms of the proteins. By using this approach, the fusion protein complex has the correct protein folding, ligand binding and catalytic functions, which are all the same within the live cell conditions. But other methods, such as the chemical linkage and FRET, could alter the protein folding in 3D structure, leading to the inactivation of the proteins, which could only provide information from the dead proteins and cells. The current study of the successful creation of the active SC-TP-Gαq and SC-TP-Gαs supports the characterization of the active membrane protein-protein interaction by using our fusion protein approach. This has provided a novel approach to further uncover the mechanisms of the signal transduction for other GPCRs with different G-protein alpha subunits in general.

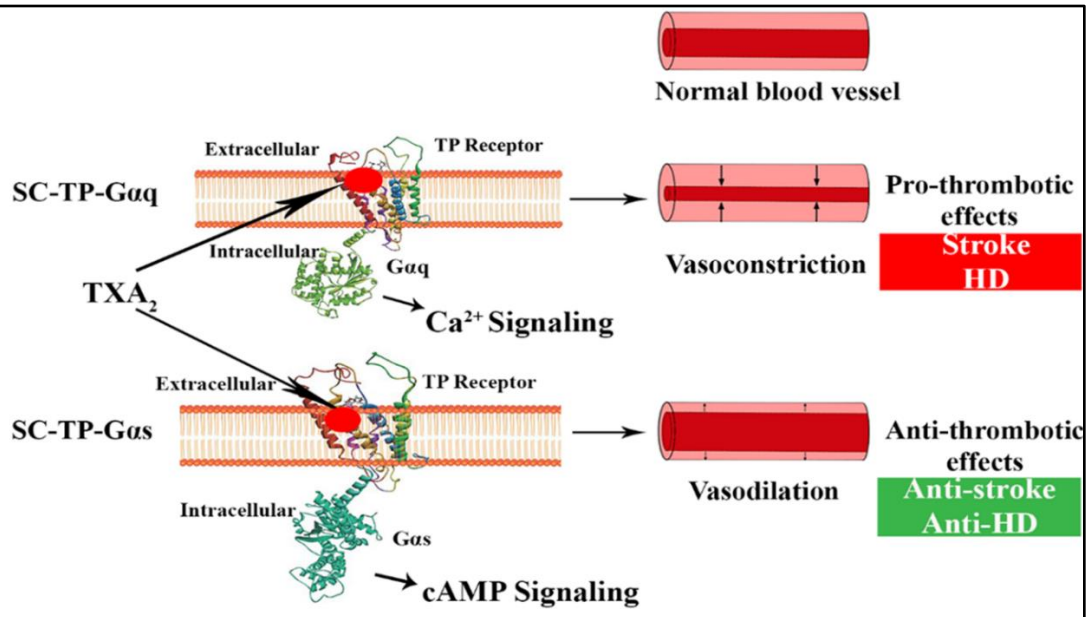

Figure 32. A diagram explaining the signaling and effects mediated by SC-TP-Gαq and SC-TP-Gαs complexes.

Upon a TP agonist, thromboxane A_2 (TXA_2) stimulation, SC-TP-Gαq is able to selectively trigger the downstream Gαq-calcium signaling, which mimics the natural signaling cascades mediated by TP receptor, and mediate vasoconstriction, exhibit pro-thrombotic effects and contribute to stroke and various cardiovascular diseases. On the other hand, under the identical TP agonist stimulation, SC-TP-Gαs is able to specifically convert the downstream signaling into Gαs-cAMP signaling, which opposes the natural signaling activities mediated by TP receptor, and induce vasodilation, demonstrate anti-thrombotic effects and prevent stroke and various thrombotic diseases.

Endogenous TXA_2 is a major pathogenic factor, which can bind to its receptor TP and cause TP coupling to Gαq, mediating calcium signaling. The GPCR-G protein complex, SC-TP-Gαq, which was created in this study, could mimic the above signaling transductions upon TXA_2 stimulation. And the results of this research verified the calcium signaling mediated by SC-TP-Gαq upon TXA_2 stimulation. The above signaling cascades are able to induce platelet aggregation, blood clotting and vasoconstriction. These activities are directly involved in promoting the progression of some thrombotic cardiovascular diseases, such as ischemia, stroke, heart arrest, pulmonary arterial hypertension and restenosis. Except SC-TP-Gαq, another recombinant fusion protein complex, SC-TP-Gαs, was created in this study, in which the Gαq subunit was replaced by the Gαs subunit. The purpose of this design is to mimic the signaling transductions mediated by the cardio-protective prostanoid, PGI_2. Different from TXA_2, after PGI_2 binds to its receptor, it can trigger the Gαs-cAMP downstream signaling. Thus, SC-TP-Gαs should reverse the activities of the TXA_2 by converting calcium signaling to cAMP signaling, which could inhibit platelet aggregation, prevent blood clot and dilate blood vessels (Figure. 32). Based on the results of this research, the ability of SC-TP-Gαs to convert the calcium signaling into the cAMP signaling was confirmed. These new findings have indicated that inducing the expression of SC-TP-Gαs in specific cells, tissues or

blood vessels, might be developed into a novel and advanced therapeutic intervention. For example, it could be used as a gene therapy reagent to be against vascular thrombosis by introducing the cDNA of SC-TP-Gαs into the endothelium or vascular smooth muscle cells locally. In this study, we utilized the platelet-delivery system to deliver SC-TP-Gαq or SC-TP-Gαs protein complex. After the establishments the stable Meg-01 cell lines expressing SC-TP-Gαq or SC-TP-Gαs, these megakaryocytes were induced maturation, and released the platelets expressing the protein complexes. The platelets expressing SC-TP-Gαs exhibited strong effects in preventing platelet aggregation. Therefore, platelets might become a novel tool to carry protein-based medicine into the human blood circulatory system. The platelet delivery system has some advantages. First, platelets don't have nuclei, so they won't cause possible nucleic acid contamination. Second, different from other cell-based delivery system, such as intramuscular injection of some stem cell therapies, intravenous infusion of platelets won't cause acute inflammation reactions. And in other cell-based delivery system, the elimination of the dead cells is always a big problem. But for the platelets, after 7 to 10 days circulating in the blood, they will be eliminated together with other dead blood cells. Furthermore, the sources for clinical platelets will not be limited any more. Recently, a research group from Japan has established a megakaryocyte cell line which can produce clinical-applicable platelets continually [129]. Last but not the least, these platelets expressing SC-

TP-Gαs could serve as a ‘cleaner’, which can continually absorb the excessive TXA_2 in blood and exhibit the anti-thrombotic effects. But there also might be some limitations in the applications of the fusion protein, SC-TP-Gαs, since the induced cAMP signaling could result in bleeding. If the cAMP signaling overbalances the calcium signaling, the risk of bleeding will be increased. Local application of the fusion protein in specific tissues, such as the stented artery, might restrict the bleeding risk. But if the platelets expressing the fusion protein are utilized to treat thrombotic diseases, more studies are needed to determine the dosage to assure the safety of the application.

Furthermore, this research has suggested that the Gα subunit could be manipulated as a regulatory and therapeutic target to control and even reverse the functions of GPCR, which might become a general method to regulate the functions of GPCRs. This approach might exhibit benefits in treating diverse diseases. In addition, the fusion protein method used in this research could also be utilized to study the signaling transductions for other GPCRs. Thus, this research has provided a new approach to manipulate the physiological effects mediated by GPCR, and a new method to understand the signaling transductions for the entire GPCR family.

VI. SUMMARY AND CONCLUSIONS

First of all, the novel engineered hybrid enzyme, COX-1-10aa-TXAS, indicated the integrated triple-catalytic activities within just a single polypeptide, by linking the C-terminus of COX-1 to the N-terminus of TXAS through a 10aa linker. Through the tripe-catalytic chain reactions, the hybrid enzyme could effectively convert endogenous AA into TXA_2. The design of this hybrid enzyme could pass the common intermediate PGH_2 to TXAS directly, which makes it possible to control cellular AA metabolism toward the production of TXA_2, and to be disfavor of other prostanoids, such as PGI_2 and PGE_2. Through redirecting the metabolism of AA, the hybrid enzyme has exhibited effective anti-bleeding properties. Thus, this hybrid enzyme could be developed into a hemostatic agent to treat bleeding. Furthermore, this hybrid enzyme could serve as a target for screening anti-stroke drugs, which could specifically suppress the production of TXA_2. This hybrid enzyme could also be used as a cellular model to understand the relationship between TXA_2 and other diseases, such as cancer and neuronal degeneration diseases. In addition, this hybrid enzyme could be further used for understanding the topology, structure and functional relationships of COX-1 and TXAS, during the biosynthesis of TXA_2.

Next, the studies of the GPCR-G protein complex, SC-TP-Gαq have led us to conclude that covalently linking the N-terminus of TP to C-terminus of Gαq could

mimic the natural calcium signaling mediated by TXA_2 activation. Furthermore, by replacing Gαq with Gαs, SC-TP-Gαs could shift the cellular signaling pathway mediated by TXA_2 from the thrombotic calcium signaling to the anti-thrombotic cAMP signaling, which could mimic the physiological effects of the vascular protector, PGI_2 Moreover, based on this research, Gα subunit could become a new therapeutic target, which could be modified and replaced in according to the needs of disease prevention and treatment. The successful modification of GPCR signaling in this study has led us to propose that this fusion protein approach could be applied to modify and control the signaling of various GPCRs, or be used as a modeling tool to understand the signaling transductions mediated by GPCRs.

REFERENCES

1. Cannon, Jeremy W. "Hemorrhagic shock." New England Journal of Medicine 378.4 (2018): 370-379.

2. Ding X, Murray PA. Cellular mechanisms of thromboxane A2-mediated contraction in pulmonary veins. American Journal of Physiology-Lung Cellular and Molecular Physiology. 2005; 289: L825-L33.

3. Yamamoto K, Ebina S, Nakanishi H, Nakahata N. Thromboxane A2 receptor-mediated signal transduction in rabbit aortic smooth muscle cells. General Pharmacology: The Vascular System. 1995; 26: 1489-98.

4. Smyth EM. Thromboxane and the thromboxane receptor in cardiovascular disease. Clinical lipidology. 2010; 5: 209-19.

5. Winn R, Harlan J, Nadir B, Harker L, Hildebrandt J. Thromboxane A2 mediates lung vasoconstriction but not permeability after endotoxin. Journal of Clinical Investigation. 1983; 72: 911-8.

6. Narumiya S, Sugimoto Y, Ushikubi F. Prostanoid Receptors: Structures, Properties, and Functions. Physiological Reviews. 1999; 79: 1193-226.

7. Ally AI, Horrobin DF. Thromboxane A2 in blood vessel walls and its physiological significance: relevance to thrombosis and hypertension. Prostaglandins and medicine. 1980 Jun 1;4(6):431-8.

8. Wendelboe AM, Raskob GE. Global burden of thrombosis: epidemiologic aspects. Circulation research. 2016 Apr 29;118(9):1340-7

9. Hansson, G.K., 2005. Inflammation, atherosclerosis, and coronary artery disease. New England Journal of Medicine, 352(16), pp.1685-1695.

10. Torrado, J., Buckley, L., Durán, A., Trujillo, P., Toldo, S., Raleigh, J.V., Abbate, A., Biondi-Zoccai, G. and Guzmán, L.A., 2018. Restenosis, stent thrombosis, and bleeding complications: navigating between Scylla and Charybdis. Journal of the American College of Cardiology, 71(15), pp.1676-1695.

11. Buccheri, D., Piraino, D., Andolina, G. and Cortese, B., 2016. Understanding and managing in-stent restenosis: a review of clinical data, from pathogenesis to treatment. Journal of thoracic disease, 8(10), p.E1150.

12. Holmes, D.R., Kereiakes, D.J., Garg, S., Serruys, P.W., Dehmer, G.J., Ellis, S.G., Williams, D.O., Kimura, T. and Moliterno, D.J., 2010. Stent thrombosis. Journal of the American College of Cardiology, 56(17), pp.1357-1365.

13. Cutlip, D.E., Baim, D.S., Ho, K.K., Popma, J.J., Lansky, A.J., Cohen, D.J., Carrozza Jr, J.P., Chauhan, M.S., Rodriguez, O. and Kuntz, R.E., 2001. Stent thrombosis in the modern era: a pooled analysis of multicenter coronary stent clinical trials. Circulation, 103(15), pp.1967-1971.

14. Moreno, R., Fernández, C., Hernández, R., Alfonso, F., Angiolillo, D.J., Sabaté, M., Escaned, J., Bañuelos, C., Fernández-Ortiz, A. and Macaya, C., 2005. Drug-eluting stent thrombosis: results from a pooled analysis including 10 randomized studies. Journal of the American College of Cardiology, 45(6), pp.954-959.

15. Wenaweser, P., Dörffler-Melly, J., Imboden, K., Windecker, S., Togni, M., Meier, B., Haeberli, A. and Hess, O.M., 2005. Stent thrombosis is associated with an impaired response to antiplatelet therapy. Journal of the American College of Cardiology, 45(11), pp.1748-1752.

16. Kounis, N.G., Koniari, I., Roumeliotis, A., Tsigas, G., Soufras, G., Grapsas, N., Davlouros, P. and Hahalis, G., 2017. Thrombotic responses to coronary

stents, bioresorbable scaffolds and the Kounis hypersensitivity-associated acute thrombotic syndrome. Journal of thoracic disease, 9(4), p.1155.

17. Virmani, R. and Farb, A., 1999. Pathology of in-stent restenosis. Current opinion in lipidology, 10(6), pp.499-506.

18. Hoffmann, R. and Mintz, G.S., 2000. Coronary in-stent restenosis—predictors, treatment and prevention. European Heart Journal, 21(21), pp.1739-1749.

19. Mitra, A.K. and Agrawal, D.K., 2006. In stent restenosis: bane of the stent era. Journal of clinical pathology, 59(3), pp.232-239.

20. Lowe, H.C., Oesterle, S.N. and Khachigian, L.M., 2002. Coronary in-stent restenosis: current status and future strategies. Journal of the American College of Cardiology, 39(2), pp.183-193.

21. Simmons, D.L., Botting, R.M. and Hla, T., 2004. Cyclooxygenase isozymes: the biology of prostaglandin synthesis and inhibition. Pharmacological reviews, 56(3), pp.387-437.

22. Allaj, V., Guo, C. and Nie, D., 2013. Non-steroid anti-inflammatory drugs, prostaglandins, and cancer. Cell & bioscience, 3(1), p.8.

23. Kang, Y.J., Mbonye, U.R., DeLong, C.J., Wada, M. and Smith, W.L., 2007. Regulation of intracellular cyclooxygenase levels by gene transcription and protein degradation. Progress in lipid research, 46(2), pp.108-125.

24. Park, J.Y., Pillinger, M.H. and Abramson, S.B., 2006. Prostaglandin E2 synthesis and secretion: the role of PGE2 synthases. Clinical immunology, 119(3), pp.229-240.

25. Vane, J.R., Bakhle, Y.S. and Botting, R.M., 1998. CYCLOOXYGENASES 1 AND 2. Annual review of pharmacology and toxicology, 38(1), pp.97-120.

26. Rouzer, C.A. and Marnett, L.J., 2009. Cyclooxygenases: structural and functional insights. Journal of lipid research, 50(Supplement), pp.S29-S34.

27. Prusakiewicz, J.J., Duggan, K.C., Rouzer, C.A. and Marnett, L.J., 2009. Differential sensitivity and mechanism of inhibition of COX-2 oxygenation of arachidonic acid and 2-arachidonoylglycerol by ibuprofen and mefenamic acid. Biochemistry, 48(31), pp.7353-7355.

28. Zarghi, A. and Arfaei, S., 2011. Selective COX-2 inhibitors: a review of their structure-activity relationships. Iranian journal of pharmaceutical research: IJPR, 10(4), p.655.

29. Zarghi, A., Arfaei, S. and Ghodsi, R., 2012. Design and synthesis of new 2, 4, 5-triarylimidazole derivatives as selective cyclooxygenase (COX-2) inhibitors. Medicinal Chemistry Research, 21(8), pp.1803-1810.

30. Zarghi, A. and Arfaei, S., 2011. Selective COX-2 Inhibitors: A Review if Their Structure Activity Relationships. 10 (4) IJPR PMC3813081

31. Zarghi, A., Reihanfard, H., Arfaei, S., Daraei, B. and Hedayati, M., 2012. Design and synthesis of new 1, 2-diaryl-4, 5, 6, 7-tetrahydro-1H-benzo [d] imidazoles as selective cyclooxygenase (COX-2) inhibitors. Medicinal Chemistry Research, 21(8), pp.1869-1875.

32. Levick, S.P., Loch, D.C., Taylor, S.M. and Janicki, J.S., 2007. Arachidonic acid metabolism as a potential mediator of cardiac fibrosis associated with inflammation. The Journal of Immunology, 178(2), pp.641-646.

33. Huwiler, A., Johansen, B., Skarstad, A. and Pfeilschifter, J., 2001. Ceramide binds to the CaLB domain of cytosolic phospholipase A2 and facilitates its membrane docking and arachidonic acid release. The FASEB Journal, 15(1), pp.7-9.

34. Huwiler, A. and Pfeilschifter, J., 2009. Lipids as targets for novel anti-inflammatory therapies. Pharmacology & therapeutics, 124(1), pp.96-112.

35. Chen, E.P. and Smyth, E.M., 2011. COX-2 and PGE2-dependent immunomodulation in breast cancer. Prostaglandins & other lipid mediators, 96(1-4), pp.14-20.

36. Smyth, E.M., Grosser, T. and FitzGerald, G.A., 2011. Lipid-derived autacoids: eicosanoids and platelet-activating factor. Goodman & Gilman's The Pharmacological Basis of Therapeutics. 201112th ed New York McGraw-Hill Professional, pp.937-959.

37. Duffin, R., O'Connor, R.A., Crittenden, S., Forster, T., Yu, C., Zheng, X., Smyth, D., Robb, C.T., Rossi, F., Skouras, C. and Tang, S., 2016. Prostaglandin E2 constrains systemic inflammation through an innate lymphoid cell–IL-22 axis. Science, 351(6279), pp.1333-1338.

38. Miyawaki, S., Imai, H., Shimizu, M., Yagi, S., Ono, H., Mukasa, A., Nakatomi, H., Shimizu, T. and Saito, N., 2013. Genetic variant RNF213 c. 14576G> A in various phenotypes of intracranial major artery stenosis/occlusion. Stroke, 44(10), pp.2894-2897.

39. Greten, F.R., Eckmann, L., Greten, T.F., Park, J.M., Li, Z.W., Egan, L.J., Kagnoff, M.F. and Karin, M., 2004. IKKβ links inflammation and tumorigenesis in a mouse model of colitis-associated cancer. Cell, 118(3), pp.285-296.

40. Wang, T., Huali, X.U., Shaochun, Q.U., Xiaofeng, Y.U. and Sui, D., 2006. Protective effects of Diemailing Injection on myocardial ischemia-reperfusion injury in rats. Journal of Jilin University (Medicine Edition), (01).

41. Satoh, N., Asano, K., Naoki, K., Fukunaga, K., Iwata, M., Kanazawa, M. and Yamaguchi, K., 1999. Plasma platelet-activating factor acetylhydrolase deficiency in Japanese patients with asthma. American journal of respiratory and critical care medicine, 159(3), pp.974-979.

42. Deng, Y., Yang, Z., Terry, T., Pan, S., Woodside, D.G., Wang, J., Ruan, K., Willerson, J.T., Dixon, R.A. and Liu, Q., 2016. Prostacyclin-producing human mesenchymal cells target H19 lncRNA to augment endogenous progenitor function in hindlimb ischaemia. Nature communications, 7(1), pp.1-12.

43. Huang J-S, Ramamurthy SK, Lin X, Le Breton GC. Cell signaling through thromboxane A2 receptors. Cellular Signaling 16(5), 521-533 (2004).

44. Devillier P, Bessard G. Thromboxane A2 and related prostaglandins in airways. Fundamental & Clinical Pharmacology 11(1), 2-18 (1997).

45. Raychowdhury MK, Yukawa M, Collins LJ, Mcgrail SH, Kent KC, Ware JA. Alternative splicing produces a divergent cytoplasmic tail in the human endothelial thromboxane A2 receptor. Journal of Biological Chemistry 269(30), 19256-19261 (1994).

46. Foulon I, Bachir D, Galacteros F, Maclouf J. Increased in vivo production of thromboxane in patients with sickle cell disease is accompanied by an impairment of platelet functions to the thromboxane A2 agonist U46619. Arteriosclerosis and thrombosis: a journal of vascular biology 13(3), 421-426 (1993).

47. Coyle AT, Kinsella BT. Characterization of promoter 3 of the human thromboxane A2 receptor gene. The FEBS journal 272(4), 1036-1053 (2005).

48. Coyle AT, Miggin SM, Kinsella BT. Characterization of the 5′ untranslated region of α and β isoforms of the human thromboxane A2 receptor (TP) Differential promoter utilization by the TP isoforms. European journal of biochemistry 269(16), 4058-4073 (2002).

49. Habib AD, Fitzgerald GA, Maclouf J. Phosphorylation of the thromboxane receptor α, the predominant isoform expressed in human platelets. Journal of Biological Chemistry 274(5), 2645-2651 (1999).

50. Rolin S, Masereel B, Dogné J-M. Prostanoids as pharmacological targets in COPD and asthma. European journal of pharmacology 533(1-3), 89-100 (2006).

51. Vezza R, Habib A, Fitzgerald GA. Differential signaling by the thromboxane receptor isoforms via the novel GTP-binding protein, Gh. Journal of Biological Chemistry 274(18), 12774-12779 (1999).

52. Hirata T, Ushikubi F, Kakizuka A, Okuma M, Narumiya S. Two thromboxane A2 receptor isoforms in human platelets. Opposite coupling to adenylyl cyclase with different sensitivity to Arg60 to Leu mutation. The Journal of clinical investigation 97(4), 949-956 (1996).

53. Hamelin E, Thériault C, Laroche G, Parent J-L. The intracellular trafficking of the G protein-coupled receptor TPβ depends on a direct interaction with Rab11. Journal of Biological Chemistry 280(43), 36195-36205 (2005).

54. Habib A, Vezza R, Créminon C, Maclouf J, Fitzgerald GA. Rapid, Agonist-dependent Phosphorylation in Vivo of Human Thromboxane Receptor Isoforms

MINIMAL INVOLVEMENT OF PROTEIN KINASE C. Journal of Biological Chemistry 272(11), 7191-7200 (1997).

55. Reid HM, Kinsella BT. The α, but not the β, isoform of the human thromboxane A(2) receptor is a target for nitric oxide-mediated desensitization. INDEPENDENT MODULATION OF TPα SIGNALING BY NITRIC OXIDE AND PROSTACYCLIN. The Journal of Biological Chemistry 291(37), 19260-19260 (2016).

56. Parent J-L, Labrecque P, Rochdi MD, Benovic JL. Role of the Differentially Spliced Carboxyl Terminus in Thromboxane A2 Receptor Trafficking IDENTIFICATION OF A DISTINCT MOTIF FOR TONIC INTERNALIZATION. Journal of Biological Chemistry 276(10), 7079-7085 (2001).

57. Parent J-L, Labrecque P, Orsini MJ, Benovic JL. Internalization of the TXA2 Receptor α and β Isoforms ROLE OF THE DIFFERENTIALLY SPLICED COOH TERMINUS IN AGONIST-PROMOTED RECEPTOR INTERNALIZATION. Journal of Biological Chemistry 274(13), 8941-8948 (1999).

58. Sasaki M, Sukegawa J, Miyosawa K, Yanagisawa T, Ohkubo S, Nakahata N. Low expression of cell-surface thromboxane A2 receptor β-isoform through the negative regulation of its membrane traffic by proteasomes. Prostaglandins & other lipid mediators 83(4), 237-249 (2007).

59. Wei J, Yan W, Li X, Ding Y, Tai H-H. Thromboxane receptor α mediates tumor growth and angiogenesis via induction of vascular endothelial growth factor expression in human lung cancer cells. Lung cancer 69(1), 26-32 (2010).

60. Rocca B, Loeb AL, Strauss Iii JF et al. Directed vascular expression of the thromboxane A 2 receptor results in intrauterine growth retardation. Nature medicine 6(2), 219 (2000).

61. Arbab, F., Goldsby, J., Matijevic-Aleksic, N., Huang, G., Ruan, K.H. and Huang, J.C., 2002. Prostacyclin is an autocrine regulator in the contraction of oviductal smooth muscle. Human Reproduction, 17(12), pp.3053-3059.

62. Deng, H., Huang, A., So, S.P., Lin, Y.Z. and Ruan, K.H., 2002. Substrate access channel topology in membrane-bound prostacyclin synthase. Biochemical Journal, 362(3), pp.545-551.

63. Ruan, K.H., So, S.P., Zheng, W., Wu, J., Li, D. and Kung, J., 2002. Solution structure and topology of the N-terminal membrane anchor domain of a microsomal cytochrome P450: prostaglandin I2 synthase. Biochemical Journal, 368(3), pp.721-728.

64. So, S.P., Wu, J., Huang, G., Huang, A., Li, D. and Ruan, K.H., 2003. Identification of residues important for ligand binding of thromboxane A2 receptor in the second extracellular loop using the NMR experiment-guided mutagenesis approach. Journal of Biological Chemistry, 278(13), pp.10922-10927.

65. Wu, J., So, S.P. and Ruan, K.H., 2003. Solution structure of the third extracellular loop of human thromboxane A2 receptor. Archives of biochemistry and biophysics, 414(2), pp.287-293.

66. Picot, D., Loll, P.J. and Garavito, R.M., 1994. The X-ray crystal structure of the membrane protein prostaglandin H2 synthase-1. Nature, 367(6460), pp.243-249.

67. Luong, C., Miller, A., Barnett, J., Chow, J., Ramesha, C. and Browner, M.F., 1996. Flexibility of the NSAID binding site in the structure of human cyclooxygenase-2. Nature structural biology, 3(11), pp.927-933.

68. Ruan, K.H., Deng, H. and So, S.P., 2006. Engineering of a protein with cyclooxygenase and prostacyclin synthase activities that converts arachidonic acid to prostacyclin. Biochemistry, 45(47), pp.14003-14011.

69. Ruan, K.H., So, S.P., Cervantes, V., Wu, H., Wijaya, C. and Jentzen, R.R., 2008. An active triple-catalytic hybrid enzyme engineered by linking cyclo-oxygenase isoform-1 to prostacyclin synthase that can constantly biosynthesize prostacyclin, the vascular protector. The FEBS journal, 275(23), pp.5820-5829.

70. Ruan, K.H., Cervantes, V. and So, S.P., 2009. Engineering of a novel hybrid enzyme: an anti-inflammatory drug target with triple catalytic activities directly converting arachidonic acid into the inflammatory prostaglandin E2. Protein Engineering, Design & Selection, 22(12), pp.733-740.

71. Zwischenberger JB, Brunston RL, Swann JR, Conti VR. Comparison of two topical collagen-based hemostatic sponges during cardiothoracic procedures. Journal of Investigative Surgery 12(2), 101-106 (1999).

72. Gabay M. Absorbable hemostatic agents. American journal of health-system pharmacy 63(13), 1244-1253 (2006).

73. Benedetto FD, Tarantino G. Topical hemostatic agents. Transfusion-Free Medicine and Surgery 143-157 (2014).

74. Kheirabadi BS, Field-Ridley A, Pearson R, Macphee M, Drohan W, Tuthill D. Comparative study of the efficacy of the common topical hemostatic agents with fibrin sealant in a rabbit aortic anastomosis model. Journal of Surgical Research 106(1), 99-107 (2002).

75. Kanko M, Liman T, Topcu S. A Low-Cost and Simple Method to Stop Intraoperative Leakage-Type Bleeding: Use of the Vancomycin–Oxidized

Regenerated Cellulose (ORC) Sandwich. Journal of Investigative Surgery 19(5), 323-327 (2006).

76. Recinos G, Inaba K, Dubose J, Demetriades D, Rhee P. Local and systemic hemostatics in trauma: a review. Ulusal Travma ve Acil Cerrahi Dergisi 14(3), 175 (2008).

77. Hidas G, Kastin A, Mullerad M, Shental J, Moskovitz B, Nativ O. Sutureless nephron-sparing surgery: use of albumin glutaraldehyde tissue adhesive (BioGlue). Urology 67(4), 697-700 (2006).

78. Fürst W, Banerjee A. Release of glutaraldehyde from an albumin-glutaraldehyde tissue adhesive causes significant in vitro and in vivo toxicity. The Annals of thoracic surgery 79(5), 1522-1528 (2005).

79. Thatte HS, Zagarins S, Khuri SF, Fischer TH. Mechanisms of Poly-N-Acetyl Glucosamine Polymer–Mediated Hemostasis: Platelet Interactions. Journal of Trauma and Acute Care Surgery 57(1), S13-S21 (2004).

80. Chou T-C, Fu E, Wu C-J, Yeh J-H. Chitosan enhances platelet adhesion and aggregation. Biochemical and Biophysical Research Communications 302(3), 480-483 (2003).

81. Thatte HS, Zagarins SE, Amiji M, Khuri SF. Poly-N-Acetyl Glucosamine–Mediated Red Blood Cell Interactions. Journal of Trauma and Acute Care Surgery 57(1), S7-S12 (2004).

82. Galownia J, Martin J, Davis ME. Aluminophosphate-based, microporous materials for blood clotting. Microporous and mesoporous materials 92(1-3), 61-63 (2006).

83. Wright JK, Kalns J, Wolf EA et al. Thermal injury resulting from application of a granular mineral hemostatic agent. Journal of Trauma and Acute Care Surgery 57(2), 224-230 (2004).

84. Pusateri AE, Delgado AV, Dick Jr EJ, Martinez RS, Holcomb JB, Ryan KL. Application of a granular mineral-based hemostatic agent (QuikClot) to reduce blood loss after grade V liver injury in swine. Journal of Trauma and Acute Care Surgery 57(3), 555-562 (2004).

85. Saed GM, Kruger M, Diamond MP. Enhanced matrix metalloproteinase expression by Tisseel in mesothelial cells, normal peritoneal fibroblasts, and adhesion fibroblasts. European Journal of Plastic Surgery 28(7), 472-479 (2006).

86. Paul BZS, Jin J, Kunapuli SP. Molecular Mechanism of Thromboxane A2-induced Platelet Aggregation: ESSENTIAL ROLE FOR P2T AC and α2ARECEPTORS. Journal of Biological Chemistry 274(41), 29108-29114 (1999).

87. Smyth EM. Thromboxane and the thromboxane receptor in cardiovascular disease. Clinical lipidology 5(2), 209-219 (2010).

88. Neamtu I, Chiriac AP, Diaconu A, Nita LE, Balan V, Nistor MT. Current Concepts on Cardiovascular Stent Devices. Mini-Reviews in Medicinal Chemistry 14(6), 505-536 (2014).

89. Im E, Hong M-K. Drug-eluting stents to prevent stent thrombosis and restenosis. Expert Review of Cardiovascular Therapy 14(1), 87-104 (2016).

90. Elmore JB, Mehanna E, Parikh SA, Zidar DA. Restenosis of the Coronary Arteries. Interventional Cardiology Clinics 5(3), 281-293 (2016).

91. Alfonso F, Byrne RA, Rivero F, Kastrati A. Current Treatment of In-Stent Restenosis. Journal of the American College of Cardiology 63(24), 2659-2673 (2014).

92. Hamid H, Coltart J. 'Miracle stents' - a future without restenosis. McGill Journal of Medicine : MJM 10(2), 105-111 (2007).

93. Smyth EM. Thromboxane and the thromboxane receptor in cardiovascular disease. Clinical lipidology 5(2), 209-219 (2010).

94. Numaguchi Y, Okumura K, Harada M et al. Catheter-based prostacyclin synthase gene transfer prevents in-stent restenosis in rabbit atheromatous arteries. Cardiovascular Research 61(1), 177-185 (2004).

95. Egan KM, Lawson JA, Fries S, Koller B, Rader DJ, Smyth EM, FitzGerald GA. COX-2-derived prostacyclin confers atheroprotection on female mice. Science. 2004; 306: 1954-7.

96. Castellana M, Wilson MZ, Xu Y, Joshi P, Cristea IM, Rabinowitz JD, Gitai Z, Wingreen NS. Enzyme clustering accelerates processing of intermediates through metabolic channeling. Nature biotechnology. 2014; 32: 1011.

97. Ruan KH, So SP, Cervantes V, Wu H, Wijaya C, Jentzen RR. An active triple-catalytic hybrid enzyme engineered by linking cyclo-oxygenase isoform-1 to prostacyclin synthase that can constantly biosynthesize prostacyclin, the vascular protector. The FEBS journal. 2008; 275: 5820-9.

98. Huang D, Ren L, Qiu C-S, Liu P, Peterson J, Yanagawa Y, Cao Y-Q. Characterization of a mouse model of headache. Pain. 2016; 157: 1744.

99. Deng H, Wu J, So S-P, Ruan K-H. Identification of the residues in the helix F/G loop important to catalytic function of membrane-bound prostacyclin synthase. Biochemistry. 2003; 42: 5609-17.

100. Ruan K-H, Deng H, Wu J, So S-P. The N-terminal membrane anchor domain of the membrane-bound prostacyclin synthase involved in the substrate presentation of the coupling reaction with cyclooxygenase. Archives of biochemistry and biophysics. 2005; 435: 372-81.

101. Ruan K-H, Deng H, So S-P. Engineering of a protein with cyclooxygenase and prostacyclin synthase activities that converts arachidonic acid to prostacyclin. Biochemistry. 2006; 45: 14003-11.

102. Ruan KH, So SP, Cervantes V, Wu H, Wijaya C, Jentzen RR. An active triple-catalytic hybrid enzyme engineered by linking cyclo-oxygenase isoform-1 to prostacyclin synthase that can constantly biosynthesize prostacyclin, the vascular protector. The FEBS journal 275, 5820-5829 (2008).

103. Castellana, M., Wilson, M.Z., Xu, Y., Joshi, P., Cristea, I.M., Rabinowitz, J.D., Gitai, Z. and Wingreen, N.S., 2014. Enzyme clustering accelerates processing of intermediates through metabolic channeling. Nature biotechnology, 32(10), p.1011.

104. Egan, K.M., Lawson, J.A., Fries, S., Koller, B., Rader, D.J., Smyth, E.M. and FitzGerald, G.A., 2004. COX-2-derived prostacyclin confers atheroprotection on female mice. Science, 306(5703), pp.1954-1957.

105. Huang, D., Ren, L., Qiu, C.S., Liu, P., Peterson, J., Yanagawa, Y. and Cao, Y.Q., 2016. Characterization of a mouse model of headache. Pain, 157(8), p.1744.

106. So S-P, Wu J, Huang G, Huang A, Li D, Ruan K-H. Identification of Residues Important for Ligand Binding of Thromboxane A2 Receptor in the Second Extracellular Loop Using the NMR Experiment-guided Mutagenesis Approach. Journal of Biological Chemistry 278, 10922-10927 (2003).

107. Akasaka H, et al. The key residue within the second extracellular loop of human EP3 involved in selectively turning down PGE2- and retaining PGE1-mediated signaling in live cells. Archives of Biochemistry and Biophysics 616, 20-29 (2017).

108. Luong C, Miller A, Barnett J, Chow J, Ramesha C, Browner MF. Flexibility of the NSAID binding site in the structure of human cyclooxygenase-2. Nature Structural and Molecular Biology. 1996; 3: 927.

109. Picot D, Loll PJ, Garavito RM. The X-ray crystal structure of the membrane protein prostaglandin H2 synthase-1. Nature. 1994; 367: 243.

110. Ruan K-H, Deng H, So S-P. Engineering of a protein with cyclooxygenase and prostacyclin synthase activities that converts arachidonic acid to prostacyclin. Biochemistry. 2006; 45: 14003-11.

111. Hui D, Huang A, Shui-Ping S, Yue-Zhen L, Ke-He R. Substrate access channel topology in membrane-bound prostacyclin synthase. Biochemical Journal. 2002; 362: 545-51.

112. Ke-He R, Shui-Ping S, Zheng W, Jiaxin W, Dawei L, Jennifer K. Solution structure and topology of the N-terminal membrane anchor domain of a microsomal cytochrome P450: prostaglandin I2 synthase. Biochemical Journal. 2002; 368: 721-8.

113. Wu J, So S-P, Ruan K-H. Determination of the membrane contact residues and solution structure of the helix F/G loop of prostaglandin I2 synthase. Archives of biochemistry and biophysics. 2003; 411: 27-35.

114. Ruan K-H. Advance in understanding the biosynthesis of prostacyclin and thromboxane A2 in the endoplasmic reticulum membrane via the cyclooxygenase pathway. Mini reviews in medicinal chemistry. 2004; 4: 639-47.

115. Ling Q-L, Mohite AJ, Murdoch E, Akasaka H, Li Q-Y, So S-P, Ruan K-H. Creating a mouse model resistant to induced ischemic stroke and cardiovascular damage. Scientific Reports. 2018; 8: 1653.

116. Ruan KH, Cervantes V, Wu J. A simple, quick, and high-yield preparation of the human thromboxane A2 receptor in full size for structural studies. Biochemistry 47, 6819-6826 (2008).

117. Ruan KH, Cervantes V, Wu J. Ligand-specific conformation determines agonist activation and antagonist blockade in purified human thromboxane A2 receptor. Biochemistry 48, 3157-3165 (2009).

118. Ruan KH, Wijaya C, Cervantes V, Wu J. Characterization of the prostaglandin H2 mimic: binding to the purified human thromboxane A2 receptor in solution. Arch Biochem Biophys 477, 396-403 (2008).

119. Chillar A, Wu J, Cervantes V, Ruan KH. Structural and functional analysis of the C-terminus of Galphaq in complex with the human thromboxane A2 receptor provides evidence of constitutive activity. Biochemistry 49, 6365-6374 (2010).

120. So S-P, Wu J, Huang G, Huang A, Li D, Ruan K-H. Identification of Residues Important for Ligand Binding of Thromboxane A2 Receptor in the

Second Extracellular Loop Using the NMR Experiment-guided Mutagenesis Approach. Journal of Biological Chemistry 278, 10922-10927 (2003).

121. Ruan K-H, Wu J, So S-P, Jenkins LA, Ruan C-H. NMR structure of the thromboxane A2 receptor ligand recognition pocket. European Journal of Biochemistry 271, 3006-3016 (2004).

122. Wu J, So S-P, Ruan K-H. Solution structure of the third extracellular loop of human thromboxane A2 receptor. Archives of Biochemistry and Biophysics 414, 287-293 (2003).

123. Ruan K-H, So S-P, Wu J, Li D, Huang A, Kung J. Solution Structure of the Second Extracellular Loop of Human Thromboxane A2 Receptor. Biochemistry 40, 275-280 (2001).

124. Tesmer VM, Kawano T, Shankaranarayanan A, Kozasa T, Tesmer JJG. Snapshot of Activated G Proteins at the Membrane: The Gα_q-GRK2-Gßγ Complex. Science 310, 1686-1690 (2005).

125. Schrage, R., Schmitz, A.L., Gaffal, E., Annala, S., Kehraus, S., Wenzel, D., Büllesbach, K.M., Bald, T., Inoue, A., Shinjo, Y. and Galandrin, S., 2015. The experimental power of FR900359 to study Gq-regulated biological processes. Nature communications, 6(1), pp.1-17.

126. Schröder, R., Janssen, N., Schmidt, J., Kebig, A., Merten, N., Hennen, S., Müller, A., Blättermann, S., Mohr-Andrä, M., Zahn, S. and Wenzel, J., 2010. Deconvolution of complex G protein–coupled receptor signaling in live cells using dynamic mass redistribution measurements. Nature biotechnology, 28(9), p.943.

127. Chillar AJ, Karimi P, Tang K, Ruan KH. An agonist sensitive, quick and simple cell-based signaling assay for determination of ligands mimicking

prostaglandin E2 or E1 activity through subtype EP1 receptor: Suitable for high throughput screening. BMC Complement Altern Med 11, 11 (2011).

128. Akasaka, H., So, S.P. and Ruan, K.H., 2015. Relationship of the topological distances and activities between mPGES-1 and COX-2 versus COX-1: Implications of the different post-translational endoplasmic reticulum organizations of COX-1 and COX-2. Biochemistry, 54(23), pp.3707-3715.

129. Nakamura, S., Takayama, N., Hirata, S., Seo, H., Endo, H., Ochi, K., Fujita, K.I., Koike, T., Harimoto, K.I., Dohda, T. and Watanabe, A., 2014. Expandable megakaryocyte cell lines enable clinically applicable generation of platelets from human induced pluripotent stem cells. Cell stem cell, 14(4), pp.535-548.